



An-Najah National University
Faculty of Graduate Studies

**DESIGN A FUZZY LOGIC
CONTROLLER TO CONTROL ACTIVE
POWER FILTER FED BY MULTILEVEL
INVERTER AND PHOTOVOLTAIC**

By

Ghadeer Ahmad Abduh

Supervisor

Dr. Kamel Saleh

**This Thesis is Submitted in Partial Fulfillment of the Requirements for the Degree of
Master of Electrical Power Engineering, Faculty of Graduate Studies, An-Najah National
University, Nablus - Palestine.**

2023

DESIGN A FUZZY LOGIC CONTROLLER TO CONTROL ACTIVE POWER FILTER FED BY MULTILEVEL INVERTER AND PHOTOVOLTAIC

By


Ghadeer Ahmad Abduh

This Thesis was Defended Successfully on 11/9/2023 and approved by

Dr. Kamel Saleh
Supervisor


Signature

Insert Name
External Examiner


Signature

Insert Name
Internal Examiner


Signature

Dedication

إلى الذي واجه نصب الحياة وشقاءها ليقرأ في عيون الأبناء لحظة سعادة

إلى من أخذ بيدي نحو تحقيق ما أصبو إليه

إلى الذي تحمل معي كل مشقة وتعب

إلى الذي أذكى جذور الأمل في نفسي

إلى روح والدي الغالي رحمه الله

إلى التي آثرت الأبناء على نفسها

إلى التي رسم حنانها ملامح شخصيتي

إلى من غرست بذور العزيمة والمحبة في حنايا روحي

إلى أُمي الغالية

إلى القلوب التي تفيض بالمحبة الصادقة والعطاء الدافق

إلى الذين بهم ومعهم يصير للحياة معنى وللنجاح قيمة

إلى إخواني الأعزاء

وإلى روح أخي الغالي وعائلته رحمهم الله

تدنو اللحظات وتفتح نوافذ المستقبل نحو ميادين الحياة الفسيحة

إلى من أمد إلي بيد العون والعطاء إلى من شجعني لتري رسالتي النور

إلى زوجي الغالي

إلى نور الحياة وامل المستقبل أبنائي الغوالي (محمد، أحمد)

إلى من رسموا إلي طريق العلم

إلى من أشعلوا لنا مصابيح النجاح

إلى أساتذتي الأفاضل

Acknowledgements

I should firstly express my great thanks to almighty Allah, who gave me power and made me able to accomplish this work.

My grateful thanks to all, who hand me help and support to collect the necessary data to fulfill my thesis.

I do express my thanks to my "Assistant Professor of Electrical Engineering" Dr. Kamel Saleh, for his continual support and guidance to carry out my work.

Finally, I can't but express my great thanks to my family and my spouse for all what they offered me through courage, motivation and support all the years of study to accomplish this work.

Declaration

I, the undersigned, declare that I submitted the thesis entitled:

**DESIGN A FUZZY LOGIC CONTROLLER TO CONTROL ACTIVE POWER
FILTER FED BY MULTILEVEL INVERTER AND PHOTOVOLTAIC**

I declare that the work provided in this thesis, unless otherwise referenced, is the researcher's own work, and has not been submitted elsewhere for any other degree or qualification.

Student's Name: _____

Signature: _____

Date: _____

List of Contents

Dedication	III
Acknowledgements	IV
Declaration	V
List of Contents	VI
List of Tables	VIII
List of Figures	IX
Abstract	XII
Chapter One	1
1.1 Encouragement	1
1.1.1 Power System Performance	1
1.1.2 Reliability of the Active Filter	1
1.2 Objectives	1
1.3 Thesis Structure	1
Chapter Two	7
Fuzzy Logic Controller (FLC)	7
2.1 Introduction	7
2.2 Design of Fuzzy Controller	7
2.3 Fundamental Components of a Fuzzy Controller	7
2.4 The Fundamentals of a Fuzzy System Fuzzification	8
Chapter Three	12
Multi-level inverter	12
3.1 Introduction	12
3.2 Types of Multilevel Converter Structure	13
3.3 Diode-Clamped Multilevel Inverter	13
3.4 Flying Capacitor Multilevel Inverter	15
3.5 Multilevel cascade inverter	16
3.6 Multilevel Inverter Design	17
Chapter Four	19
Shunt Active Filter	19
4.1 Introduction	19
4.2 Techniques for Extracting Harmonic Currents	21
4.3 Theorem of Instantaneous (Active & Reactive) Power	22
4.4 Instantaneous Current Component Theory	26
4.5 Controller for Shunt Active Power Filters (SHAPF)	28
4.6 Direct Control Approach	28

4.7 Indirect Control Approach.....	28
4.7.1 Algorithm Based on PQ Theory	29
4.7.2 Synchronous Reference-based indirect control	30
4.7.3 DC voltage controller-based indirect control.....	31
4.8 Shunt Active Power Filter controller design	31
Chapter Five.....	34
Compensation Scenarios and System Outcome	34
5.1 Effects of various System Compensation scenarios on individual non-linear loads	34
5.2 Comparison between PI and Fuzzy logic controller.....	39
5.3 Effects of System Compensation scenarios on IEEE networks	43
5.3.1 Results and Analysis.....	45
5.3.1.1 Scenario 1	45
5.3.1.2 Scenario 2	46
Chapter Six.....	48
Compensation Scenarios and System Outcome Results and Recommendations.....	48
List of Abbreviations	50
Reference	50
المُلخَص	ب

List of Tables

Table 2.1: Error and Change of Error for FLC	9
Table 2.2: Error and Change of Error for FLC with 27*27 membership	79
Table 3.1: Three-level diode-clamped inverter condition switching	14
Table 3.2: The multi-level inverter's DC sources.....	17
Table 5.1: Total harmonics distortion of Source and inverter currents	37

List of Figures

Figure 2.1: structure of Fuzzy logic controller	7
Figure 5.1: Schematic for a system simulation with non-linear load in combination	35
Figure 5.2: Schematic of System active power and reactive power behavior under different operation scenarios	36
Figure 5.3: Schematic of source and inverter current and THD during four scenarios ..	38
Figure 5.4: Schematic for a- fuzzy logic system / b-PI simulation with non-linear load in combination	40
Figure 5.5: Schematic a- I_d / I_q ref and measured for PI system / b- I_d / I_q ref and measured for Fuzzy system simulation with non-linear load in combination	78
Figure 5.6: currents waveforms of : a-PI controller and THD without and with APF / b- Fuzzy Logic controller and THD without and with APF.	42
Figure 5.9: Schematic of combined system simulation with IEEE 15 Bus network	44
a-(APF at load) / b-(APF at swing bus1)	44
Figure 5. 8: APF connected to bus no 1 of the IEEE 15 bus networks.....	45
Figure 5.11: APF connected to bus no5 of the IEEE 15 bus network.	47

List of Appendices

Figure 1.1	General schematic of the designed system.	53
Figure 2.2	The fundamental design of a fuzzy controller.	53
Figure 2.3	Fuzzy system components.	53
Figure 2.4	Block diagram of fuzzy controller	54
Figure 2.5	Membership function plot of 2 input of fuzzy controller	54
Figure 2.6	Membership function plot of output of fuzzy controller	54
Figure 2.7	Rule editor of fuzzy controller Rule viewer of fuzzy controller	55
Figure 2.8	Rule viewer of fuzzy controller	55
Figure 2.9	Surface view of fuzzy controller	56
Figure 2.10	Arrangement of fuzzy controller in nonlinear system.	56
Figure 2.11	Fuzzy Logic controller by using MATLAB/SIMULINK	57
Figure 3.1	Schematic of a single-phase inverter showing the DC voltage levels	57
Figure 3.2	Diagram of a three-level inverter with a diode-clamped topology	58
Figure 3.3	Circuit architecture diagram for a capacitor-clamped multilevel inverter (three levels)	58
Figure 3.4	Design of a 3-level cascaded multilevel inverter (Y arrangement)	59
Figure 3.5	H-bridge inverter with three separate DC sources and 27 levels for one leg	59
Figure 3.6	multi-level inverter controller flowchart	60
Figure 3.7	MATLAB/SIMULINK-based 27-level inverter design	60
Figure 4.1	Passive shunt high pass filter	61
Figure 4.2	Shunt active power filter scheme	61
Figure 4.3	hybrid power filtering technique	62
Figure 4.4	Schematic of p-q theory principle	62
Figure 4.5	The p-q theory power components	62
Figure 4.6	An illustration of the p-q theory in action for eliminating harmonics	63
Figure 4.7	An example of how the p-q theory can be used to reduce harmonics and improve PF	63
Figure 4.8	I_d - I_q theory for reference current extraction illustrated	63
Figure 4.9	Direct Control Method Schematic	64
Figure 4.10	Illustration of the current closed-loop controller	64

Figure 4.11 <i>Direct Control Technique Illustration</i>	64
Figure 4.12 <i>Diagram illustrating a strategy for indirect control based on p-q theory</i> .	65
Figure 4.13 <i>Id-Iq theory-based schematic for an indirect control approach</i>	65
Figure 4.14 <i>Diagram of an indirect control method using a DC voltage controller</i>	66
Figure 4.15 <i>Schematic of SAF with switches and Dc source</i>	66
Figure 4.16 <i>Current controller</i>	67
Figure 4.17 <i>Shunt active power filter controller by using MATLAB/SIMULINK</i>	67
Figure 5. 9 <i>Operation of the SAPF during under load disturbance</i>	82
Figure 5. 10 <i>The source current of operation of the SAPF during under load disturbance</i>	83
Figure 5. 11 <i>source current when APF connected to bus no 1 of the IEEE 15 bus networks</i>	83
Figure 5.10 <i>currents waveforms at buses 9,11,15 when APF connected to bus 1 of the IEEE 15 bus network</i>	84
Figure 5.11 <i>THD at buses 9,11,15 when APF connected to bus no 1 of the IEEE 15 bus network</i>	85
Figure 5.12 <i>Source current when APF connected to bus no5 of the IEEE 15 bus network</i>	85
Figure 5.13 <i>currents waveforms at buses 9,11,15 when APF connected to bus 5 of the IEEE 15 bus network</i>	86
Figure 5.14 <i>THD when APF connected to bus no5 of the IEEE 15 bus network</i>	86

DESIGN A FUZZY LOGIC CONTROLLER TO CONTROL ACTIVE POWER FILTER FED BY MULTILEVEL INVERTER AND PHOTOVOLTAIC

By

Ghadeer Ahmad Abduh

Supervisor

Dr. Kamel Saleh

Abstract

New electrical systems commonly use nonlinear loads, which increase harmonic pollution in the primary power system.

When power electronic equipment with semi-conductors is utilized, harmonic currents occur, affecting quality of power and generating non-sinusoidal currents taken from the AC sources. This result in a current discontinuity and an increase in the system's harmonics.

Harmony in the power network generates a variety of issues, including voltage deformities at the Point of Common Coupling (PCC), altering peak and RMS values of line used, and a variety of other issues.

In addition to the challenges caused by harmonic current, reactive power is another problem with the quality of the electricity in the power system. To improve the quality of the power delivered to the network, electrical filters must be employed to cancel harmonics and reactive power.

The power quality is developed using a variety of filter topologies, including passive, active, and hybrid.

A shunt active filter is employed in this project to increase the quality of the electric power. This active filter can perform a variety of tasks, including reducing harmonics, adjusting reactive energy, improving Power Factor (PF), inserting real power source.

The primary goal of this project is to apply a fuzzy logic controller to optimize the performance of the Shunt Active Power Filter in order to lower harmonic distortion. To

decrease the harmonic current and raise the power factor to unity, the Fuzzy Logic Controller for the three-phase Shunt Active Power Filter is intended to replace the Proportional Integral controller.

The results were confirmed from the calculated values of the THD of the source currents. The THD was reduced from 16.67% before using the APF to 2.62 % after using the APF for PI controller and 16.67% to 1.42% for FLC. These results of the THD for FLC is even better than the results obtain of PI controller.

MATLAB/SIMULINK has been used in this study to combine various renewable energy sources with a 27-level H-Bridge multi-level inverter with a shunt active power filter. The system has been built to function in a variety of operational scenarios.

Keywords: Fuzzy Logic Controller, Shunt Active Power Filter, Photovoltaic, Multilevel Inverter, Total Harmonic Distortion.

Chapter One

1.1 Encouragement

1.1.1 Power System Performance

The System of Power quality is a crucial thing in the system power for a variety of causes, thus an active filter must be created to remove harmonics, make up for reactive power, and develop power factor in order to prevent issues that might arise in the power system.

1.1.2 Reliability of the Active Filter

Passive and active components that are used to create an active filter, are what determine its dependability. The active filter may function in fault, steady-state, and transient situations, the quality of the power system may also be improved.

1.2 Objectives

The thesis shows the following objectives:

1. The design includes the type selection and photovoltaic size array necessary to satisfy the reactive loads and real power requirements for the voltage and current regularities. It also has the capacity to filter harmonics and insert active power and reactive power.
- 2- executing the intended module using the MATLAB/SIMULINK software.
- 3- Using Fuzzy Logic Controller.
- 4- Using Load Flow Programming to make load flow analysis for the system with a standard IEEE network.

1.3 Thesis Structure

Chapter One: The effects of employing nonlinear loads more frequently, which causes harmonics in the power system, as well as the effects of harmonics on the grids and the equipment are covered in this chapter. The use of power filters, whether passive, active, or hybrid, is one method for minimizing harmonics and compensating for reactive power that is covered in this chapter. Describe the purpose and objectives of this research in your conclusion.

Chapter Two: Fuzzy Logic Controller (FLC): In this chapter, we discussed the fuzzy logic controller, in order to ensure that the performance goals will be achieved, it merges plant output data $y(t)$ and compares it to the reference input $r(t)$. It then calculates how the plant input $u(t)$ should be.

Chapter Four

Shunt Active Filter Multi-level inverter design: This chapter describes the design of multilevel inverters, the types of multilevel converter structures, and the factors that led to the selection of an H-bridge with a 27-level inverter for this project. It also displays each type's features. Finally, it uses MATLAB/SIMULINK to demonstrate the intended multilevel inverter model with controller and DC sources for one leg.

Chapter Four: Shunt Active Filter: This chapter explains the many types of active power filters and their features. It also explains how to extract harmonic currents by using numerous equations from the instantaneous power theory and instantaneous current component theory. lastly displays the full control strategy for SHAPF that was examined using MATLAB program.

Chapter Five:

Compensation Scenarios and System Outcome: This chapter uses MATALAB/SIMLUINK to present a system schematic overview with a separate nonlinear load and an IEEE network. This chapter also illustrates how the system behaves and how it affects the source and networks in various compensation scenarios for various operational conditions.

1.4 LITERATURE REVIEW

1.4.1 (THD) Total Harmonic Distortion

A measurement of the harmonic distortion contained in current or voltage is called the total harmonic distortion (THD) of a signal. It is described as the ratio of the sum of all harmonic power components that make up the basic component. The insertion of causes harmonic distortion when waveforms with multiples of the fundamental frequency (Mohammed, 2012). The following list of the most popular harmonics indexes is provided: 2012 (Hussein).

$$THD_V(\%) = \frac{\sqrt{\sum_{h=2}^a V_h^2}}{V_1} \quad (1.1)$$

$$THD_I(\%) = \frac{\sqrt{\sum_{h=2}^a I_h^2}}{I_1} \quad (1.2)$$

Total harmonic distortion is typically represented as a percentage and is defined as the ratio of the rms values of the harmonic components to the rms values of the fundamental components. This index is used to determine how far a periodic waveform with harmonics deviates from a pure sine wave. The THD is 0 for a perfect sine wave at fundamental frequency.

The Total Harmonic Distortion (THD) is a valuable tool for a variety of tasks, but it excels for harmonic index measurement. Its drawback, however, is that because voltage stress within a capacitor is tied to the peak magnitude of the voltage waveform, it is not a suitable indicator of that stress (Mohammed, 2012).

1.4.1.1 Effect of Harmonics on Power Factor

The impact of harmonics on the power factor is discussed in this article. The electrical power system's harmonics are brought on by the nonlinear loads, which negatively impact the power factor. The performance of electrical machinery and apparatus is impacted by the increased power loss brought on by harmonics' degradation of power factor. We must first comprehend the various terms used to describe power factor before we can comprehend how harmonics lead to lower power factor (Electrical Volt , 2022).

The power factor is the ratio of real or active power to apparent power.

$$Power\ Factor, \cos\phi = \frac{Active\ Power}{Apparent\ Power} \quad (1.3)$$

$$Power\ Factor, \cos\phi = \frac{P}{S}$$

More total harmonic distortion in a load result in a higher demand for reactive power and a lower distortion power factor. The total harmonic distortion that the load produces determines the distortion power factor.

The mathematical equations listed below can be used to express the distortion power factor.

$$\text{Distortion Power Factor} = \frac{1}{\sqrt{1+THD^2}} \quad (1.4)$$

The mathematical equations listed below can be used to express an electrical network's actual power factor. (Electrical Volt, 2022)

$$\text{Power Factor} = \cos \phi \times 1$$

$$\text{Power factor} = \cos \phi \times \frac{1}{\sqrt{1+THD^2}} \quad (1.5)$$

$$\text{Power factor} = \frac{\cos \phi}{\sqrt{1+THD^2}}$$

1.4.2 Filters

There are three basic kinds of filters, each of which offers a special way to lessen and get rid of harmonics. The structures of these harmonic filters can be broadly divided into passive, active, and hybrid types. The kind of filter to apply depends on the issue at hand as well as the implementation's financial implications (Nalini et al., 2011).

1.4.2.1 Active Filters

In order to successfully replace some of the distorted current wave coming from the load, active filters use active components like IGBT transistors to introduce negative harmonics into the network (Nalini et al., 2011). When the orders of harmonic currents vary, an active filter is used. The sort of harmonic sources available in the power system and the effects that various filter 17 solutions would have on the overall system performance are taken into consideration while choosing the structure, which can either be of the series or parallel type (Nalini et al., 2011).

The ability to correct for harmonics without worrying about reactive power at fundamental frequencies is a benefit of active filters. Active filters have the added benefit of being able to adapt to shifting load and harmonic conditions, as opposed to passive filters, whose harmonic response is fixed. (Sankara, 2002; Nalini et al., 2011).

Shunt active filter, Series active filter, and Hybrid active filter are the three categories that active filters can be categorized under based on the connection scheme. Hybrid

active filters combine an active filter and a passive filter, with the passive filter performing basic filtering (5th order, for example), and the active filter, through precise control, covering higher harmonics (Balasubramaniam et al., 2014).

1.4.3 Harmonics Current Extraction Strategies

Dc voltage control techniques and the extraction method form the harmonics current extraction strategies. The frequency domain method and the time domain method are the two main strategies for harmonic detection that have been proposed in the literature (Rathika & Devaraj, 2011).

The Time domain techniques are used for computing the because they require less computation. Identify the most recent. Synchronous reference (d-q-0) and time domain methods are the two most popular techniques. (P-Q) theory and the instantaneous real-reactive power theory (Rathika & Devaraj, 2011).

1.4.3.1 Synchronous Reference Frame (d-q)

The time-domain reference signal estimating methods serve as the foundation for the synchronous system theory, often known as the d-q theory. In addition to handling standard voltage and current waveforms, it may operate in steady-state or transient conditions (Balasubramaniam et al., 2014). The straightforwardness of the computations that entail algebraic calculation is another essential component of this theory (Hemachandra et al., 2015).

The direct (d-q) and inverse (d-q) -1 park transformations make up the fundamental structure of the synchronous reference frame (d-q-0) theory (Balasubramaniam et al., 2014; Hemachandra et al., 2015).

Following is the transformation equation: 2014 (Sunitha & Kartheck).

$$\begin{bmatrix} id \\ iq \\ io \end{bmatrix} = \sqrt{\frac{3}{2}} \begin{bmatrix} \cos\theta & \cos(\theta - \frac{2\pi}{3}) & \cos(\theta + \frac{2\pi}{3}) \\ -\sin\theta & -\sin(\theta - \frac{2\pi}{3}) & -\sin(\theta + \frac{2\pi}{3}) \\ \frac{1}{\sqrt{2}} & \frac{1}{\sqrt{2}} & \frac{1}{\sqrt{2}} \end{bmatrix} \begin{bmatrix} ia \\ ib \\ ic \end{bmatrix} \quad (1.6)$$

1.4.4 Fuzzy logic controller

Solar photovoltaic (PV) and wind farm systems of renewable energy installations have been regarded as the promising generating source that would satisfy the ongoing demand for energy. Both end users of electric power and electric utilities have grown more concerned about the issue of the quality of the electric network as a result of the high inbound penetration of distribution generators (DG). Capacitive coupling with the grounding systems, which are now necessary due to the high frequency current forced by the power converters, is one specific issue lying under the umbrella idea. Total harmonic distortion (THD), which is induced by the frequent use of power electronic equipment, is constrained by the allowable range of power quality standards (IEEE-519). This study examines the THD in PV systems when capacitive coupling is used to lower THD. In order to negate the harmonic design of a non-linear load, fuzzy logic controllers are used. Results indicate that THD for power in PV systems has decreased by roughly 13%, while THD for current in PV systems has decreased by around 23% (Ali,Tawala,Marwala, boukkaibet. 2021).

Throughout this work, we have demonstrated the efficiency of shunt active power filtering, particularly when fuzzy logic and the band-pass filter approach are used to calculate current references. The power supply current distortion was actually reduced to a tolerable level (THD = 0.99% in 80 ms with fuzzy correctors compared to 1.14% in 80 ms with classical correctors) and the power factor was adjusted (power supply voltage and current became in phase), (Benalladz, hinddjegloud,2016).

Chapter Two

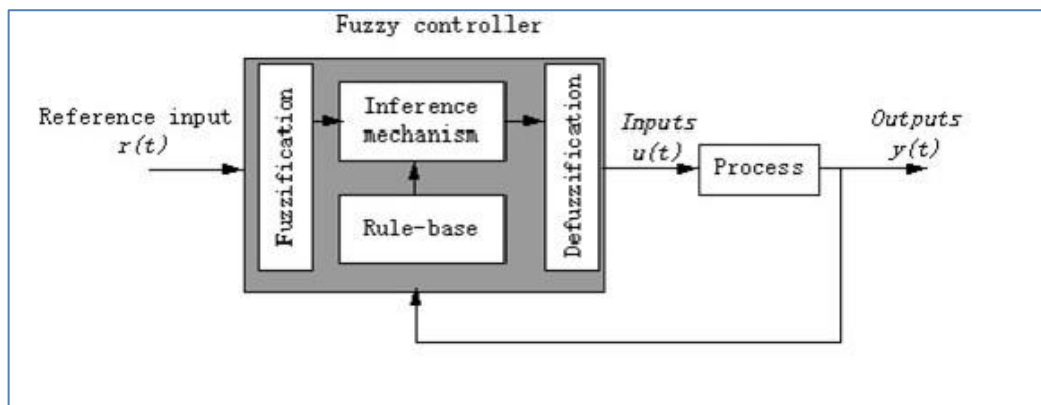
Fuzzy Logic Controller (FLC)

2.1 Introduction

Fuzzy logic control is taken from fuzzy set theory introduced by Zadeh in 1965. In the fuzzy logic concept, the transition is taken from membership and non-membership tasks. Therefore, boundaries of fuzzy sets can be hidden and ambiguous, making it helpful for approximate systems. FLC is an attractive choice when short mathematical formulas are impossible to help [1].

Figure 2.1:

Structure of Fuzzy logic controller



In general, the fuzzy controller should be represented as an artificial decision-maker that operates in a real-time closed-loop session or loop. In order to ensure that the performance goals will be achieved, it merges plant output data $y(t)$ and compares it to the reference input $r(t)$. It then calculates how the plant input $u(t)$ should be.

2.2 Design of Fuzzy Controller

Because the rules are frequently nonlinear, there is no design process like root-locus design, frequency response design, pole placement design, or stability margins in fuzzy control.

2.3 Fundamental Components of a Fuzzy Controller

A fuzzy controller may be thought of as a system that communicates data similarly to a conventional controller, with inputs holding details about the plant that needs to be regulated and an output, or the variable being controlled. Both the input current and

output one values are clear from the outside without any hazy information. A fuzzy controller's input values are either control errors produced from the set-point values and controlled variables, or measured values from the plant that are either plant output values or plant states [1].

A static control law is one that is expressed as a fuzzy system. This indicates that a fuzzy controller, like a conventional state-feedback controller, is a static transfer element since the fuzzy rule-based representation of a fuzzy controller lacks any dynamics. In addition, a fuzzy controller is often a fixed nonlinear static transfer element because of the nonlinear features of the computational steps that make up its computational structure. The three blocks in Figure 2.2 in appendix a show the three basic phases that make up a fuzzy controller's computational structure [2].

1. At the input, signal conditioning and filtering (input filter).
2. Fuzzy logic system.
3. At the output, signal conditioning and filtering (output filter).

2.4 The Fundamentals of a Fuzzy System Fuzzification

Figure 2.3 in appendix a depicts a fuzzy system's components. Crisp values from the input signals are converted to fuzzy sets in the fuzzification step. The defuzzification block, which converts an output fuzzy set back to a crisp value, produces the output u directly. The collection of membership functions in charge of the relational portion's rule base and transforming part includes as [2].

Figures 2.4 in appendix a show the fuzzy controller with a fuzzy system that has two inputs (E and ΔE) and one output .

a. Fuzzification

The first component of the fuzzy system is fuzzification, which looks up each piece of input data in one or more membership functions to convert it to degrees of membership.

b. Rule format

Basically, a linguistic controller contains rules in the if-then format, but they can be presented in different formats. In many systems, the rules are presented to the end user in a format similar to the following.

1. If error is NB and change in error is NB then output is NB.
2. If error is NM and change in error is NM then output is NM.
3. If error is NS and change in error is NS then output is NS.
4. If error is ZE and change in error is ZE then output is ZE.
5. If error is PS and change in error is PS then output is PS.
6. If error is PM and change in error is PM then output is PM.
7. If error is PB and change in error is PB then output is PB.
8. If error is PS and change in error is PB then output is PB.
9. If error is PS and change in error is PM then output is PB.
10. If error is PM and change in error is NB then output is NS.
11. If error is PM and change in error is NM then output is ZE.
12. If error is PM and change in error is NS then output is PS.
13. If error is PM and change in error is NS then output is PS.
14. If error is PM and change in error is PB then output is PB.

The simulation was implanted on 49 rules (membership function) upon this, the names positive, negative, zero, small, medium, and big are labels of fuzzy sets. A more compact representation is as follows:

Table 2.1

Error and Change of Error for FLC

Error	Change in error	Output	Change in Error			
				Neg	Zero	Pos
NB	NB	NB				
NM	NM	NM				
NS	NS	NS				
ZE	ZE	ZE				
PS	PS	PS				
PM	PM	PM				
			Change in Error			
			Neg	NB	NM	Zero
			Zero	NM	Zero	PM
			Pos	Zero	PM	PB

c. Defuzzification

The output fuzzy set needs to be transformed into a number that may be used as a control signal for the process. Defuzzification is the process in question. In Figure, the output surface is displayed [2].

The system was developed through simulating $27*27= 729$ rules; however, the system was unfortunately working slowly because of the high memory needed.

Chapter Three

Multi-level inverter

3.1 Introduction

A specific output voltage and frequency are used by the inverter, a form of energy electronic equipment, to convert DC electricity into AC power. Currently, an interesting area of industrial applications is multilevel converters. Conventional power electronic converters can only change the output voltage between two voltage levels. A multilevel inverter creates the necessary output voltage by using a variety of DC voltage levels as input. The input side voltage levels are often provided by fuel cells, capacitor voltage sources, renewable energy sources, and other sources [3].

Due to the low power rating of the medium voltage grid, only one power semiconductor switch may be connected directly. Therefore, a multilayer power inverter may be used in place of a standard converter in situations that call for medium power and high voltage. A multilayer converter achieves large power ratings and produces an output signal that is superior with fewer harmonics and nearly similar to the reference signal.

Multilevel converters' core concept was originally presented in 1975. A converter having three or more levels is referred to as "multilevel". A number of topologies are used in the design of the multilevel converter [4].

To create a high-power converter, however, a series of power semiconductor switches with multiple dc sources should be employed in the design. The power switches' commutation combines this diverse dc to create a big power output. However, the only variable that impacts the rated voltage of the switches is the rating of the connected DC sources of voltage.

The major problem with the multilevel converter is the use of so many power semiconductor switches. Each switch requires a separate driving circuit. As a result, the system will be more expensive and complicated [4].

3.2 Types of Multilevel Converter Structure

The multilayer converter is composed of three or more layers. Since it uses a bi-directional switch or may operate both as an inverter and a rectifier, it is frequently referred to as a converter rather than an inverter. THD will decrease and system work will increase as the levels rise.

The voltage of the DC-link (V_{dc}) can be obtained from any DC source that is able to produce dependable DC power (VSI) when employing a multilayer Voltage Source Inverter. As shown in Figure 3-1 in appendix a, a number of interconnected capacitors serve as a power reservoir to create a variety of dc voltage values for the inverter. According to the formula below, each capacitor has a voltage V_C .

$$V_C = \frac{V_{dc}}{n-1} \quad (3.1)$$

where n is the number of levels.

A schematic representation of various types and degrees of inverters is shown in Figure 3-1 in appendix a (one phase leg). Different locations for the semiconductor switches could be employed to produce various dc values. The level- n inverter creates a resulting voltage with n -voltage values, whereas the two-level inverter makes an output voltage with two values. Figure 3-1 shows a schematic representation of a one phase inverter with two, three, and n levels of dc voltage as (a), (b), and (c), respectively.

These converters have been implemented using one of three primary multilevel converter structures:

- Diode Clamped Converters
- Flying Capacitors Converters
- Cascaded H-Bridge Converters

3.3 Diode-Clamped Multilevel Inverter

The diode clamped multilevel inverter (DCMLI) design is often used to fix the dc voltage in order to acquire multiple values or ways in the resulted voltage.

For instance, a three-level inverter is created utilizing two pairs of diodes and switches using the diode clamped topology. Using diodes and the complementary nature of each pair of switches, the midpoint voltage may be calculated. In this architecture, the three inverter phases use the dc bus, which can be separated into three levels using two capacitors. Clamping diodes Dc1 and Dc2 limit the voltage stress across each switching set to Vdc, as shown in Figure 3-2 in appendix a.

Each capacitor is subject to a voltage of $V_{dc}/2$, where ($V_{c1}=V_{c2}=V_{dc}/2$).

Three different switch states can be used with three-level inverters to provide three different output values, as shown in Figure 3-3. There should always be two switches switched on.

Table 3.1

Three-level diode-clamped inverter condition switching

Switch status	State	Voltage
S1=ON, S2=ON S1'=OFF, S2'=OFF	S=+ve	$V_o=V_{dc}/2$
S1=OFF, S2=ON S1'=ON, S2'=OFF	S=0	$V_o=0$
S1=OFF, S2=OFF S1'=ON, S2'=ON	S=-ve	$V_o=-V_{dc}/2$

Normally, $2(N - 1)$ switching sets for each leg, $(N-1)$ dc-link capacitors, and $(N - 1) * (N - 2)$ clamping diodes are used in the design of a N level diode clamped inverter. Several levels have an impact on the output quality voltage. A significant volume of waveform and a tighter proximity to sinusoidal or reference output are indicated by raising the values. Since there are more switching elements and clamping diodes as N rises, the intended inverter will become more complex.

The advantages of DCMLI are listed below:

- The converter requires less capacitance since all of the phases are connected to the same dc bus.
- The capacitors may be pre-charged collectively.
- low harmonics while using many levels.

The following is a list of DCMLI's disadvantages:

- Because the dc intermediate levels tend to overcharge or even discharge without a careful monitoring or control, a real power flow is challenging for one inverter [5].
- The system is challenging since it takes several clamping diodes to provide high-quality output [6].

3.4 Flying Capacitor Multilevel Inverter

The capacitor fixed inverter, sometimes referred to as the flying capacitor (FCMLI), was put forward by Foch and Meynard in 1992 [6].

These inverters have the same construction as clamped-diode types, except instead of clamping diodes, capacitors are used. Each flying capacitor has a different voltage than the capacitors behind it because they are linked in series. Where the choice of the two adjacent capacitor legs determines the voltage steps of the output waveform. Figure 3-3 below shows the three-level capacitor clamped inverter configuration.

The benefits of (FCMLI) are seen below:

- The capacitors that are connected with the same leg are charged to different voltage values in the capacitor-fixed voltage design, which allows the usage of many levels. The series-connected capacitors in the diode fixed topology have the same voltage.
- The inverter has the ability to regulate both reactive and actual power
- The inverter can handle both deep voltage sags and brief power interruptions.

The FCMLI's shortcomings, however, may be summed up as follows:

- The control and modulation procedures are challenging since any modulation requires charging the capacitors beforehand.
- The control gets quite challenging when several capacitors are being used.

3.5 Multilevel cascade inverter

The cascaded multilevel inverter (CMLI), also known as the series H-bridge inverter, is another type of multilevel inverter. In 1975, the H-bridge inverter was first proposed. Due to its adaptability and versatility, the CMLI has been used in a variety of applications, particularly high-power ones. A group of single-phase full bridges make up each of the inverter's phases. CMLI needs three-phase legs of a series H-bridge converter in order to produce a three-phase output AC waveform. It is straightforward to scale the voltage level while using this design since it relies on series power conversion cells. Using a PV system, rectifying diodes, or other sources of DC, each full-bridge converter receives its own DC supply [7].

As seen in Figure 3-4 in appendix a, the topology of these converters is based on a series of connections between H-bridge converters with distinct DC sources.

The voltages produced by the different cells are added to create the output phase voltage. Each single-phase full-bridge converter's output is converted to three voltage levels by a three-level inverter: $+V_{dc}$, $0V_{dc}$, and $-V_{dc}$ (positive voltage, zero voltage, and negative voltage). where the desired output might be produced by manipulating the power switches. The three levels of the output ac voltage span the $+V_{dc}$ to $-V_{dc}$ range.

The cascaded converter's output voltage can be connected in either a wye (Y) or a delta (Δ) configuration based on the three-phase system.

The profits of CMLI are shown below:

- 1- The DC buses regulation's simplicity
- 2- Modularity is possible for control. Contrary to capacitor clamped and diode clamped inverters, which call for a central controller to perform the modulation for individual
- 3- This kind of inverter uses fewer parts than others for the same output voltage

The disadvantage of DCMLI is that many dc sources need to be used for real power conversions [8].

3.6 Multilevel Inverter Design

For this project, an H-bridge with a 27-level inverter was used because of the following:

- 1- Reducing the distortion in the output waveform will require more (12) levels.
- 2- Compared to traditional inverters It works well in high-power and demanding applications.,.
- 3- Because it comprises of Modula table cells, it is easier to regulate than other types of inverters.
- 4- As the number of levels is raised, the voltage stress on the switches will lessen.
- 5- Because an inverter structure is made up of several single-phase, full-bridge converters that are each fed by a different DC source, there is no requirement for voltage balance (sharing) circuits or voltage matching of the switching devices.
- 6- Soft-switching can be used to control switches.
- 7- For each H-bridge, a separate DC energy source may be used.

The inverter has three H-bridges with also three unequally DC sources distributed, as shown in Figure 3-5 in appendix a and Table 3-2 below

Table 3.2

The multi-level inverter's DC sources

Inverter Bus name	Required input voltage
Vdc1	36 V
Vdc2	108 V
Vdc3	324 V

How the switches are regulated based on the magnitude of the signal referred. The modification method employed is capacity modification, which is a simple and basic process. By comparing the amplitudes of the signal referred to and also the defeneded ranges, this method produces the pulses depicted in the following graph (3.6).

Where (a) is the signal's single value, (is) divided by its maximum value, and (y) is the reference signal's value, also divided by its maximum value.

Following is the crucial definition of capacity modification.

- The highest value of the reference signal input is split by two.
- Multiply one by (one minus the number of levels) divided by two to obtain the range of each step, as shown below. This results in a step range of 0.0769.
- Before creating the right pulses to create the proper level, one must first determine the range to which the value belongs and measure the capacity of the input or reference signal.
- For instance, if the signal's amplitude is 0.01 and it falls inside the first range, the output should be level 1. (0.038 to 0.0769).
- For positive references signal values, the pulses were supplied to the switches in the following order: (P 1, P 2, P 3, P 4, P 5, P 6, P 7, P 8, P 9, P 10, P 11, P 12).
- When a reference of signal level is negative (P 3, P 4, P 1, P 2, P 7, P 8, P 5, P 6, P 11, P 12, P 9,
- P 10).
- This means that only a first dc voltage should be connected and a other two should be unplugged if the output voltage is level one, or 36 volts, and the input reference signal value is 0.060.
- To do this, the controller creates the following pulses for the switches: (110010101010).

The following Figure 3-7 in appendix a shows the multilevel inverter model that was created using MATLAB/SIMULINK, together with a controller and DC sources for one leg. Inverter output behavior with its controller is discussed in Chapter * of this research based on various operational settings.

Chapter Four

Shunt Active Filter

4.1 Introduction

Active power filters (APF) are filters that are capable of eliminating harmonics. Harmonics in the power system that are much below the filter's switching frequency can be removed using active power filters. Higher order harmonics as well as lower order harmonics are filtered out of the power system using active power filters

Power filters are available in a wide range of configurations, including series, parallel, and hybrid filters (a filter that combines passive and active filters to maximize filter performance). In order to reduce and correct for load voltage harmonics, series active filters are placed in series between the source and the loads. Current harmonics of non-linear loads are also compensated using shunt active filters [9].

The parallel active filter is used to filter harmonics from the current source. Due to the component in a series filter should be able to pass a complete current through, which necessitates greater value for the elements employed, compared to other types, like series active filters, it has lower component values. [10].

Voltage source active power filters (VSAPFs) and current source active power filters are the two primary divisions of shunt active power filters (SAPFs) (CSAPFs). The storage element that is employed with these filters—capacitors with VSAPFs and inductors with CSAPFs—determines the kind of filter.

In this study, the VSAPF was chosen over the CSAPF because it is less costly, lighter, more efficient, and simpler to manage [11].

There are two techniques to deal with harmonic pollution. The first strategy is to employ appropriate circuits that may decrease or eliminate pollution.

Transformer-less systems UPS with PWM rectifiers, which cause the current's harmonics to be low, are one example of these uses. As a result, a little degree of distortion may persist, and filtering equipment is not required in this scenario. The

second way is to use power filtering equipment, which employs strategies to reduce total harmonic distortion (THD) in current systems.

There are three types of techniques to choose from:

- Passive Filters
- Active Filters
- Hybrid filters.

The traditional filter is the passive filtering method shown in Figure 4.1 in appendix a.

The passive filter principle is to block harmonics by connecting a high series impedance in series (a series passive filter) or to compensate harmonics by connecting a low impedance as a parallel current to the load (a shunt passive filter). Depending on the nonlinear load, a combination of series and shunt may be used in various situations [12].

Because passive filters are really cheap, simple and highly efficient (for particular frequency), they are already selected by filter designers.

Although they have numerous profits, they are dependent on system factors. When employing passive filters, a problem of rebound with the system hindering will occur, and it can be helpful to filter a harmonic frequency certain. As a result, active filters are employed [13-14].

A concept of active filters was studied in the 1970s. However, the concept became financially and scientifically feasible after quick, inexpensive semiconductor devices like MOSFETs (IGBTs) and high-performance, efficient Digital Signal Processors (DSPs) were made accessible. The active filter's basic principle is to introduce voltage/current with the same magnitude and opposite of the harmonics, causing harmonics to be rejected from the system, and advancements in power electronics control theory allow the active filter to be more practical, commercially successful, and efficient in filtering harmonics as show in figure 4.2 in appendix a [15].

Active filters, unlike passive filters, have a modest physical size and may perform a variety of jobs in the power system, including compensating reactive power, inserting active power, and tolerating faults and working correctly under bad conditions. They are effective solutions for a variety of power quality issues. Although active filters are more effective at filtering than passive filters, they are more expensive [16].

Active filters have the following drawbacks: - The passive filter (used in hybrid) removes high power and low order harmonics, whereas the active filter removes high order and low power harmonics requires high converter ratings.

- Is more expensive when compared to passive filter.

As a result, a new form of filter known as a hybrid power filter was developed to eliminate the issues associated with passive and active filters. The first type of filter in a hybrid filter is an active filter, while the second type is a passive filter. Hybrid filters are utilized to lower the system's start-up expenses while boosting its effectiveness.

While the active filter eliminates high order and low power harmonics, the passive filter (used in hybrid) only eliminates high power and low order harmonics.

The goal of hybrid filtering is to increase the filtering efficiency of a passive filter while attenuating series and parallel resonances with a small rated active filter. On the other side, hybrid filters require more technical work than passive filter design because they perform fewer tasks than pure active filters in figure 4.3 in appendix a show the hybrid technique [17].

4.2 Techniques for Extracting Harmonic Currents

The reference extraction technique used determines how effective the APF is. The reference signal may be extracted using a variety of methods. Time domain and frequency domain are the two primary approaches. In order to generate a reference signal from distorted load voltage or current, an immediate estimate is generated in the time domain. Results will be quicker since the time domain approach is easier to use and requires less calculations than the frequency domain method [18].

4.3 Theorem of Instantaneous (Active & Reactive) Power

All p-q theories, also referred to as the "instantaneous power theory," describes the significance of the real and imaginary power that exists in a three-phase circuit at any given moment in time. Additionally, it clarifies the path taken by energy in a three-phase circuit as it moves from a source to a load or between phases. Using this method, flexible AC transmission system (FACTS) compensators may be developed and comprehended [19].

The p-q theory's time domain foundation enables real-time control of the APFs for both steady-state and transient operation, as well as for a variety of voltage and current waveforms.

The instantaneous values of the voltage and current waveforms in a three-phase power system are used to calculate power using the instantaneous power technique (p-q theory).

In order to use this theory, three-phase current and voltage from a-b-c must first be converted to the instantaneous power is calculated using α - β coordinates, which is equivalent to the Clarke transformation, an algebraic transformation. It uses the Clarke transformation, which consists of a matrix connecting three-phase components to stationary reference frames with a 0 in the middle. As illustrated in Figure 4-4 in appendix a below, the reference current is then calculated using the real and reactive power of the non-linear load.

In order to regulate active filters in three-phase power systems, Akagi et al. presented the "Generalized

Theory of the Instantaneous Reactive Power in Three-Phase Circuits" [20].

The following can be used to represent the three-phase systems without a zero-sequence:

$$X_a + X_b + X_c = 0 \quad (4.1)$$

Equation (4.1) above suggests that there are only two variables because of the 3rd variable's link (a function) to the other two variables.

The following voltage and current matrices might be produced to switch from the a-b-c to the

α - β -0 system.

$$\begin{bmatrix} V_o \\ V_\alpha \\ V_\beta \end{bmatrix} = \sqrt{\frac{2}{3}} \times \begin{bmatrix} \frac{1}{\sqrt{2}} & \frac{1}{\sqrt{2}} & \frac{1}{\sqrt{2}} \\ 1 & -0.5 & -0.5 \\ 0 & \frac{\sqrt{3}}{2} & -\frac{\sqrt{3}}{2} \end{bmatrix} \times \begin{bmatrix} V_a \\ V_b \\ V_c \end{bmatrix} \quad (4.2)$$

$$\begin{bmatrix} I_o \\ I_\alpha \\ I_\beta \end{bmatrix} = \sqrt{\frac{2}{3}} \times \begin{bmatrix} \frac{1}{\sqrt{2}} & \frac{1}{\sqrt{2}} & \frac{1}{\sqrt{2}} \\ 1 & -0.5 & -0.5 \\ 0 & \frac{\sqrt{3}}{2} & -\frac{\sqrt{3}}{2} \end{bmatrix} \times \begin{bmatrix} I_a \\ I_b \\ I_c \end{bmatrix} \quad (4.3)$$

From the equations above, the following new connection may be derived:

$$I_N = I_a + I_b + I_c = \sqrt{3} I_o \quad (4.4)$$

The power may then be described as follows:

$$\begin{bmatrix} p_o \\ p_{\alpha\beta} \\ q_{\alpha\beta} \end{bmatrix} = \begin{bmatrix} V_o & 0 & 0 \\ 0 & V_\alpha & V_\beta \\ 0 & -V_\beta & V_\alpha \end{bmatrix} \begin{bmatrix} I_o \\ I_\alpha \\ I_\beta \end{bmatrix} \quad (4.5)$$

Where:

The phase voltages and currents are v_a , v_b , v_c and i_a , i_b , i_c , respectively.

p_o : A zero-sequence's immediate power.

$p_{\alpha\beta}$: the instantaneous real power.

$q_{\alpha\beta}$: the instantaneous imaginary power

By replacing the currents in the previous expression with power and voltages, the current matrix may be re-expressed as follows:

$$\begin{bmatrix} I_o \\ I_\alpha \\ I_\beta \end{bmatrix} = \frac{1}{V_o \times V_{\alpha\beta^2}} \times \begin{bmatrix} V_{\alpha\beta} & 0 & 0 \\ 0 & V_o \times V_\alpha & -V_o \times V_\beta \\ 0 & V_o \times V_\beta & V_o \times V_\alpha \end{bmatrix} \times \begin{bmatrix} p_o \\ p_{\alpha\beta} \\ q_{\alpha\beta} \end{bmatrix} \quad (4.6)$$

Where:

$$V_{\alpha\beta^2} = V_\alpha^2 + V_\beta^2 \quad (4.7)$$

In the p-q theory, the following are the six different types of power:

- $\overline{p0}$: instantaneous power that travels through voltage and current from the source to the load (Zero-sequence components).
- $\widetilde{p0}$: A Instantaneous zero-sequence power at a different value. It describes the amount of energy that is transported over time via the voltage and current zero-sequence components from the power source to the load.
- \overline{p} : The average value of the instantaneous real power. It has to do with how much energy is equally transported over time from the power source to the load using the a-b-c coordinates. (In actuality, it is the preferred power element.)
- \widetilde{p} : The alternative value of instantaneous real power. The a-b-c coordinates are used to convey energy per unit of time from the power source to the load.
- \overline{q} : Average value of instantaneous imaginary power. It is a component of the reactive energy that the basic components of current and voltage create.
- \widetilde{q} : One of the harmonic currents produced by the instantaneous reactive power of ac is the alternating value of instantaneous imaginary power [20].

In figure 4.5 **in appendix a** shows the active power filter that must compensate for the other components of the power as \overline{p} which is the only usable and desirable component. The zero- voltage and zero- current components will both have 0 values if the neutral wire is not attached. Thus, the following may be deduced from the aforementioned voltage and current transform matrices:

$$\begin{bmatrix} V_\alpha \\ V_\beta \end{bmatrix} = \sqrt{\frac{2}{3}} \times \begin{bmatrix} 1 & -0.5 & -0.5 \\ 0 & \frac{\sqrt{3}}{2} & -\frac{\sqrt{3}}{2} \end{bmatrix} \times \begin{bmatrix} V_a \\ V_b \\ V_c \end{bmatrix} \quad (4.8)$$

$$\begin{bmatrix} Il\alpha \\ Il\beta \end{bmatrix} = \sqrt{\frac{2}{3}} \times \begin{bmatrix} 1 & -0.5 & -0.5 \\ 0 & \frac{\sqrt{3}}{2} & -\frac{\sqrt{3}}{2} \end{bmatrix} \times \begin{bmatrix} Ia \\ Ib \\ Ic \end{bmatrix} \quad (4.9)$$

These equations display the load's instantaneous power. (pl and ql)

$$\begin{bmatrix} pl \\ ql \end{bmatrix} = \begin{bmatrix} V\alpha & V\beta \\ V\beta & -V\alpha \end{bmatrix} \begin{bmatrix} Il\alpha \\ Il\beta \end{bmatrix} \quad (4.10)$$

The following results from breaking down the above equation

$$pl = \tilde{p}l + Pl \quad (4.11)$$

$$ql = \tilde{q}l + Ql \quad (4.12)$$

While the $\tilde{q}l$ and $\tilde{p}l$ are oscillatory terms, the Ql and Pl are average terms.

The aforementioned equations show a number of things, including the following:

- The mean power under sinusoidal and balanced conditions represents the basic harmonic current.
- Every higher harmonic's related oscillation term [21].

According to the design, the average power terms might be eliminated by using a high pass filter (HPF) or low pass filter (LPF), as shown in Figures 4-6 in appendix a below.

The remaining terms then need to be compensated as follows:

$$pc = -pl \sim \text{ \& } qc = ql \sim \quad (4.13)$$

Compensating the current as follow:

$$\begin{bmatrix} Ic\alpha \\ Ic\beta \end{bmatrix} = \frac{1}{V\alpha \times V\beta^2} \times \begin{bmatrix} V\alpha & V\beta \\ V\beta & -V\alpha \end{bmatrix} \begin{bmatrix} pc \\ qc \end{bmatrix} \quad (4.14)$$

Where:

$$V\alpha\beta^2 = V\alpha^2 + V\beta^2 \quad (4.7)$$

As seen below, the reference current that the inverter must generate shifts from the α - β coordinate to the a-b-c coordinate:

$$\begin{bmatrix} Ica^* \\ Icb^* \\ Icc^* \end{bmatrix} = \sqrt{\frac{2}{3}} \times \begin{bmatrix} 1 & 0 \\ -0.5 & \frac{\sqrt{3}}{2} \\ -0.5 & -\frac{\sqrt{3}}{2} \end{bmatrix} \times \begin{bmatrix} Ica \\ Icb \end{bmatrix} \quad (4.15)$$

If the reference signal needs to be corrected solely, reactive power needs to be given directly to it.

Figures 4-6 in appendix a in the accompanying image simply eliminate harmonics. Reactive power must have two components, ($\tilde{q}l$)&(Ql) in order to improve its power factor. The control method is shown in the Figure 4-7 in appendix a.

4.4 Instantaneous Current Component Theory

This approach generates reference currents using the id-iq theory, or the instantaneous active and reactive current components of the nonlinear load. In synchronous reference frames, the three phase current components a, b, and c are rotated by an angle depending on the park transformation, much to how they are converted into α - β -0 components in stationary frames. A control method is also described for constructing the PI controller, which is essential for generating the error signal required for switching, as well as for regulating the DC voltage across the DC bus capacitor.

Under distorted voltage situations, it is shown that this approach outperforms the instantaneous active and reactive power method [22].

This method obtains the reference signal by using the nonlinear load's instantaneous active and reactive current components. Separating harmonic and fundamental contents will be made easier by obtaining (d-q) current components. This method works better when there is imbalance or less-than-ideal voltages. For this approach, the source just has to provide the d-axis component. The transform is defined by the subsequent equations:

$$\begin{bmatrix} Id \\ Iq \\ Io \end{bmatrix} = \sqrt{\frac{3}{2}} \times \begin{bmatrix} \cos\theta & \cos(\theta - \frac{2\pi}{3}) & \cos(\theta + \frac{2\pi}{3}) \\ -\sin\theta & -\sin(\theta - \frac{2\pi}{3}) & -\sin(\theta + \frac{2\pi}{3}) \\ \frac{1}{\sqrt{2}} & \frac{1}{\sqrt{2}} & \frac{1}{\sqrt{2}} \end{bmatrix} \times \begin{bmatrix} Ia \\ Ib \\ Ic \end{bmatrix} \quad (4.16)$$

when the synchronous reference's angular position is indicated by θ .

The basic frequency's linear function is denoted by. This angle is rotating synchronously and continuously with the three-phase voltage. A low pass filter is used to isolate the harmonic current component.

$$Idl = \widetilde{il\bar{d}} + \overline{il\bar{d}} \quad (4.17)$$

$$Iql = \widetilde{il\bar{q}} + \overline{il\bar{q}} \quad (4.18)$$

The oscillatory terms are the $\widetilde{il\bar{d}}$ and $\widetilde{il\bar{q}}$ whereas the average terms are the $\overline{il\bar{d}}$ and $\overline{il\bar{q}}$. The equations above show several things, including what follows:

- Under sinusoidal and balanced conditions, the average current is related to the fundamental harmonic current.
- The oscillation parameters connected to each higher harmonic.

Iql will be used to account for reactive power and improve power factor during the creation of the reference signal, and an alternate component termed Idl ($\widetilde{il\bar{d}}$) will be included to remove the harmonics.

The reference signal for the active power filter (APF) changes to:

$$\begin{bmatrix} Ifd^* \\ Ifq^* \end{bmatrix} = \begin{bmatrix} \widetilde{il\bar{d}} \\ il\bar{q} \end{bmatrix} \quad (4.19)$$

Using the inverse park transform, the following results are obtained for the 3-phase system's reference signal for the APF currents:

$$\begin{bmatrix} Ifa \\ Ifb \\ Ifc \end{bmatrix} = \frac{\sqrt{3}}{2} \times \begin{bmatrix} \cos\theta & -\sin\theta \\ \cos(\theta - \frac{2\pi}{3}) & -\sin(\theta - \frac{2\pi}{3}) \\ \cos(\theta + \frac{2\pi}{3}) & \sin(\theta + \frac{2\pi}{3}) \end{bmatrix} \times \begin{bmatrix} Ifd^* \\ Ifq^* \end{bmatrix} \quad (4.20)$$

A phase locked loop (PLL), displayed in the image that follows 4.8 in appendix a, can be used to estimate the angular location of the synchronous reference.

4.5 Controller for Shunt Active Power Filters (SHAPF)

Enhancing the shunt active power filter control techniques, such as reducing the THD value, increasing the system's power factor, or improving the SAPF's performance when the non-linear loads vary, is essential for improved results. One of two methods that depend on the measured current can be used to regulate the SAPF in order to account for harmonic currents:

- Direct Control Approach
- Indirect Control Approach.

4.6 Direct Control Approach

The reference signal that will be utilized to account for harmonics that are created from the load currents and the reference signal are both necessary components of this approach. The SAPF will generate currents in this case that are exclusively reliant on the load current and not the source current.

The voltage and current equations for a filter may be obtained using all information in Figures 4-9 in appendix a as follows:

$$Vf(s) = Vs(s) + \{SLf \times If(s)\} + \{Rf \times If(s)\} \quad (5.21)$$

$$If(S) = \frac{Vf(s)-Vs(s)}{SLf+Rf} \quad (5.22)$$

The system's current close loop controller is displayed in Figure 4-10 in appendix a as a result of the aforementioned calculations.

4.7 Indirect Control Approach

This technique does not monitor or worry about filter currents; instead, it is focused on source currents. The grid receives a sine-wave reference current that is used to compare the measured current to the reference current. The error is then supplied to the current controller, which generates pulses for the SHAPF. In comparison to the direct approach, this system's control is simpler and makes use of fewer sensors. Figure 4-11 in appendix a diagram for the indirect strategy.

The method used to construct the filter reference currents and the grid reference currents is the same. Grid current detection may be done in many different ways. Some of these methods rely on the DC voltage controller, the instantaneous current components (id-iq), and the instantaneous power (p-q) theories [23][21].

4.7.1 Algorithm Based on PQ Theory

This strategy relies on the immediate active power. The indirect technique eliminates the alternative component and reserves the direct term (DC term) for the generation of grid currents. This method permits simultaneous correction of the harmonic current and the reactive power because it is necessary to decrease both [24].

The indirect control technique based on the p-q theory diagram is shown in the figure 4.12 in appendix a.

The following equations could be obtained by assuming that the voltages at point PCC are V_{sa} , V_{sb} , and V_{sc} and the load currents are I_{La} , I_{Lb} , and I_{Lc} .

$$\begin{bmatrix} V_{s\alpha} \\ V_{s\beta} \end{bmatrix} = \sqrt{\frac{3}{2}} \times \begin{bmatrix} 1 & -0.5 & -0.5 \\ 0 & \frac{\sqrt{3}}{2} & -\frac{\sqrt{3}}{2} \end{bmatrix} \times \begin{bmatrix} V_{sa} \\ V_{sb} \\ V_{sc} \end{bmatrix} \quad (4.28)$$

$$\begin{bmatrix} I_{L\alpha} \\ I_{L\beta} \end{bmatrix} = \sqrt{\frac{3}{2}} \times \begin{bmatrix} 1 & -0.5 & -0.5 \\ 0 & \frac{\sqrt{3}}{2} & -\frac{\sqrt{3}}{2} \end{bmatrix} \times \begin{bmatrix} I_{La} \\ I_{Lb} \\ I_{Lc} \end{bmatrix} \quad (4.29)$$

The direct active power can be expressed as follows:

$$Pl = (V_{s\alpha} \times I_{L\alpha}) + (V_{s\beta} \times I_{L\beta}) \quad (4.30)$$

As previously mentioned, there are two components that make up active power: direct power, which has to do with basic voltage and current, and alternative power, which has to do with harmonics.

$$Pl = \bar{p}l + \tilde{p}l \quad (4.31)$$

The reference power may appear something like this if we examine it from the source side.

$$P_S^* = \bar{p}l + Pdc^* \quad (4.32)$$

By utilizing a low pass filter, we can isolate the direct active power.

As a result, the grid reference current changed to:

$$I_{S\alpha}^* = \frac{Vs\alpha}{Vs\alpha^2 + Vs\beta^2} \times P_S^* \quad (4.33)$$

$$I_{S\beta}^* = \frac{Vs\beta}{Vs\alpha^2 + Vs\beta^2} \times P_S^* \quad (4.34)$$

The reference currents shift to the configuration shown below:

$$\begin{bmatrix} I_{S\alpha}^* \\ I_{S\beta}^* \\ I_{Sc}^* \end{bmatrix} = \sqrt{\frac{3}{2}} \times \begin{bmatrix} 1 & 0 \\ -0.5 & \frac{\sqrt{3}}{2} \\ -0.5 & -\frac{\sqrt{3}}{2} \end{bmatrix} \times \begin{bmatrix} I_{S\alpha}^* \\ I_{S\beta}^* \end{bmatrix} \quad (4.35)$$

4.7.2 Synchronous Reference-based indirect control

The calculation of synchronous reference currents is the only distinction between this approach and the p-q theory. Additionally, it uses the load currents and PLL to calculate an angular location for the voltage. The following is the procedure for determining the direct load current components (I_{ld}):

$$I_{ld} = \sqrt{\frac{2}{3}} \times \left\{ (I_{la} \times \cos(\omega t)) + \left(I_{lb} \times \cos\left(\omega t - \frac{2\pi}{3}\right) \right) + \left(I_{lc} \times \cos\left(\omega t + \frac{2\pi}{3}\right) \right) \right\} \quad (5.36)$$

This current has two components: direct and alternating components, according to the equation below.

$$I_{ld} = \bar{I}l\bar{d} + \widetilde{I}l\widetilde{d} \quad (5.37)$$

A suitable low pass filter with a high enough cut-off frequency (almost 20 Hz) can be used to separate the direct current component, and this current is connected to the grid's

fundamentals. Since this method has the ability to set I_q to zero, it can simultaneously correct for harmonics and reactive power.

The following equation describes how to express the reference signal:

$$\begin{bmatrix} I_{sa}^* \\ I_{sb}^* \\ I_{sc}^* \end{bmatrix} = \begin{bmatrix} \cos\theta & -\sin\theta \\ \cos(\theta - \frac{2\pi}{3}) & -\sin(\theta - \frac{2\pi}{3}) \\ \cos(\theta + \frac{2\pi}{3}) & \sin(\theta + \frac{2\pi}{3}) \end{bmatrix} \times \begin{bmatrix} I_{sd}^* \\ I_{sq}^* \end{bmatrix} \quad (5.38)$$

The schematic of the Indirect Control Technique Based on Synchronous Reference is shown in Figure 4-13 in appendix a below (Id-Iq).

4.7.3 DC voltage controller-based indirect control

The main concept behind this approach is to compute the peak value of the grid's reference current using a DC regulator. Multiplying the peak grid current value by the PCC voltage unit vectors will do this.

The reference current is expressed in the following equations:

$$I_{sa}^* = I_{speak}^* \times \sin\theta \quad (5.39)$$

$$I_{sb}^* = I_{speak}^* \times \sin(\theta - \frac{2\pi}{3}) \quad (5.40)$$

$$I_{sc}^* = I_{speak}^* \times \sin(\theta + \frac{2\pi}{3}) \quad (5.41)$$

You may create an angular position with the PLL. The schematic of an indirect control technique-based DC voltage controller is shown in Figure 4-14 in appendix a below.

4.8 Shunt Active Power Filter controller design

The Approach to Indirect Control This simulation was developed using the Synchronous Reference (Id-Iq) theory, which is discussed in section 4.3.3.2. The reference signal must be generated in the interim by integrating the PI controller with the APF controller. The chosen strategy focuses on direct technique control, requiring the identification of the load current and its harmonics. The input for the PI Controller (I_{invd}) is the difference between the alternating component of the load current (I_{ld}) and

the d-component of the inverter current, and the input for the second PI Controller is the difference between the q-axes currents of the inverter (I_{invq}) and the load (I_{Lq}).

Think about the voltages at the sources (V_a , V_b , and V_c) and the voltages at the inverter's output (V_{a1} , V_{b1} , and V_{c1}) as shown in Figure 4-15 in appendix a.

The resistor (R) and inductor (L) have been connected for each phase between the inverter output and the PCC.

The following equations express source voltages

$$V_a = (R \times i_1) + \left(L \frac{di_1}{dt}\right) + V_{a1} \quad (4.42)$$

$$V_b = (R \times i_2) + \left(L \frac{di_2}{dt}\right) + V_{b1} \quad (4.43)$$

$$V_c = (R \times i_3) + \left(L \frac{di_3}{dt}\right) + V_{c1} \quad (4.44)$$

The equations above are transformed into the following by applying the d-q variables:

$$L \frac{di_d}{dt} = (-I_d \times R) + (V_{ad} - V_{a1d}) - (\omega L \times I_q) = V_d - (I_d \times R) \quad (4.45)$$

$$L \frac{di_q}{dt} = (-I_q \times R) + (V_{aq} - V_{a1q}) - (\omega L \times I_d) = V_q - (I_q \times R) \quad (4.46)$$

Where:

$$V_d = (V_{ad} - V_{a1d}) - (\omega L \times I_q) \quad (4.47)$$

$$V_q = (V_{aq} - V_{a1q}) - (\omega L \times I_d) \quad (4.48)$$

Using our previous equations, we can create an illustration of a PI controller, as shown in figure 4-16 in appendix a.

The PI controller's transfer feature is:

$$G_{pi}(s) = K_p + \frac{K_{ii}}{s} \quad (4.49)$$

Using the following assumptions and comparing the controller's transfer function to a second-order transfer function's canonic form:

- Damping factor value is 0.707
- band width is 200 Hz.

K_p and K_{ii} 's values are as follows: $K_1 = 1000$ and $K_2 = 10,000$, respectively [18].

Figure 4-17 in appendix a displays the overall control approach for SHAPF, which was evaluated using MATLAB software.

Chapter Five

Compensation Scenarios and System Outcome

Several renewable energy sources have been used in conjunction with their controllers and a multi-level inverter with an active filter to accomplish the goals of this research.

Two separate operating conditions were used to evaluate the system: the first merely featured a non-linear load and a DC load, while the second examined how the system affected the IEEE Network. The controllers are made to function in accordance with the following scenarios under each of these operational conditions:

1. 0-0.08s: The active filter is connected but without making any compensation through controlling the reference currents of the inverter to zero.
2. 0.08-0.16s: The active filter is controlled to compensate the harmonics only.
3. 0.16-0.24s: The active filter is controlled to compensate the harmonics in addition to injecting reactive power.
4. 0.24-0.30s: The active filter is controlled to compensate the harmonics, inject reactive power, and injecting real power.

5.1 Effects of various System Compensation scenarios on individual non-linear loads

The first requirement for operation is connecting to a separate load. There are two different kinds of loads; one of which is a resistance and inductor load (RL), which is a load with specifications of 6.0 kWp of active power and 2 KVar of reactive power. The additional load is 3-phase a rectifier attached to a load that is resistive with an 8.0 kWp consumption. The controlled voltage sources are supplied by the reference signal of the proposed controller.

The entire system is depicted in Figure 5.1 below after being connected to a load and having a simulation run in MATLAB/SIMULINK.

Figure 5.1

Schematic for a system simulation with non-linear load in combination

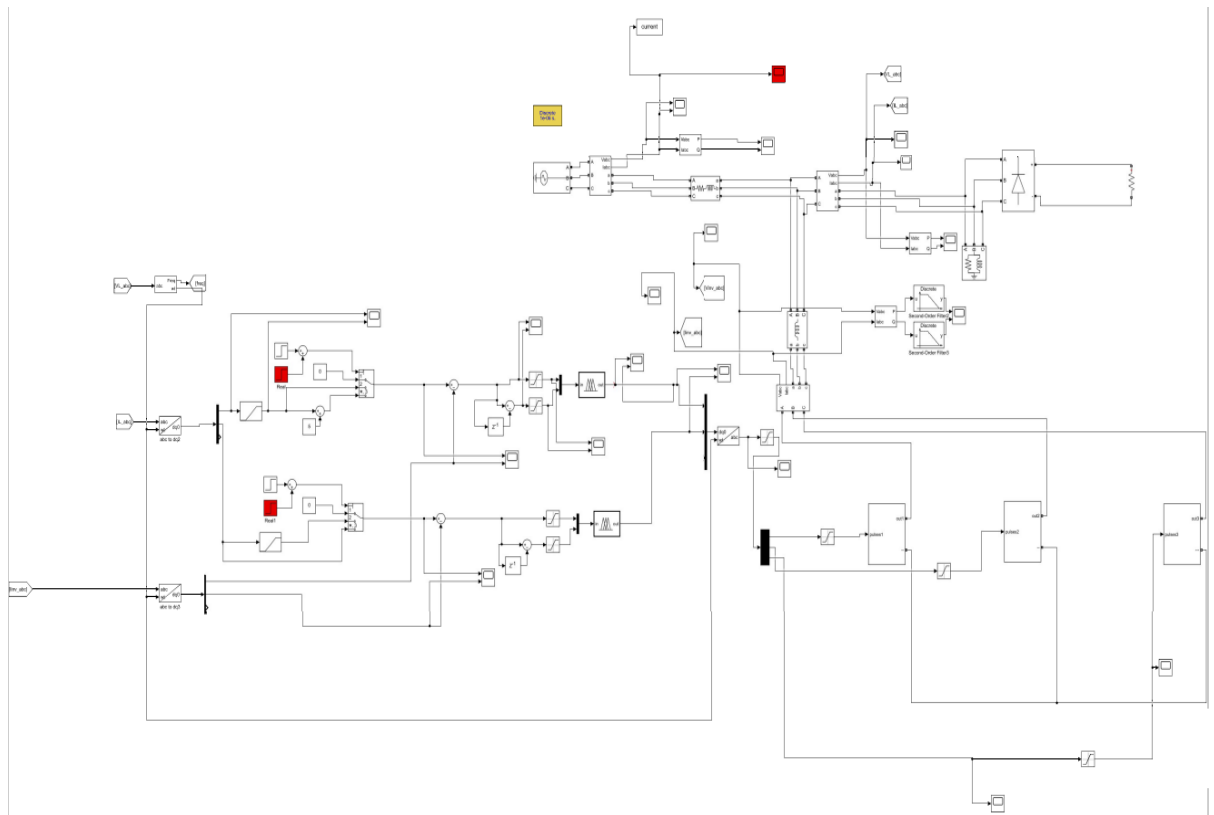


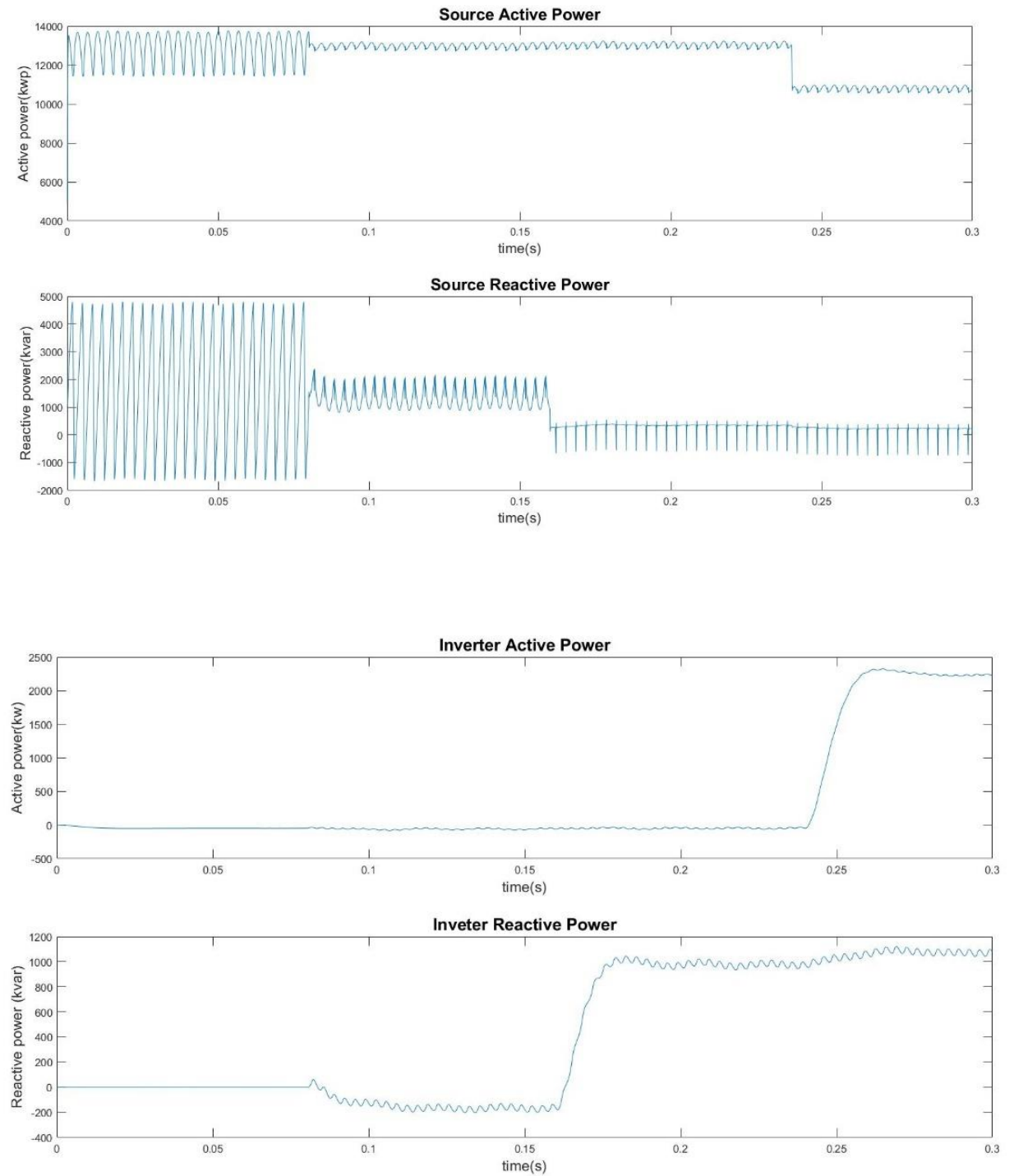
Figure 5-2 demonstrates that the source reactive power harmonics have been reduced while being balanced for the load by the inverter when it begins to operate after ($t \geq 0.08s$). Whereas the source reactive power is roughly zero during reactive power injection operation scenarios ($t \geq 0.16s$), the inverter's output reactive power increases in response to the load's need for reactive power. Reactive power at the load is constant during all processes.

last operation scenario ($t \geq 0.24s$), but this amount is also added to the harmonic reduction in the prior scenario by the inverter because the load active power is constant throughout all operations. Figure 5-2-1 appendix a illustrates the source and inverter active and reactive power under operation scenarios.

Figures 5-2 below illustrates the source and inverter active and reactive power characteristics under the abovementioned operation scenarios, respectively.

Figure 5.2

Schematic of System active power and reactive power behavior under different operation scenarios



The following four possibilities are illustrated as before and after operation scenarios in the Figures 5-3 below by the curves of the current behavior for the source and the inverter:

- 0-0.08: I_{inv} is 0, and IS is not impacted.
- 0.08-0.16: I_{inv} has harmonics rather than the source since the IS's harmonics are removed.
- 0.16-0.24: Due to the injection of reactive power and the harmonic elimination procedure in the preceding paragraph, I_{inv} is larger and IS is slightly smaller.
- 0.24-0.3: In addition to the previously mentioned effect, the high-power injection also causes a reduction in IS and an increase in I_{inv} magnitude.
 - The figure 5-3-1 appendix a shows the result of FFT analysis as a fundamental value (50Hz) and total harmonic distortion (THD) for the source and inverter during each operation scenarios
 - The table below displays results of the FFT analysis for the source and inverter for each of the aforementioned operation situations as a fundamental value (50Hz) and total harmonic distortion (THD).

Table 5.1

Total harmonics distortion of Source and inverter currents

Scenario#	Inverter output current		Source output current	
	Fundamental (50Hz)	THD%	Fundamental (50HZ)	THD%
0-0.08	0.1099	8.10%	26.53	16.72%
0.08-0.16	0.1036	4778.2%	26.62	2.93%
0.16-0.24	2.505	201.38%	26.62	1.42%
0.24-0.3	5.488	92.99%	22.03	1.77%

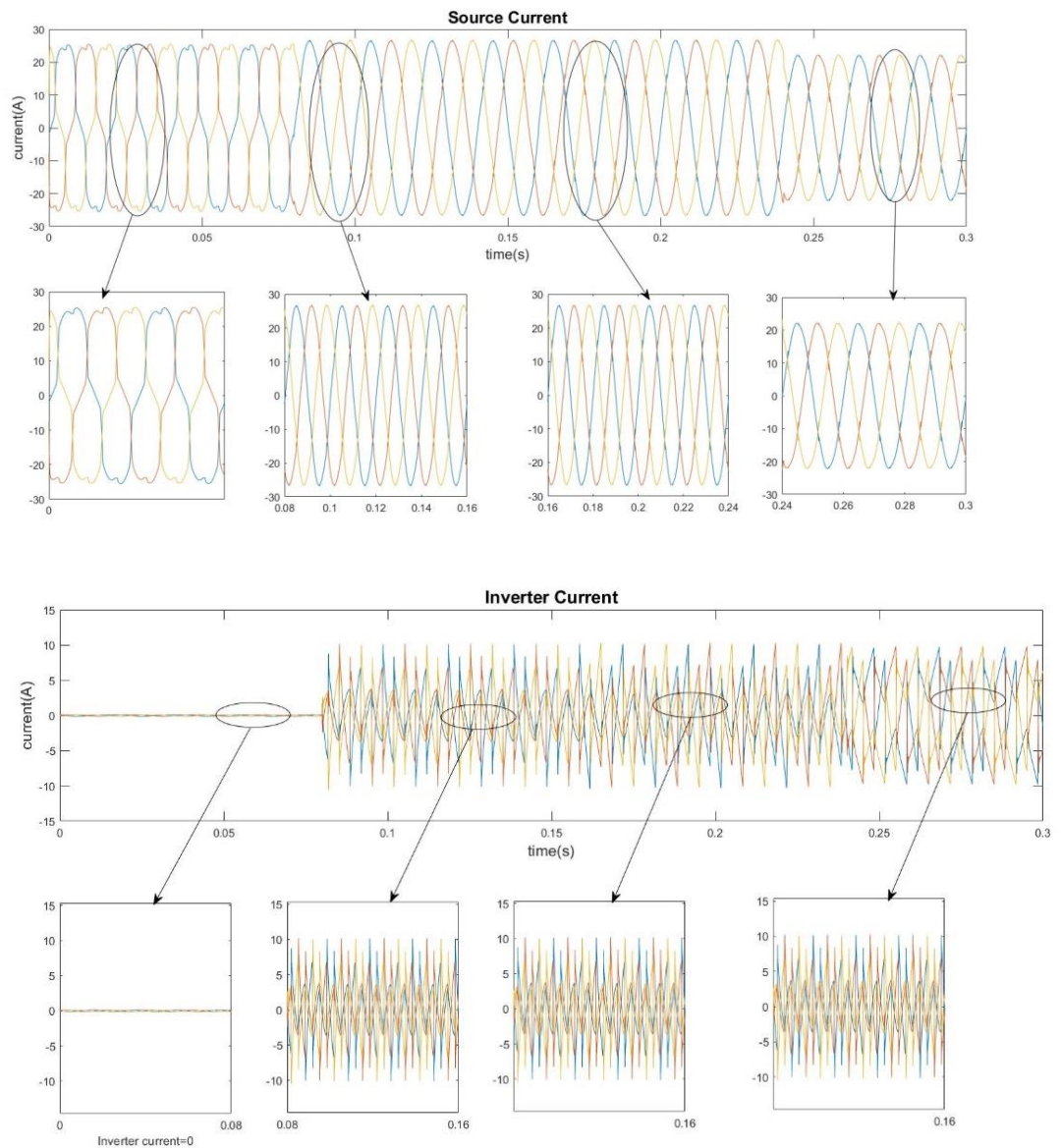
By applying formula 1.3 and according to the load applied where the real power consumed by this load was 6 kW and the reactive power was 2 kVAR, the displacement power factor for this load is 0.95. For this load and after applying our proposed

approach to decrease the THD where the best value obtained for this THD was 1.77 %, and by using the formula 1.4, the distortion power factor calculated according to this THD value is 0.9997 (approximately 1). So, the true power factor for this best case and according to formula 1.5 is 0.948. Surely, the true power factor takes lower values for other cases where the THD shows higher values.

In comparison with the results of [26] for the THD value obtained for their proposed approach where the best value of the THD was 1.9%, the results obtained by executing our proposed approach show lower value for the THD which is 1.77 %.

Figure 5.3

Schematic of source and inverter current and THD during four scenarios



5.2 Comparison between PI and Fuzzy logic controller

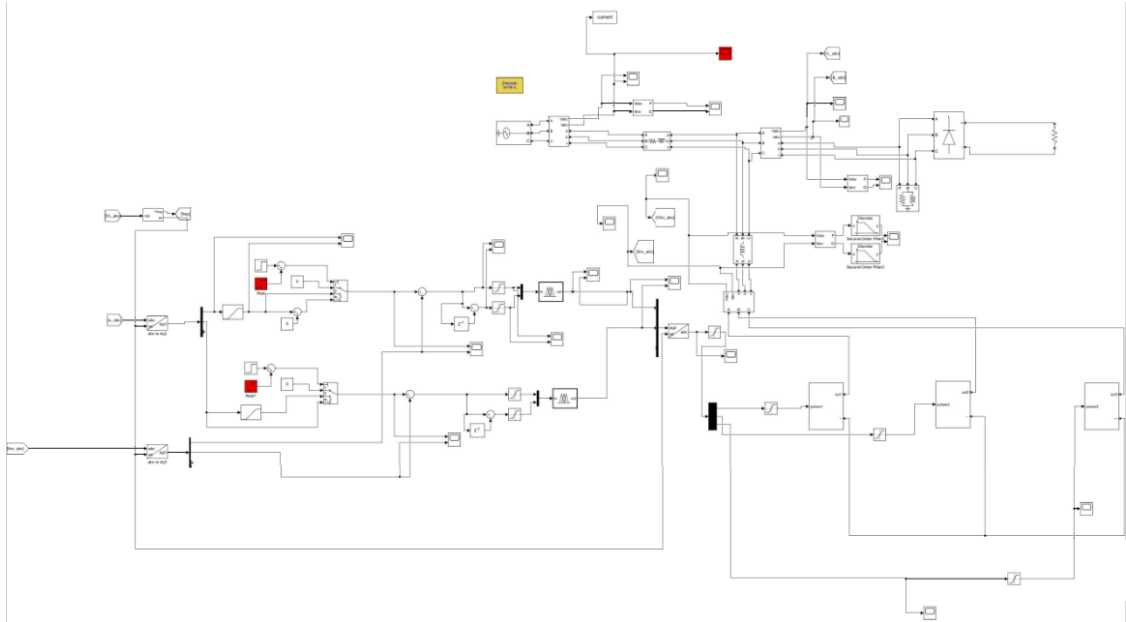
The primary goal of this project is to apply a fuzzy logic controller to optimize the performance of the Shunt Active Power Filter in order to lower harmonic distortion. To decrease the harmonic current and raise the power factor to unity, the Fuzzy Logic Controller for the three-phase Shunt Active Power Filter is intended to take the place of the Proportional Integral controller.

We simulated in MATLAB/SIMULINK and compared the system by using PI and fuzzy system, and the results were as follows:

Figure 5.4

Schematic for a- fuzzy logic system / b-PI simulation with non-linear load in combination

a- Fuzzy



b- PI

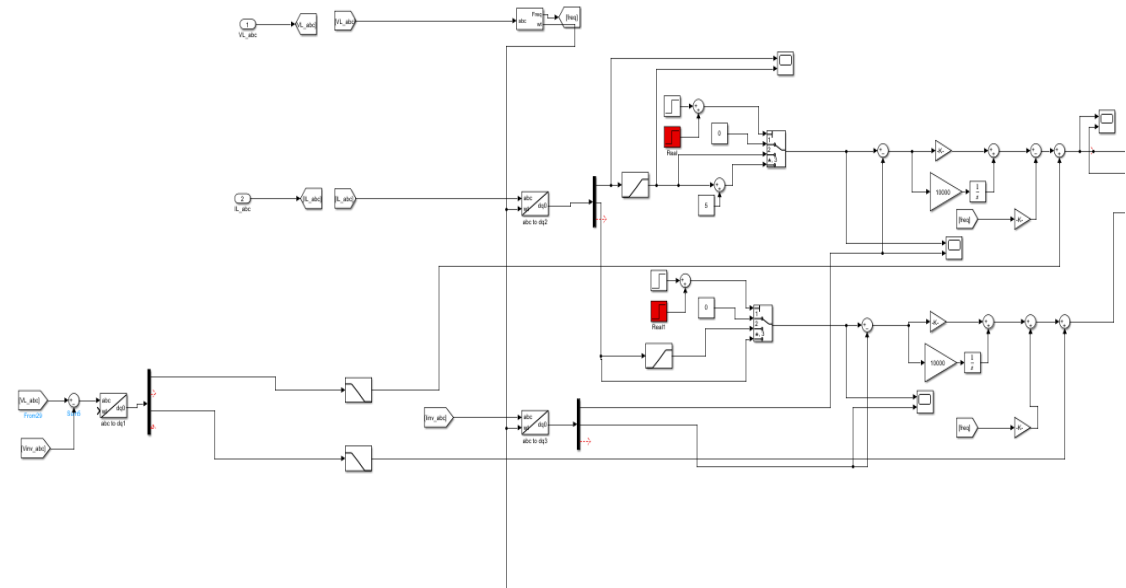


Figure 5-5 (a) appendix a Id ref and measured for Pi controller and Iq ref and measured for Pi controller during all scenarios.

Figure 5-5 (b) appendix a Id ref and measured for Fuzzy Logic controller and Iq ref and measured for Fuzzy logic controller during all scenarios.

In the figure it can be notice that the controllers could track the inputs with minim steady state and transient errors.

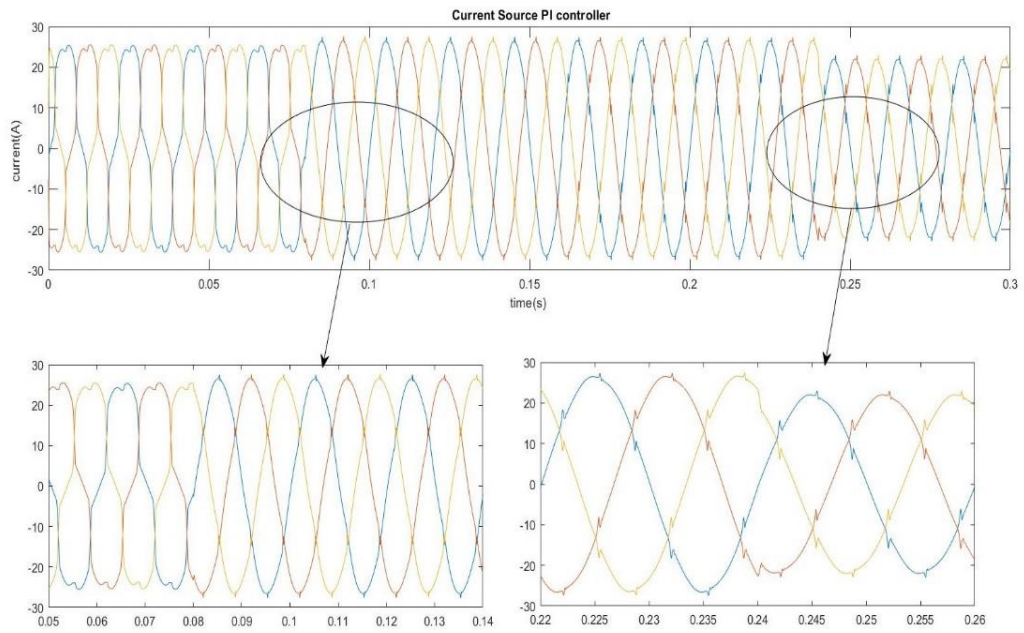
The Figure5-6 shows the result of FFT analysis as a fundamental value (50Hz) and total harmonic distortion (THD) for current source of PI controller and Fuzzy Logic controller.

The current wave form of the source currents for PI and Fuzzy logic controller was measured and the THD was calculated as shown in figure above. The current waveforms in addition to the Fast Fourier Transform (FFT) shows, the above-mentioned results also were confirmed from the calculated values of the THD of the source currents. The THD was reduced from 16.67% before using the APF to 2.65 % after using the APF for PI controller as shows in a figure 5-6-1 appendix a shows (a) and 16.72% to 1.42% for FLC shows in figure 5-6-1 appendix a shows (b). These results of the THD for FLC is even better than the results obtained of PI controller.

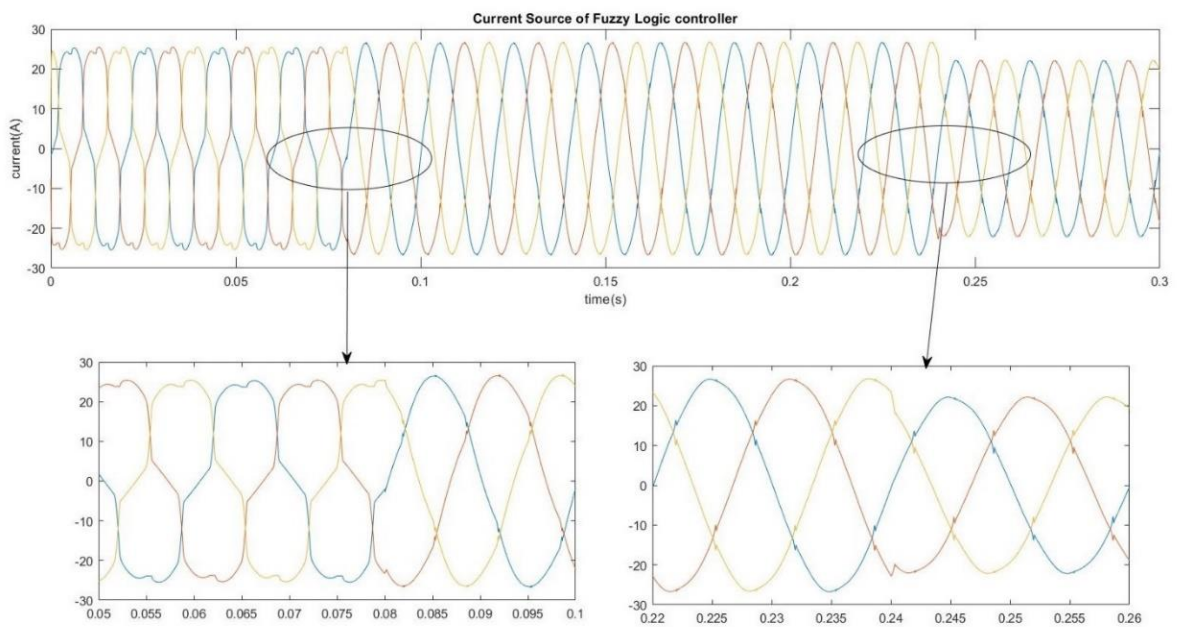
Figure 5.6

currents waveforms of : a-PI controller without and with APF / b- Fuzzy Logic controller.

a- PI controller



b- Fuzzy Logic controller



5.3 Operation of the SAPF during under load disturbance

The system is designed in Figure 5-7 in appendix a, operation of the SAPF under load disturbance and having a simulation run in MATLAB/SIMULINK.

In figure 5-8 in appendix a, shows the source current for this scenario

following scenarios under each of these operational conditions:

2. 0-0.05s: The active filter is connected but without making any compensation through controlling the reference currents of the inverter is zero.
2. 0.05-0.1s: The active filter is controlled to compensate the harmonics only.
3. AT 0.1: The results shows is introduced that the active filter is capable to maintain its performance of filtering the harmonics load during the sudden change in load.

5.4 Effects of System Compensation scenarios on IEEE networks

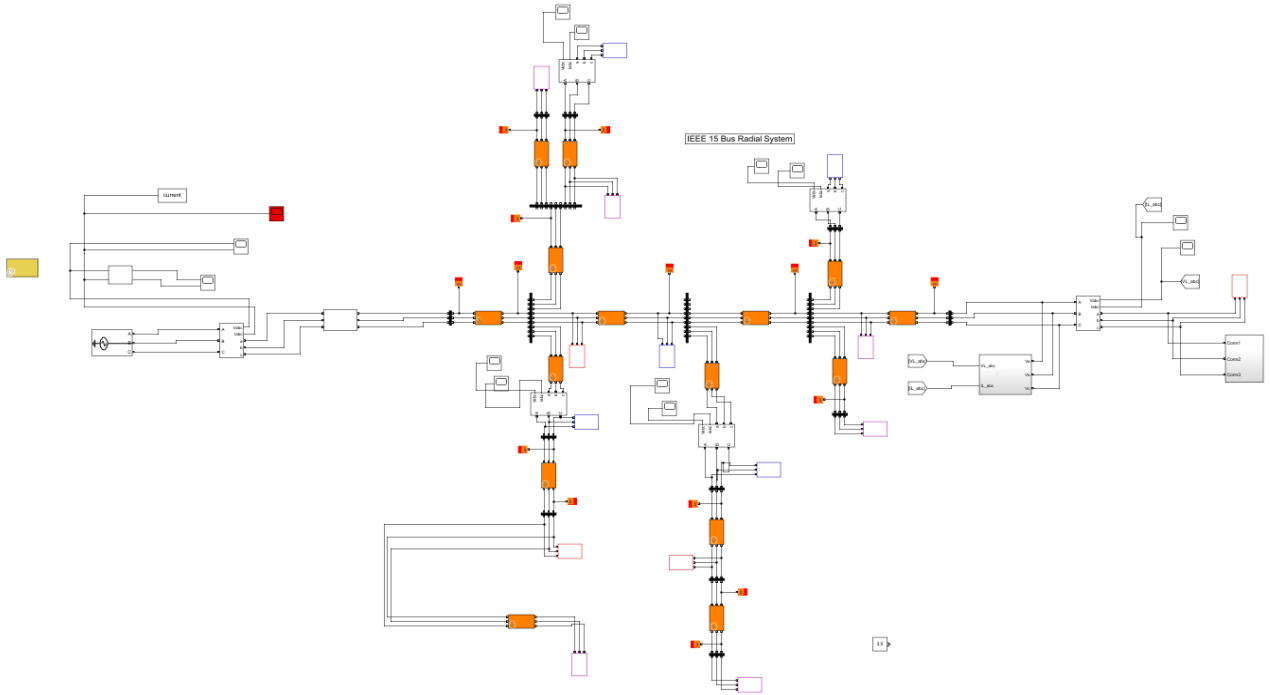
The second operational need is joining an IEEE 15 bus radial network, where there are 15 load buses carrying various loads and one swing bus. The entire system is depicted in the Figure 5-10 (a) add APF at bus5 and harmonic source, and Figure 5-10 (b) add APF at swing bus1 after being connected to an IEEE standard network and simulating it in MATLAB/SIMULINK.

Figure 5.10

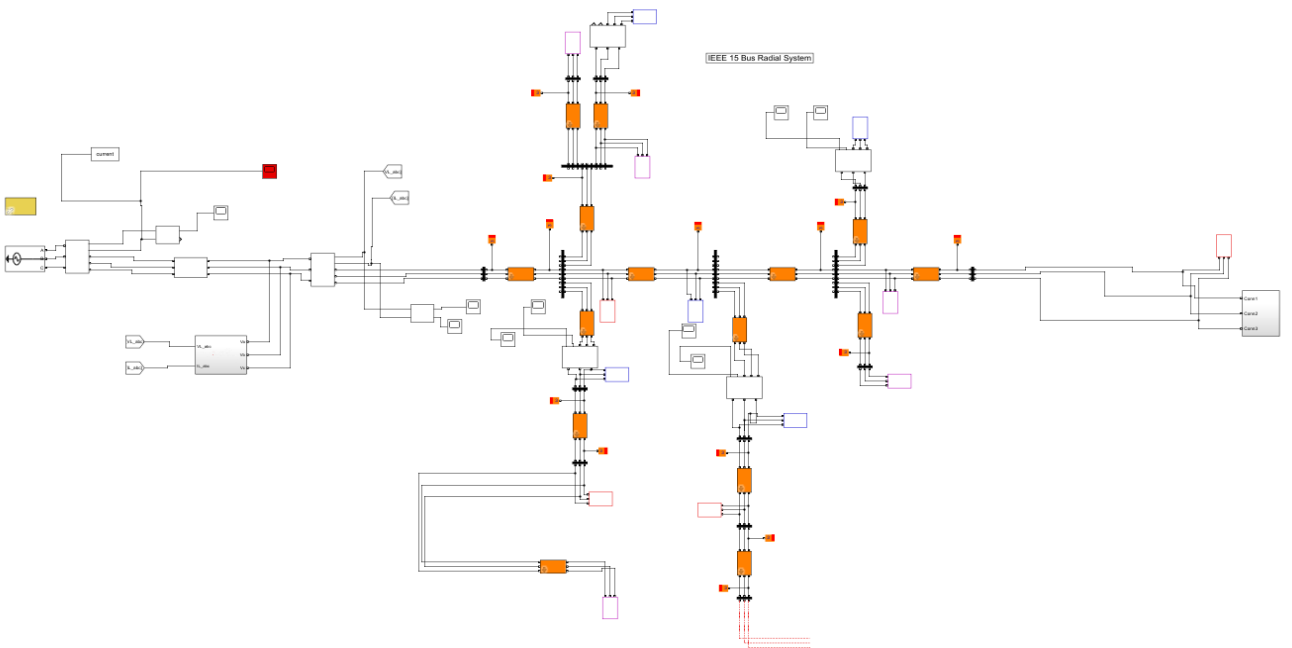
Schematic of combined system simulation with IEEE 15 Bus network

a-(APF at load) / b-(APF at swing bus1)

a-



b-



5.2.1 Results and Analysis

Numerous scenarios, including the ones listed below, have been thought of while using a single nonlinear load and an IEEE 15 bus network operating at 400 V.

1- The first scenario involves testing the proposed APF's functionality on an IEEE 15-bus network with a nonlinearized load on bus 5. The SAPF is placed near the source in this case, and therefore the harmonics within the network are not important.

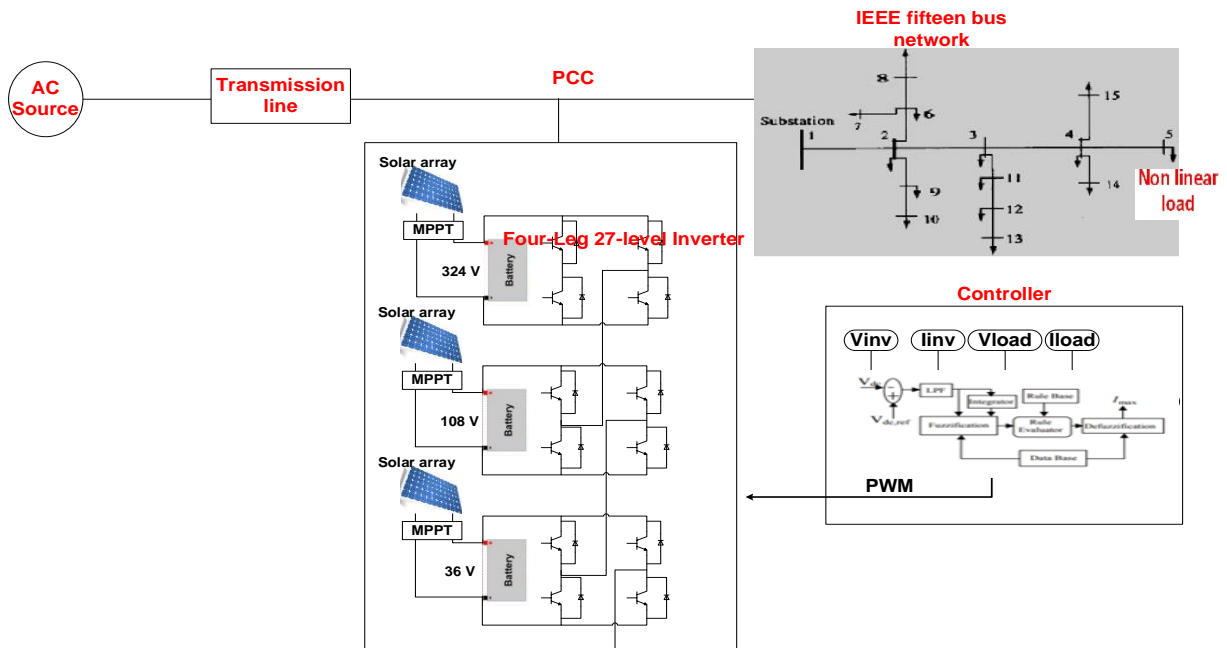
2- To see how the SAPF affects the losses and harmonics of the other buses, the second scenario involves placing the SAPF inside the network next to the bus that is carrying the nonlinear load (bus 5).

5.2.1.1 Scenario 1

As shown in figure 5-11, an IEEE 15 bus network with a 400 V nominal voltage was used in this test. The load at Bus no 5 was made nonlinear. As a result of the APF's connection to Bus No. 1, the entire network is handled as a single load.

Figure 5.11

APF connected to bus no 1 of the IEEE 15 bus networks



The source currents at Bus No. 1 were measured for their current waveforms, and the THD was calculated as shown in figure 5-12 in appendix a. The Fast Fourier Transform (FFT) and the current waveforms both reveal a dramatic decrease in the source currents' harmonic content, which turned nearly sinusoidal.

The results indicated above were also supported by the calculated THD values for the source currents. Before utilizing the APF, the THD was 13.65%; after using the APF, it was 2.64%.

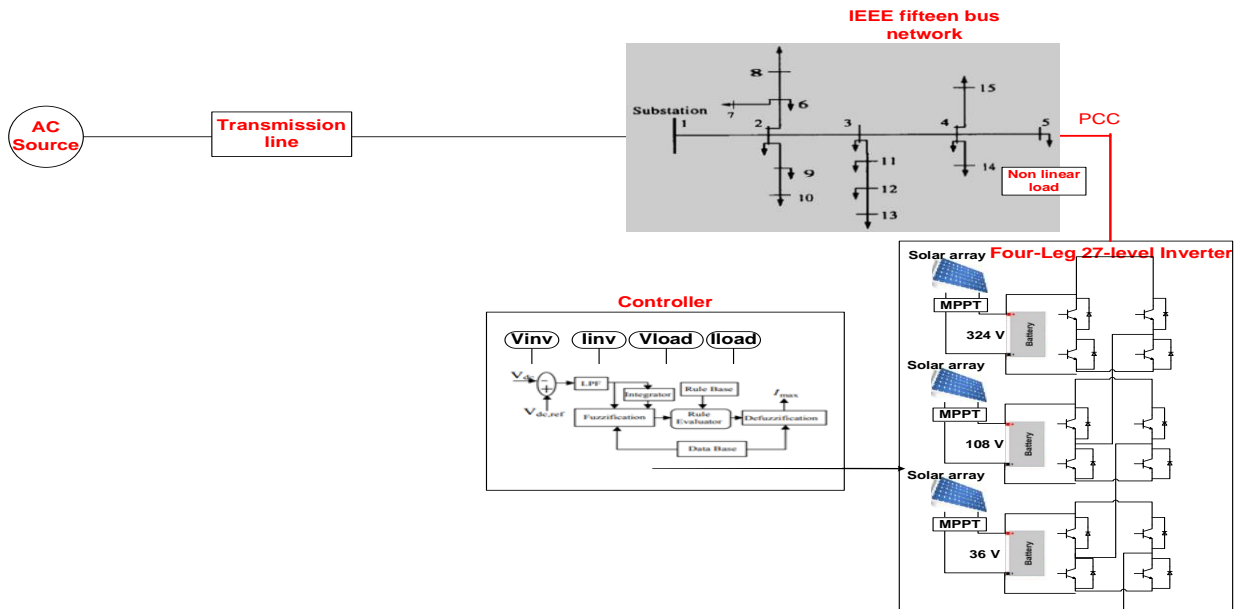
The current wave forms at buses 9, 11, and 15 were measured in order to examine the impact of the APF on the THD over the whole network in this instance. Figure 5-9 in appendix a present the findings. Figure 5-9 demonstrates that the current waveforms at these buses have slightly improved, indicating that the network's overall harmonic distortion is still significant. The calculated THD at these buses before and after employing the APF is shown in Figure 5-10 in appendix a. The calculation shows that the APF at this location is ineffective at lowering THD in the network because it is located distant from the location of the nonlinear load at bus5.

5.2.1.2 Scenario 2

The results obtained from the previous scenario (i.e., connecting the APF at the connection point at bus 1 point and far from the nonlinear load) shows an improvement in the THD of the source current but the currents in the network still distorted and the THD of this current is still high which will cause many power quality issues to the network. in this scenario, the APF was connected at bus 5 near the nonlinear load as shown in figure 5-13.

Figure 5.13

APF connected to bus no5 of the IEEE 15 bus network.



The source currents at Bus 1 were measured for their current wave forms, and the THD was computed as shown in figure 5-12 in appendix a. The Fast Fourier Transform (FFT) and the current waveforms both reveal a dramatic decrease in the source currents' harmonic content, which turned nearly sinusoidal. The results indicated above were also supported by the calculated THD values for the source currents. Before utilizing the APF, the THD was 13.84%; after using the APF, it was 2.05%. These source current measurements are significantly better than those attained by connecting the APF to bus1.

The current waveforms were once again measured at buses 9, 11, and 15 to examine the impact of the APF on the THD over the whole network in this instance. Figure 5-13 in appendix a presents the findings. The current waveforms at these buses have much improved, as seen in Figure 5-13 in appendix a, indicating that the network's overall harmonic distortion is quite low. The predicted THD at these buses before and after employing the APF is shown in Figure 5-14 in appendix a. Given that it is close to where the nonlinear load at bus 5 is, the results show that the APF at this location is effective in lowering THD in the network.

Chapter Six

Compensation Scenarios and System Outcome Results and Recommendations

An active power filter has been created to do the following tasks:

- It is capable of reducing harmonics.
- Improve power factor and reactive power correction.
- Active power injected.

The major goal is to employ a fuzzy logic controller to optimize the Shunt Active Power Filter's performance in order to lower harmonic distortion. In order to decrease the harmonic current and raise the power factor to unity, the fuzzy logic controller for the three-phase shunt active power filter is intended to take the role of the traditional proportional integral (PI) controller.

A distribution system equipped with a Shunt Active Power Filter and a Fuzzy Logic Controller is the subject of simulation. With the aid of MATLAB/SIMULINK, the power system model is simulated.

The results simulation of this project shows that, the objective of this project by reducing the Total Harmonic Distortion.

Current controller is used to generate gating signals to control the electronics switches in the SAPF. The SAPF will produce the compensating current that necessarily has the same magnitude as a source of current but different in phase. The simulation result has proved to validity of employing Shunt Active Power Filter with Fuzzy Logic Controller in distribution system as the THD is reduce from 16.72% to 1.77%.

As a future recommendation:

- Improve the Palestine distribution networks.
- Exchange between scenarios based on weather conditions and demand load.

List of Abbreviations

Abbreviation	Meaning
AC	Alternative Current
DC	Direct Current
PF	Power Factor
THD	Total Harmonic Distortion
Voc	Open-Circuit Voltage
Isc	Short circuit Current
PCC	Point of Common Coupling
Kwh	Kilowatt Hour
FLC	Fuzzy Logic Controller
PI	Proportional integral
DCMIL	Diode Clamped Converter
FCMIL	Flying Capacitor Multilevel Inverter
CMIL	Cascaded Multilevel Inverter
SAPF	Shunt Active Power Filter
PWM	Pulse Width Modulation
MOSFET	Metal- Oxide- Semiconverter Field- Effect Transistor
IGBT	Insulated – Gate Bipolar Transistor
DSP	Digital Signal Processor
PLL	Phase Locked Loop
FFT	Fast Fourier Transformer
IEEE	Institute of Electrical and Electronics Engineer

Reference

- [1]Karuppanan, P., & Kamalakanta, M. (2011). (*PI, PID and Fuzzy Logic Controlled Cascaded Voltage Source Inverter based Active Filter for Power Line Conditioners*). Article in WSEAS Transactions on Power Systems .
- [2]Devendra , K. C. (2010). " *Modeling and simulation of system using MATLAB, and Simulink*".
- [3]Krishna, R., & Suresh, L. (2016). " *A brief review on multi-level inverter topologies,*" . IEEE.
- [4]Rodriguez, J., Lai, J., & Peng, F. (2002). *Multilevel Inverters: A Survey of Topologies, Controls, and Applications*. IEEE.
- [5]Zhengl, X., Song, L., & Hongying, P. (2012). *Study of Five-level diodes-clamped Inverter Modulation Technology Based on Three-harmonic Injection Method*. 2nd International Conference on Electronic & Mechanical Engineering and Information Technology.
- [6]Meynard, T., & Foch, H. (1992). *Multi-level conversion: High voltage choppers and voltages source inverters*. IEEE PESC'92.
- [7]Krishna, R., & Suresh, L. (2013). *A brief review on multi-level inverter topologies*. International Conference on Power, Energy and Control (ICPEC).
- [8]Ganiyu , A., Ajenikoko, O., & Olaluwoye. (2015). Effect of Reactive Power Flow on Transmission Efficiency and Power Factor. *International Journal of Recent Scientific Research*.
- [9]Rodriguez, J., Lai, J., & Peng, F. (2002). *Multilevel Inverters: A Survey of Topologies, Controls, and Applications*
- [10]Zhengl, X., Song, L., & Hongying, P. (2012). *Study of Five-level diodes-clamped Inverter Modulation Technology Based on Three-harmonic Injection Method*. 2nd International Conference on Electronic & Mechanical Engineering and Information Technology.

- [11]Clark, S., Famouri, P., & Cooley, W. (1997). *Elimination of supply harmonics*. IEEE Industry Applications Magazine B.
- [12]Moran, L., Dixon, J., Espinoza, J., & Wallace, R. (2019). Using active power filters to improve power Quality. IEEE Transactions
- [13]Miller, T., & Wiley, J. (1982). *Reactive Power Control in Electric Systems*. A Wiley Interscience Publication
- [14]Gyugyi, L., & Strycula, E. (1976). Active AC power filters. IEEE Industrial Applications Society Annual Meeting
- [15]Antchev, H. (2018). *Classical and Recent Aspects of Active Power Filters for Power Quality Improvement*. Classical and Recent Aspects of Power System.
- [16]Jacob, A., Abraham, B., Prakash, N., & Philip, R. (2018). *A Review of Active Power Filters in Power System Applications*. IEEE.
- [17]Routimo, M., Salo, M., & Tuusa, H. (2007). *Comparison of Voltage and Current Sources Active Power Filters*. IEEE.
- [18]Candrsekaran, S., & Ragavan, K. (2013). Reference current extraction through sliding DFT assisted single phase p-q theory for shunt active power filter. IJEEPS.
- [19]Afonso, L., Feritas, M., & Martins, S. (2003). *p-q Theory Power Components Calculations*. IEEE.
- [20]Akagi, H. (1996). *New Trends in Active Filters for Power Conditioning*. IEEE.
- [21]Santosh, D., Madhu, B., & Kanojiya, M. (2011-2012). *Instantaneous Active and Reactive Current Component Method for Active Filters under Balanced & Unbalanced mains Voltage Conditions for 3-ph 3-wire System*. IEEE.
- [22]Moran, L., Dixon, J., Espinoza, J., & Wallace, R. (2019). *Using active power filters to improve power Quality*. IEEE Transactions.

- [23] Miller, T., & Wiley, J. (1982). *Reactive Power Control in Electric Systems*. A Wiley Intercedence Publication.
- [24] Gyugyi, L., & Strycula, E. (1976). *Active AC power filters*. IEEE Industrial Applications Society Annual Meeting.
- [25] Antchev, H. (2018). *Classical and Recent Aspects of Active Power Filters for Power Quality Improvement*. Classical and Recent Aspects of Power System.
- 26 Kenjrawy H, Makdisie C, Mohammad N, “ New Modulation Technique in Smart Grid Interfaced Multilevel UPQC-PV Controlled via Fuzzy Logic Controller” *Electronics* 2022, Mar 2022.

Appendices

Figures

The overall schematic for the system that was created for this study is shown in Figure 1.

Figure 1.1

General schematic of the designed system.

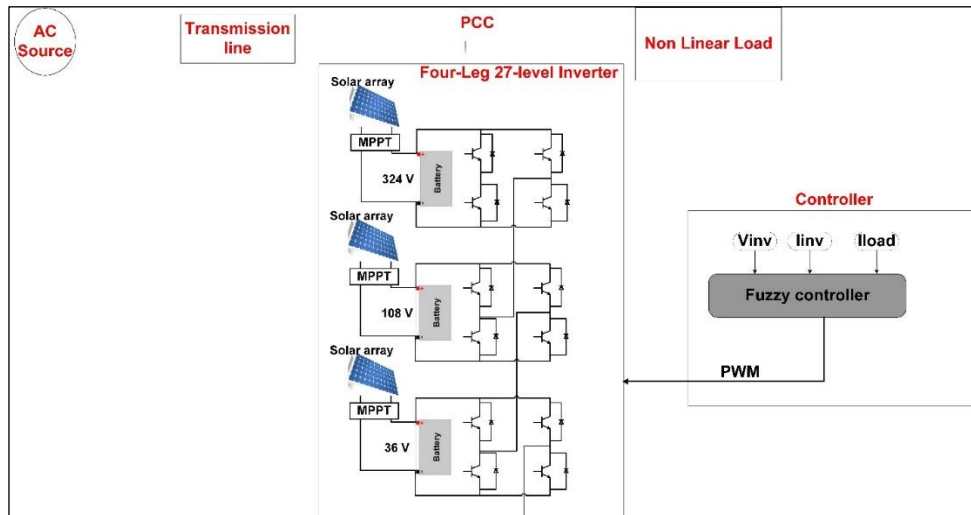


Figure 2.2

The fundamental design of a fuzzy controller.

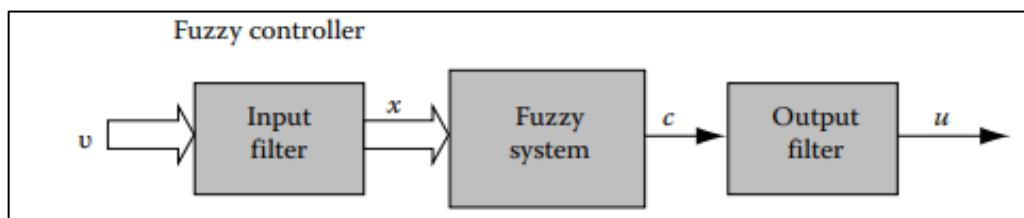


Figure 2.3

Fuzzy system components.

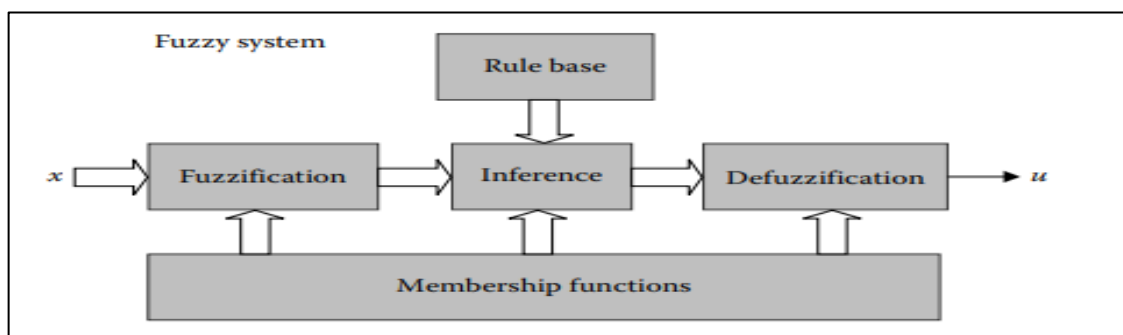


Figure 2.4

Block diagram of fuzzy controller

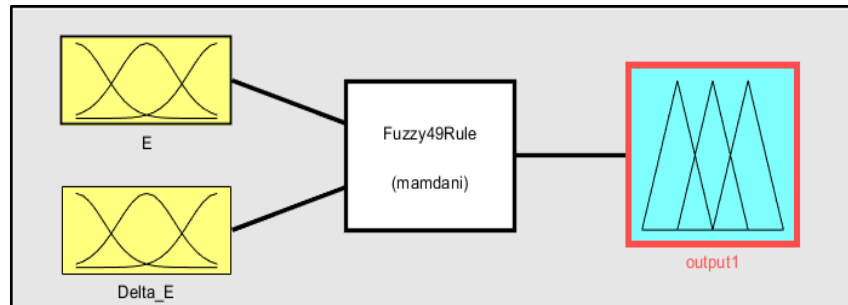


Figure 2.5

Membership function plot of 2 input of fuzzy controller

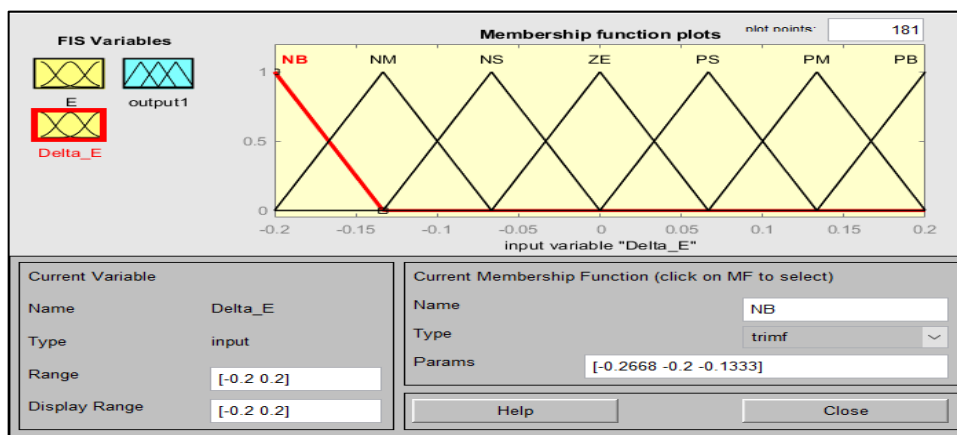


Figure 2.6

Membership function plot of output of fuzzy controller

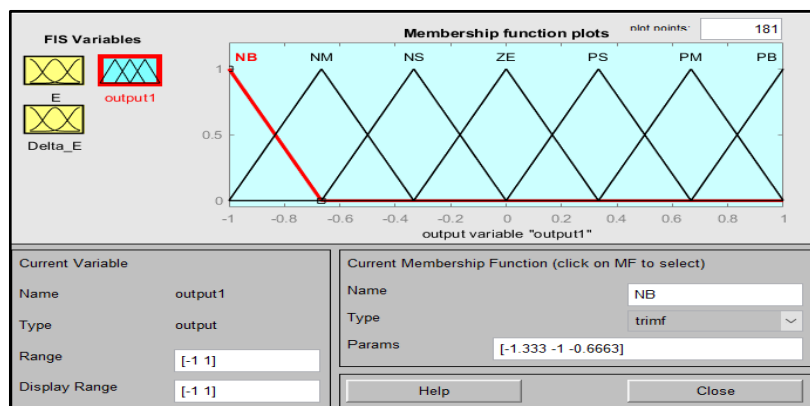


Figure 2.7

Rule editor of fuzzy controller Rule viewer of fuzzy controller

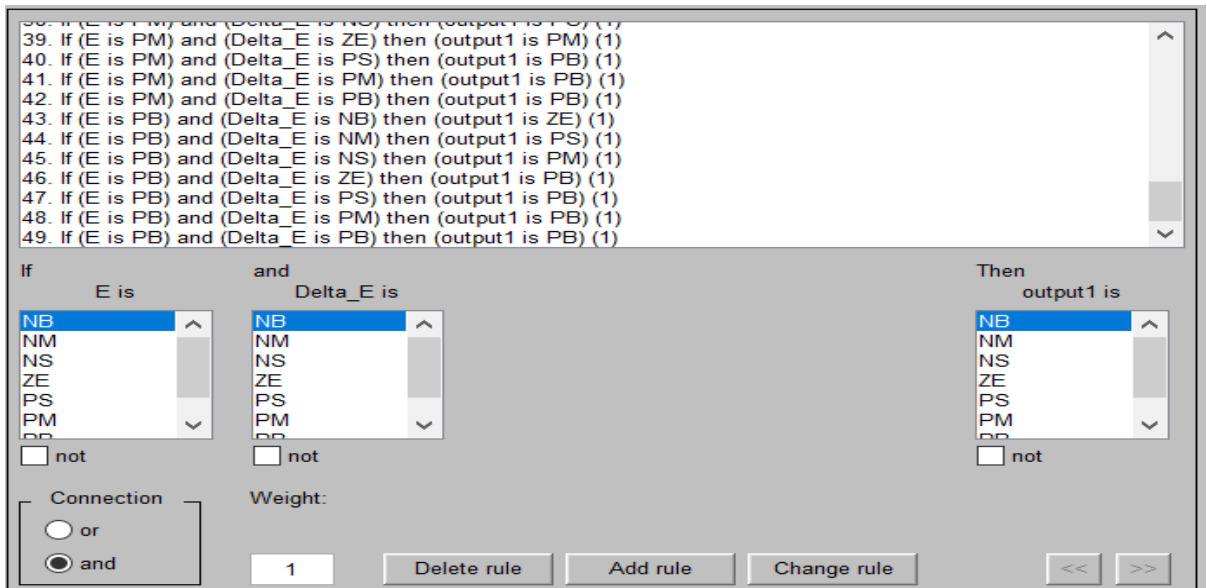


Figure 2.8

Rule viewer of fuzzy controller

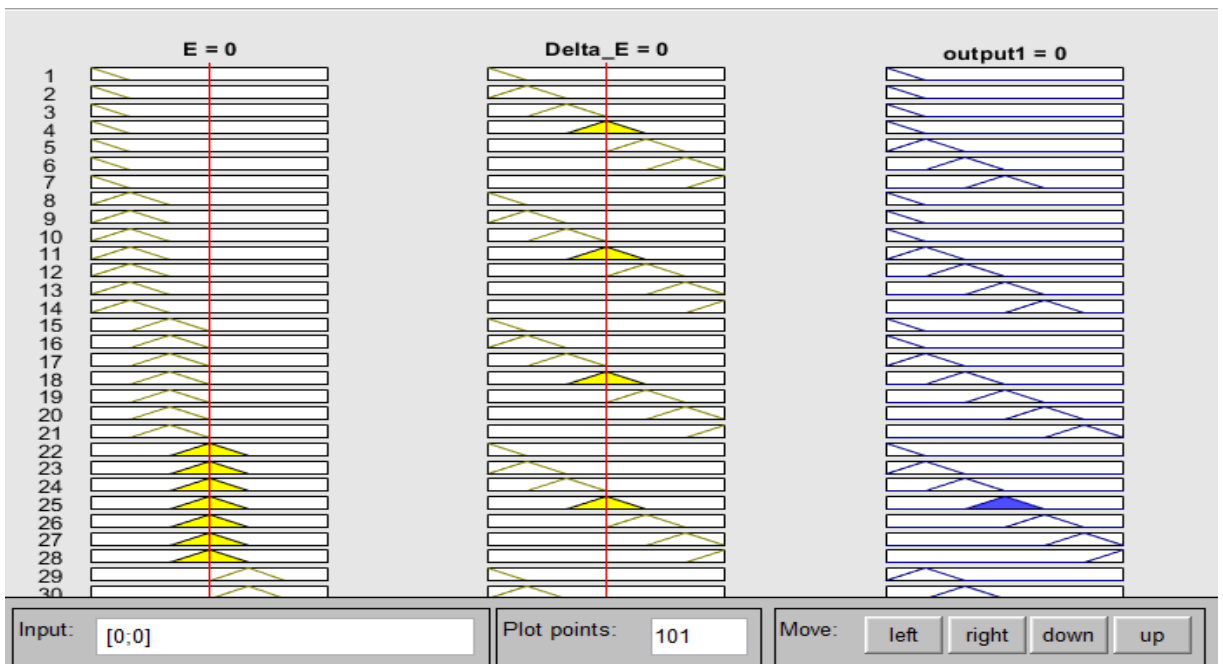


Figure 2.9

Surface view of fuzzy controller

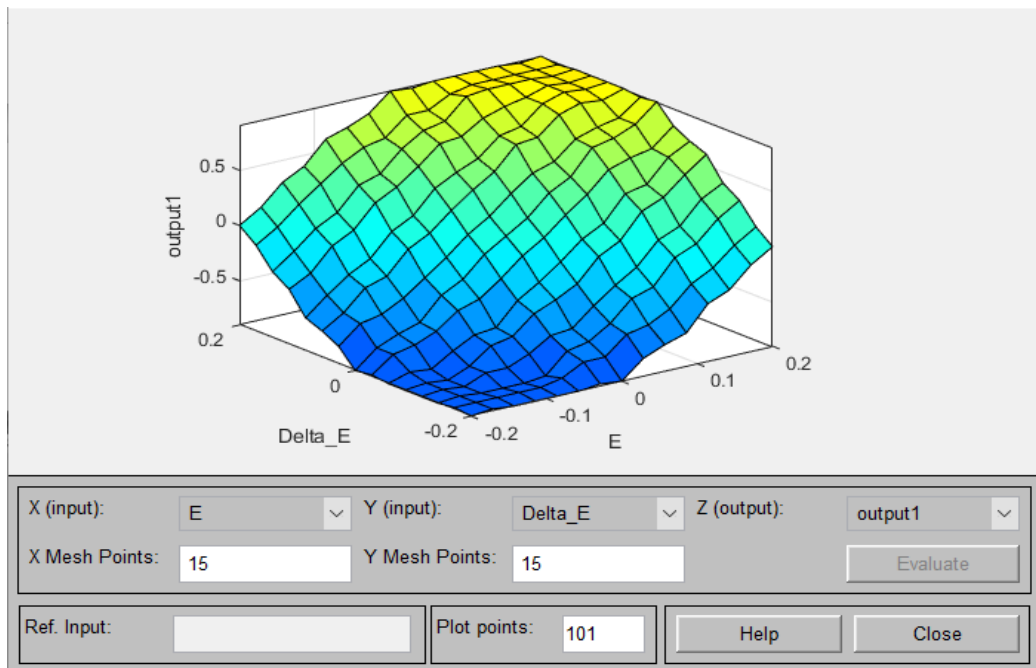


Figure 2.10

Arrangement of fuzzy controller in nonlinear system.

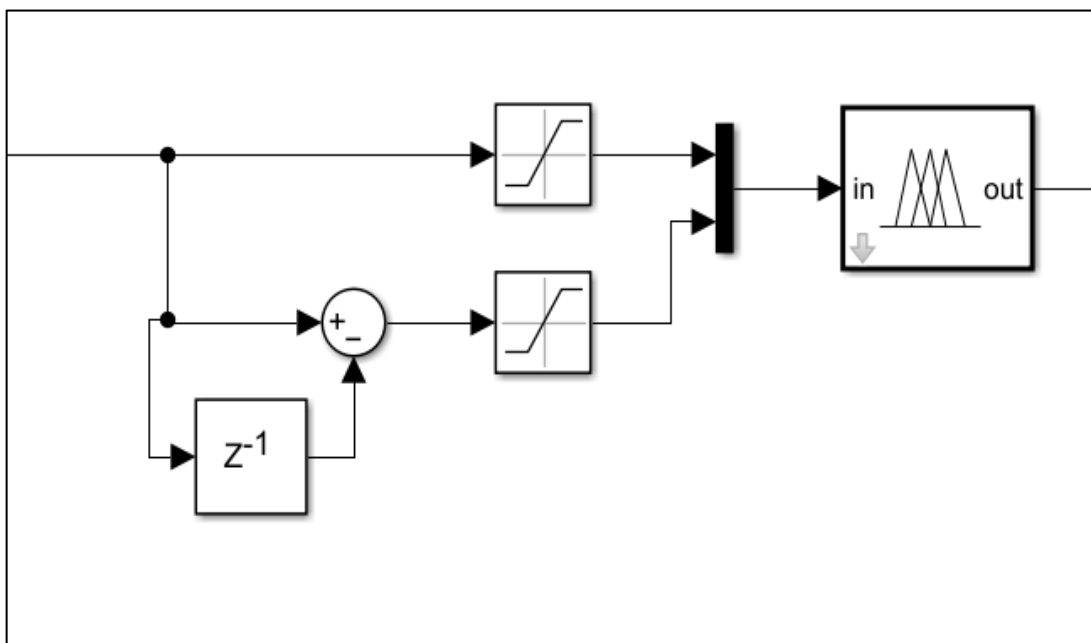


Figure 2.11

Fuzzy Logic controller by using MATLAB/SIMULINK

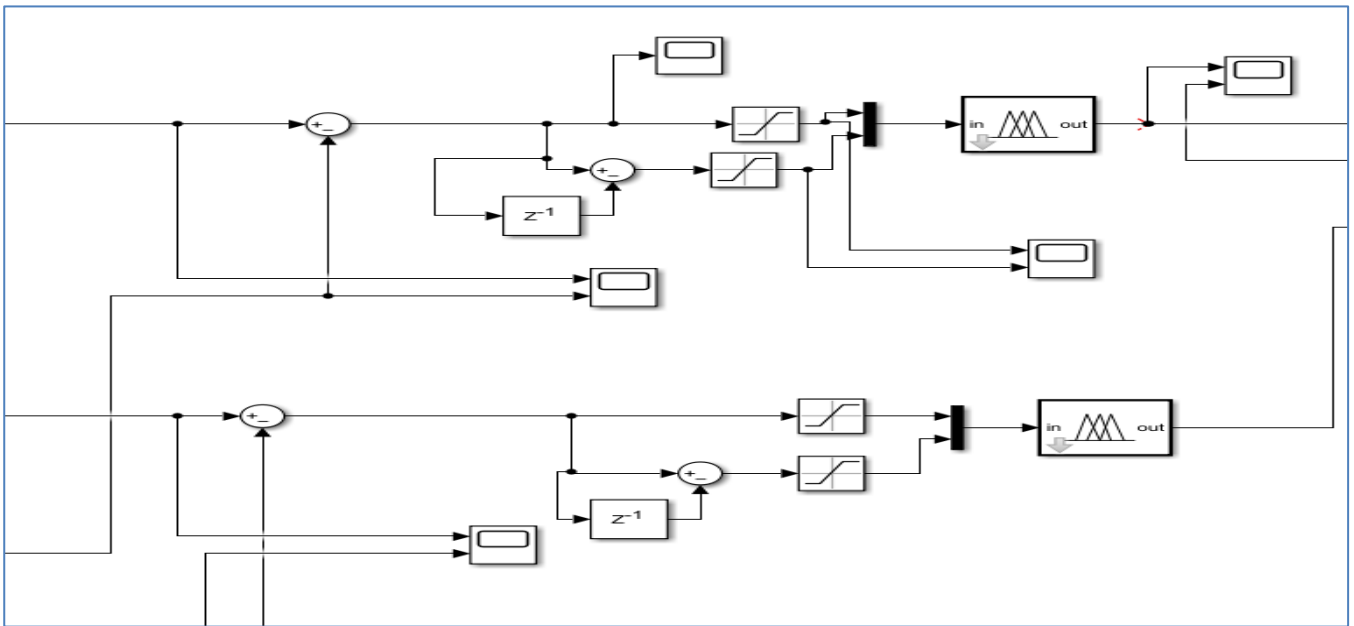


Figure 3.1

Schematic of a single-phase inverter showing the DC voltage levels

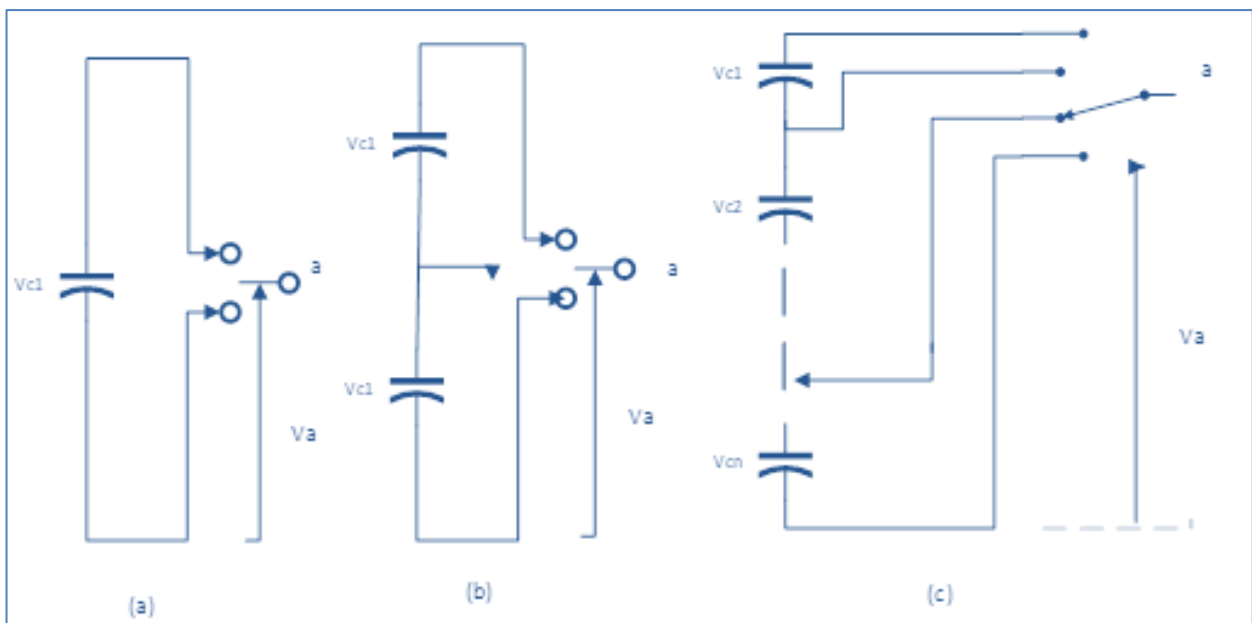


Figure 3.2

Diagram of a three-level inverter with a diode-clamped topology

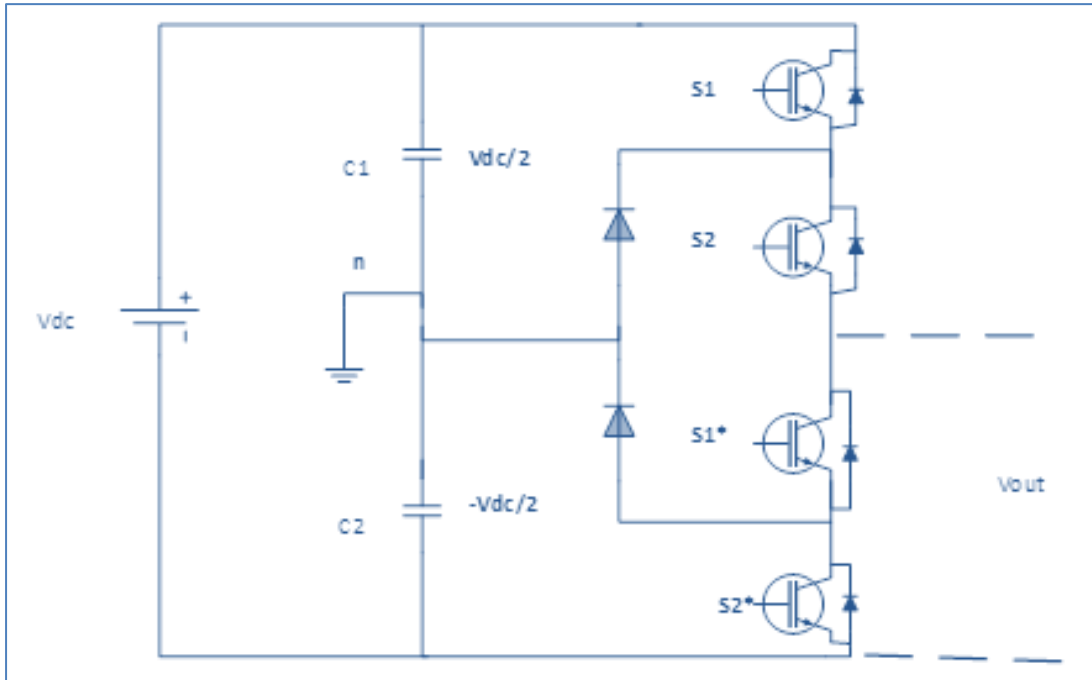


Figure 3.3

Circuit architecture diagram for a capacitor-clamped multilevel inverter (three levels)

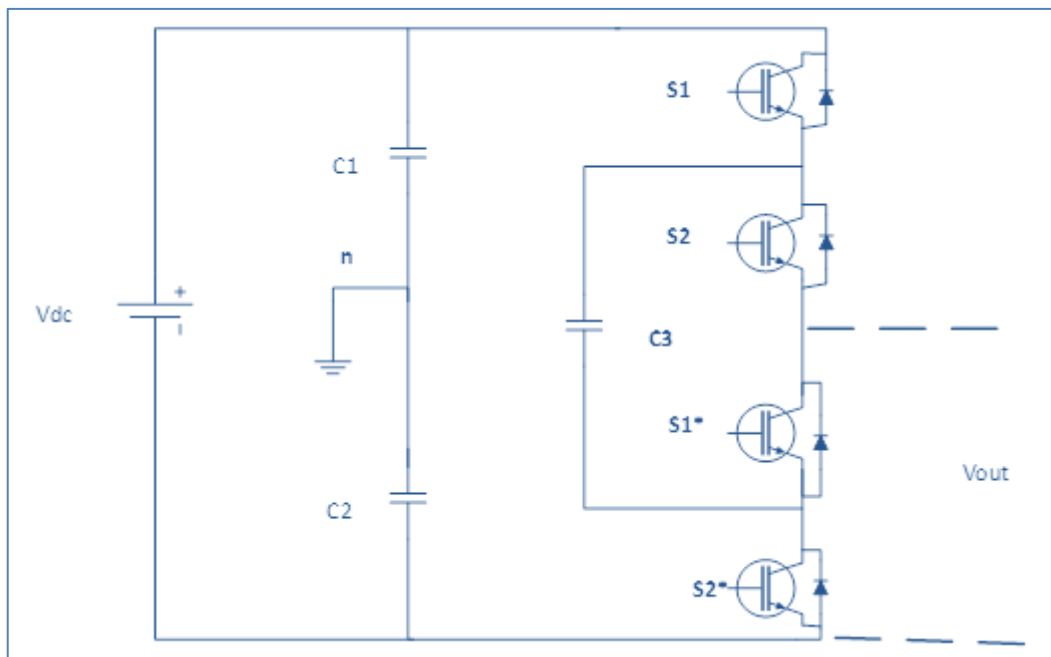


Figure 3.4

Design of a 3-level cascaded multilevel inverter (Y arrangement)

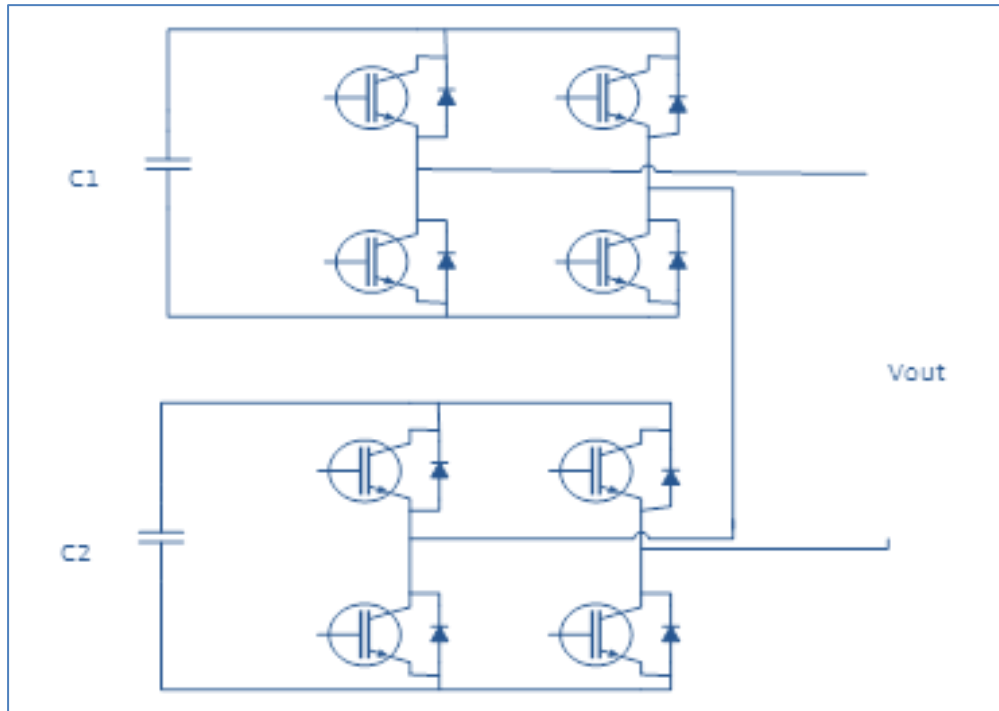


Figure 3.5

H-bridge inverter with three separate DC sources and 27 levels for one leg

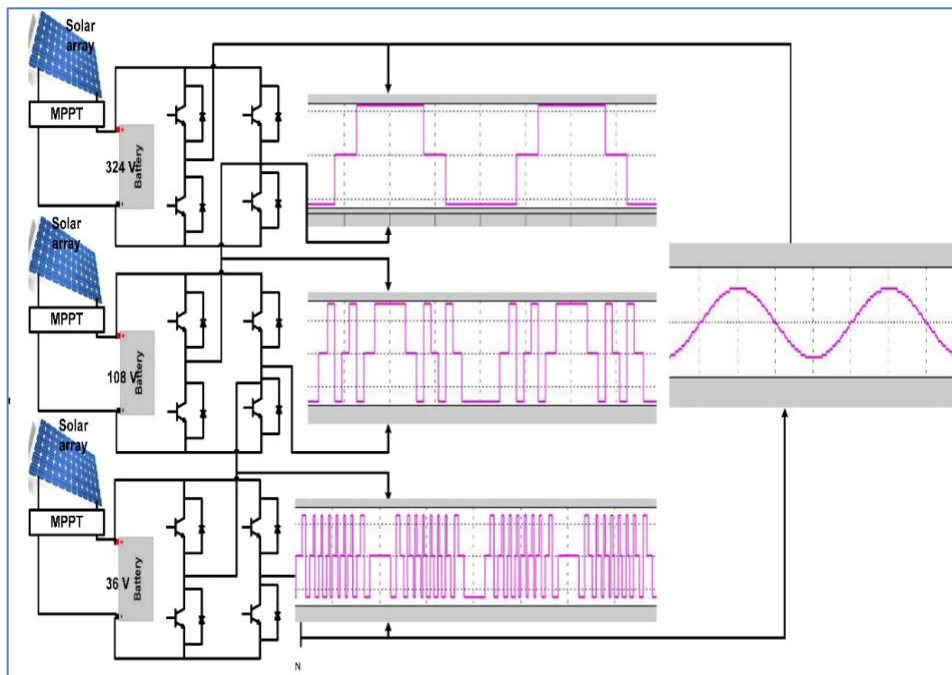


Figure 3.6

multi-level inverter controller flowchart

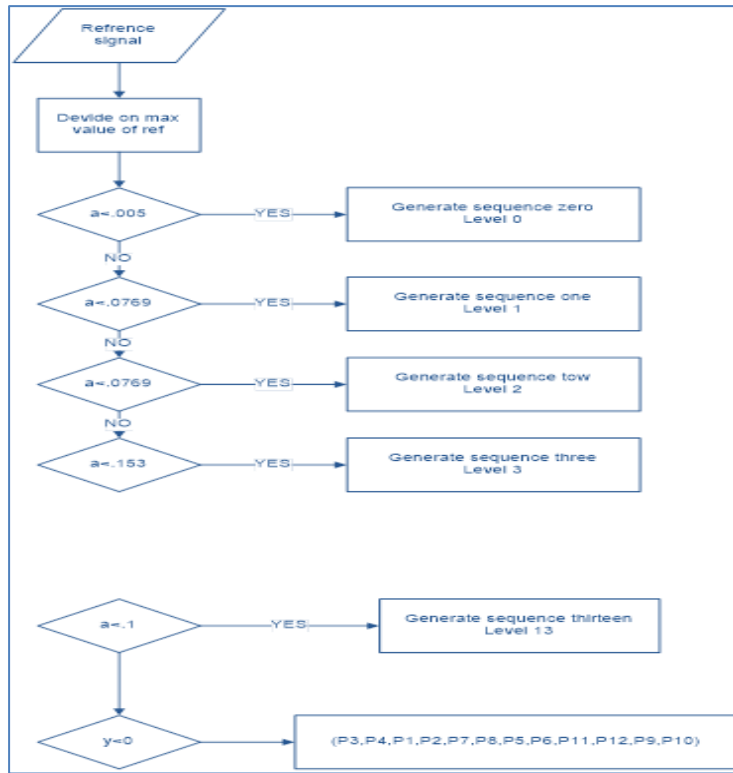


Figure 3.7

MATLAB/SIMULINK-based 27-level inverter design

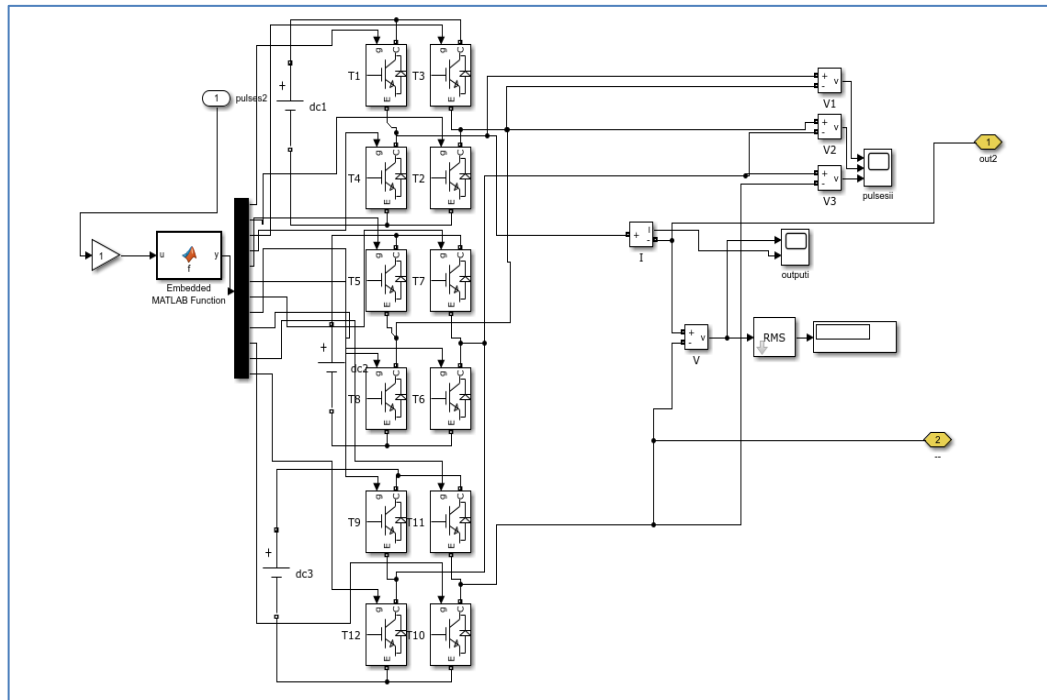


Figure 4.1

Passive shunt high pass filter

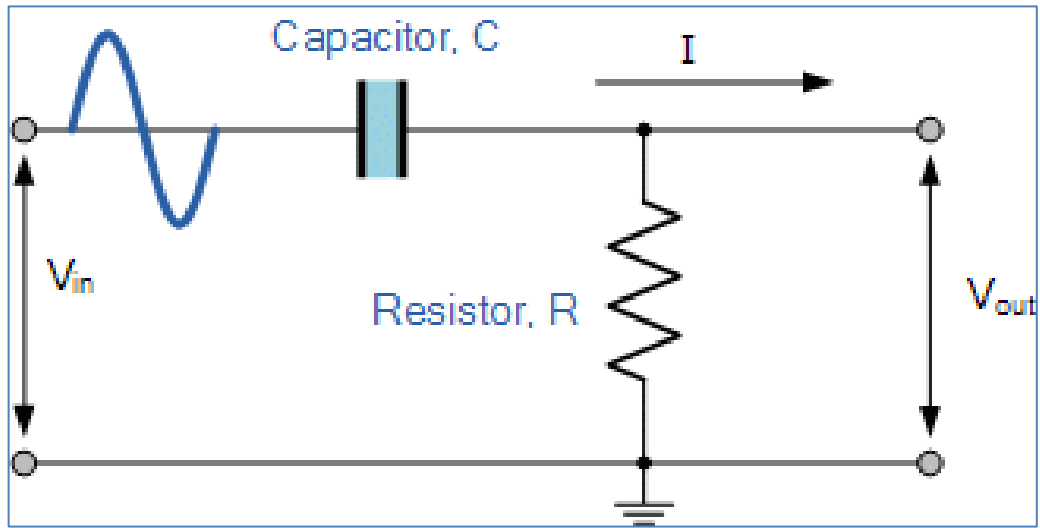


Figure 4.2

Shunt active power filter scheme

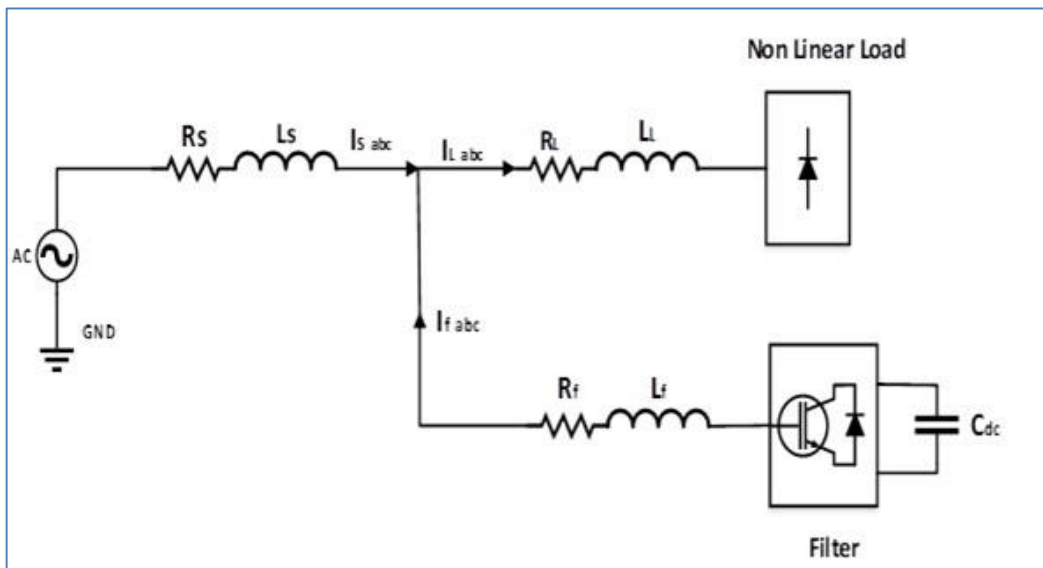


Figure 4.3

hybrid power filtering technique

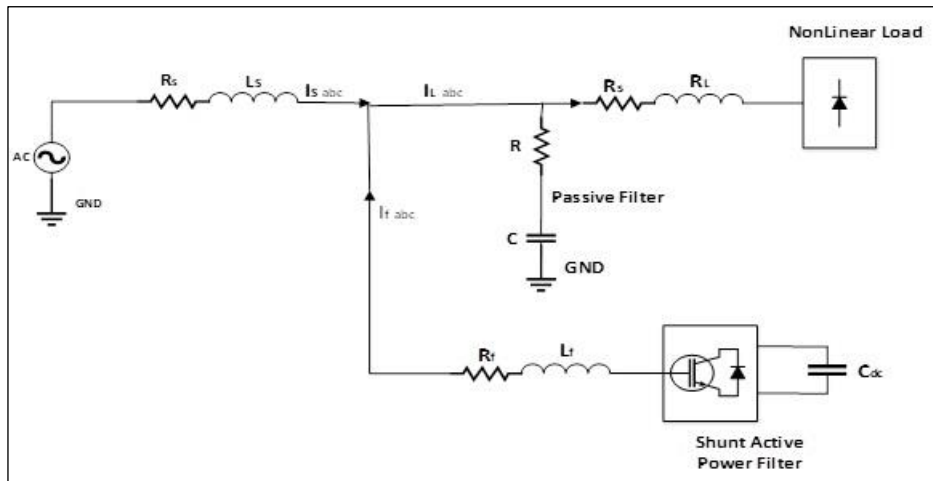


Figure 4.4

Schematic of p-q theory principle

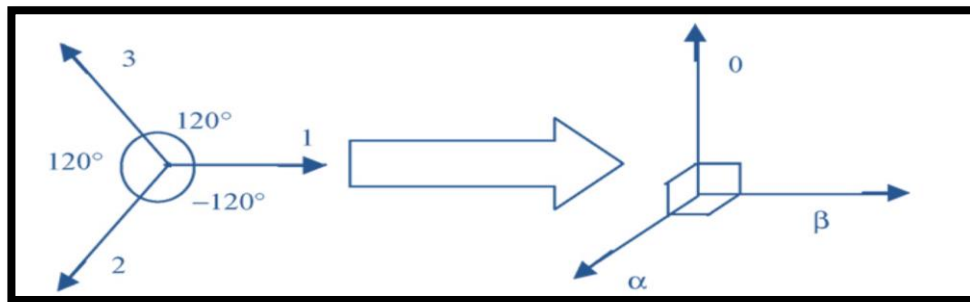


Figure 4.5

The p-q theory power components

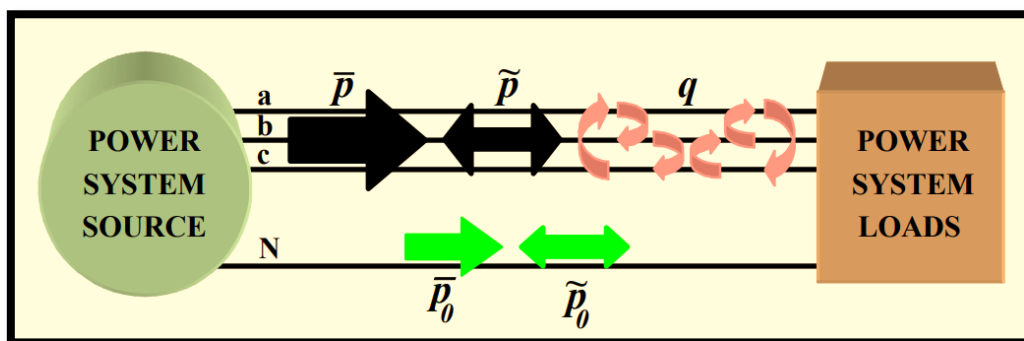


Figure 4.6

An illustration of the p-q theory in action for eliminating harmonics

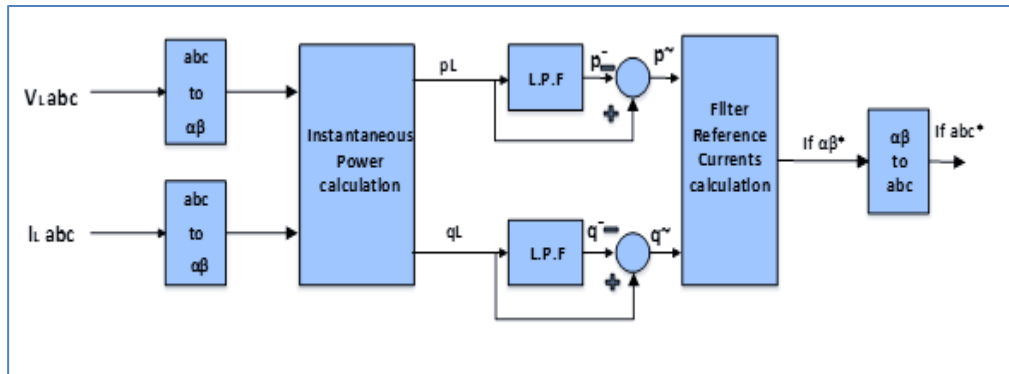


Figure 4.7

An example of how the p-q theory can be used to reduce harmonics and improve PF

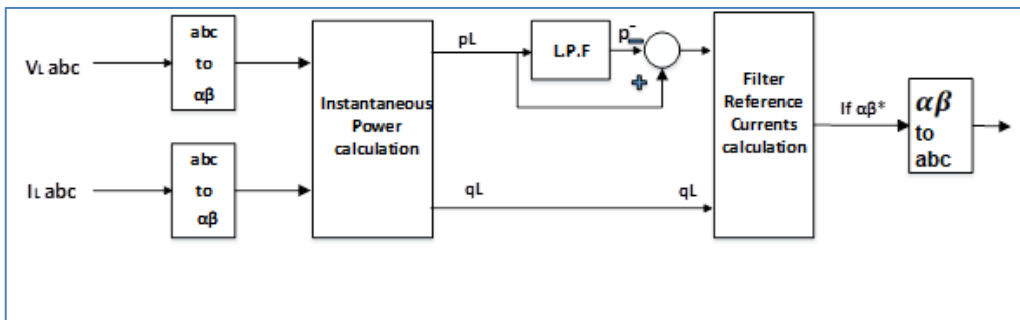


Figure 4.8

I_d - I_q theory for reference current extraction illustrated

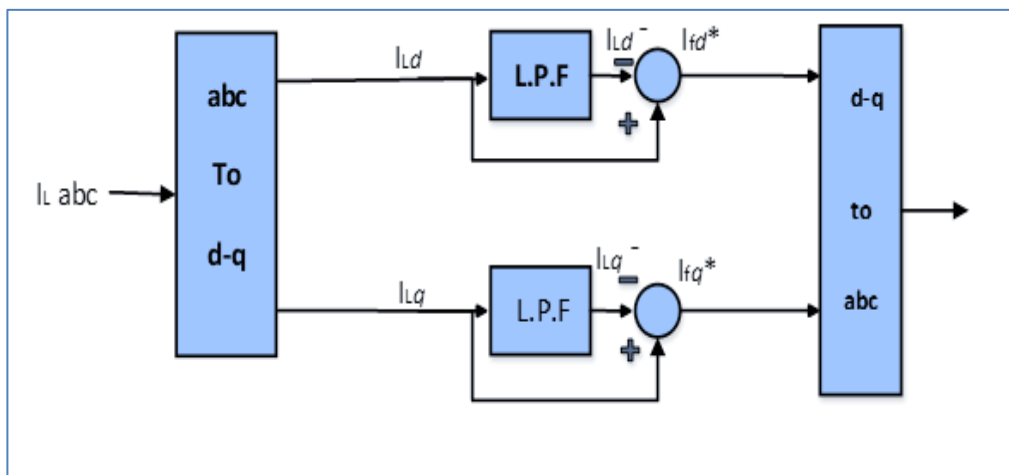


Figure 4.9

Direct Control Method Schematic

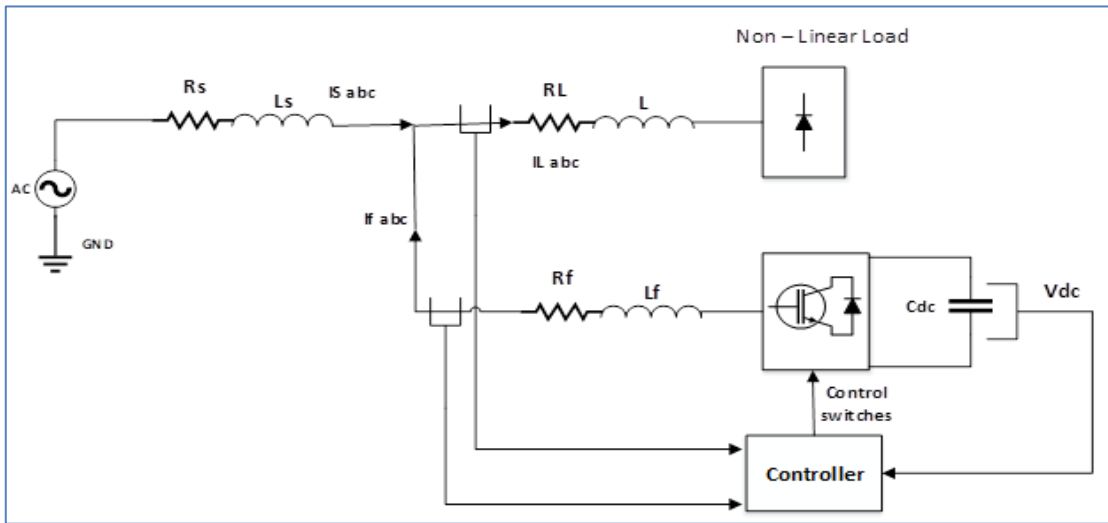


Figure 4.10

Illustration of the current closed-loop controller

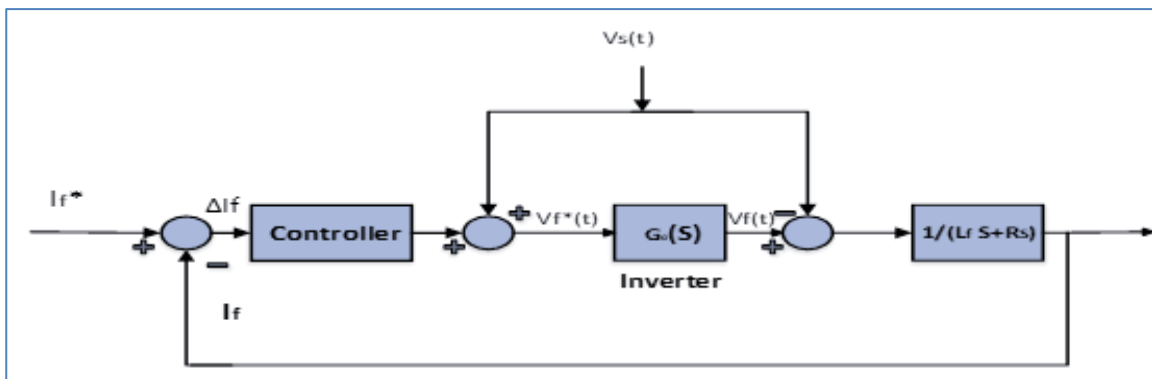


Figure 4.11

Direct Control Technique Illustration

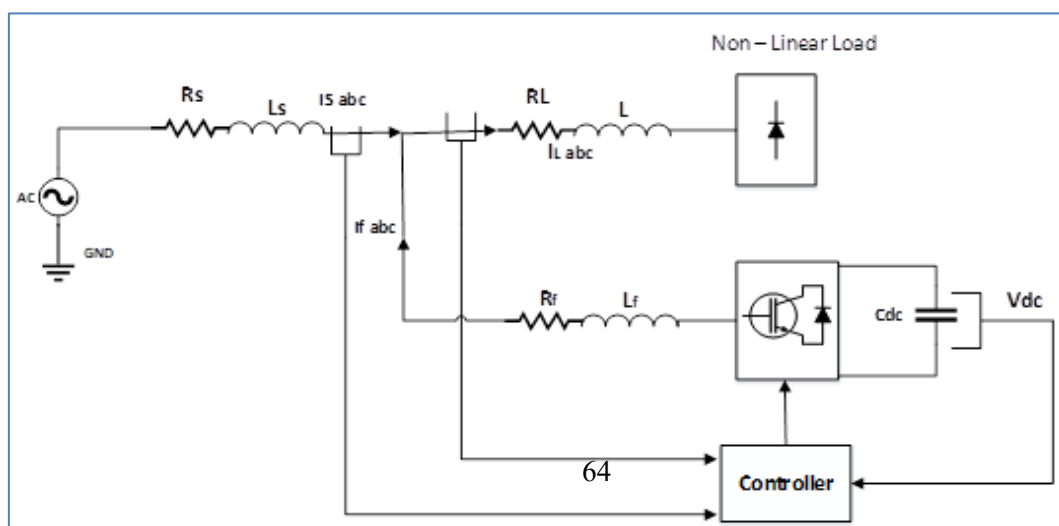


Figure 4.12

Diagram illustrating a strategy for indirect control based on p-q theory

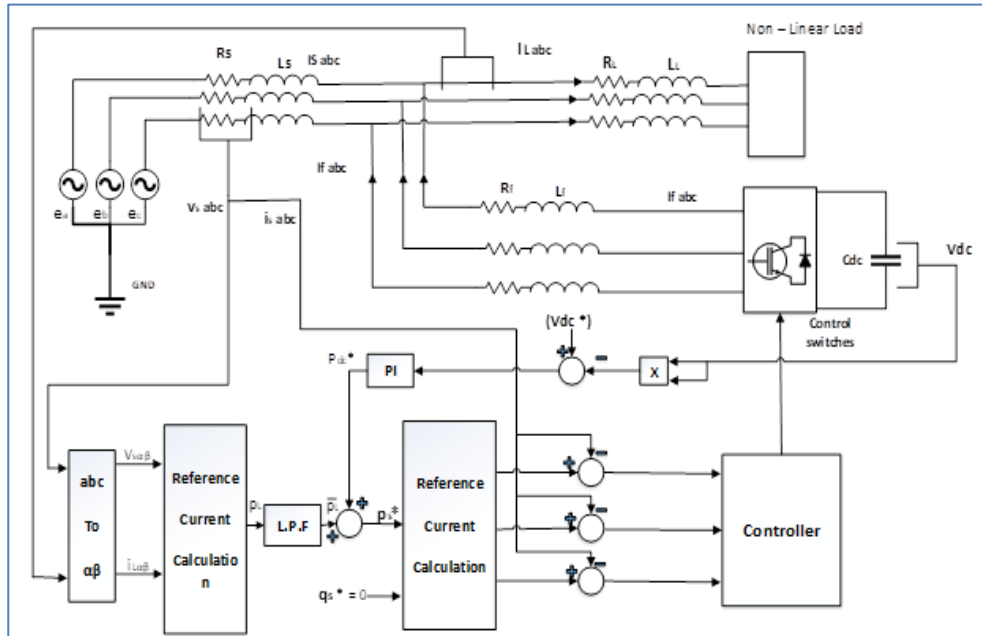


Figure 4.13

Id-Iq theory-based schematic for an indirect control approach

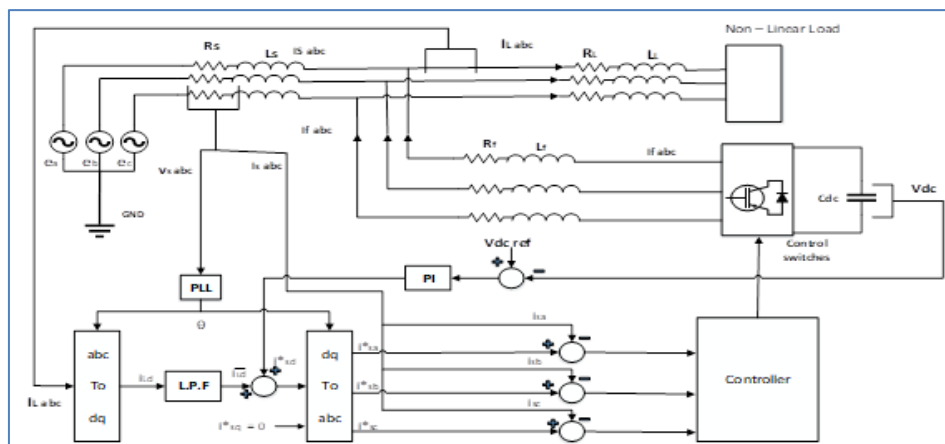


Figure 4.14

Diagram of an indirect control method using a DC voltage controller

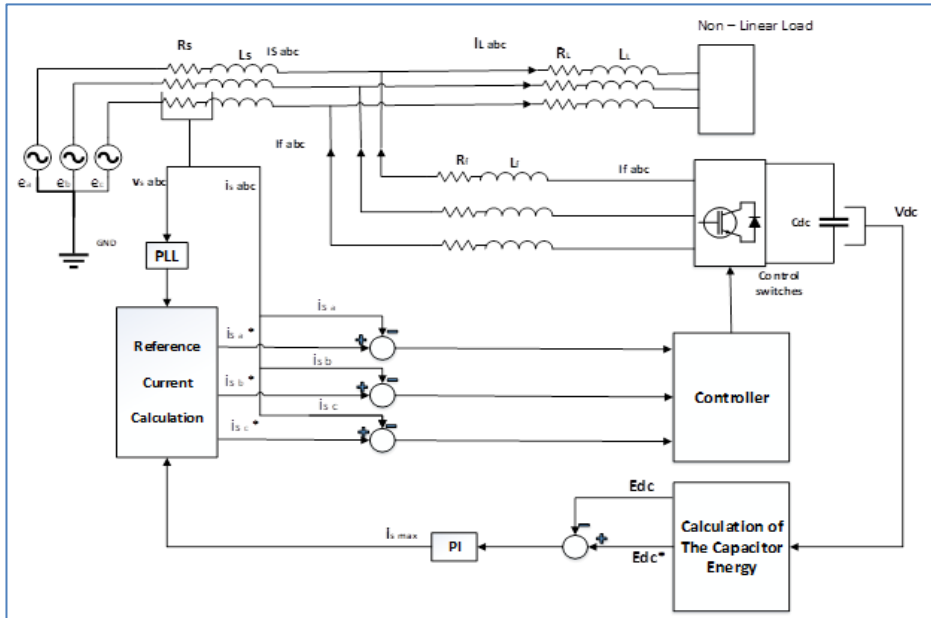


Figure 4.15

Schematic of SAF with switches and Dc source

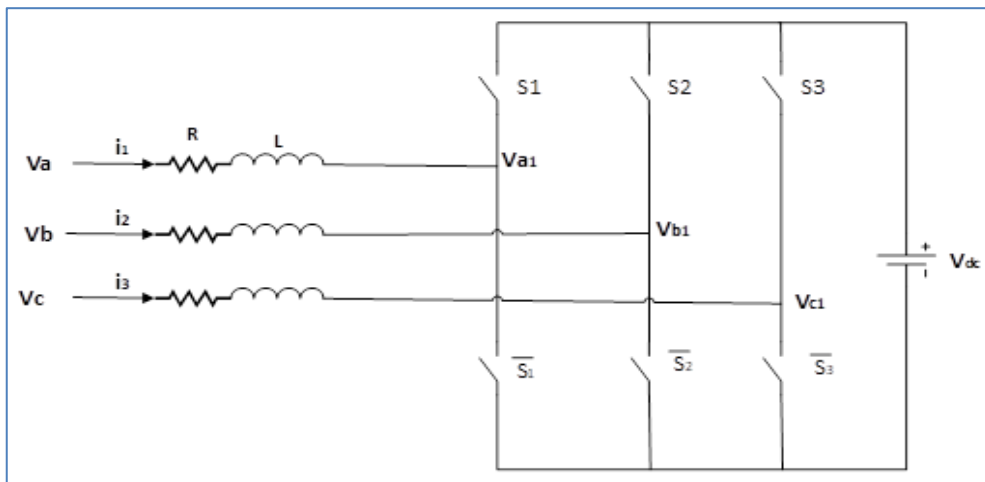


Figure 4.16

Current controller

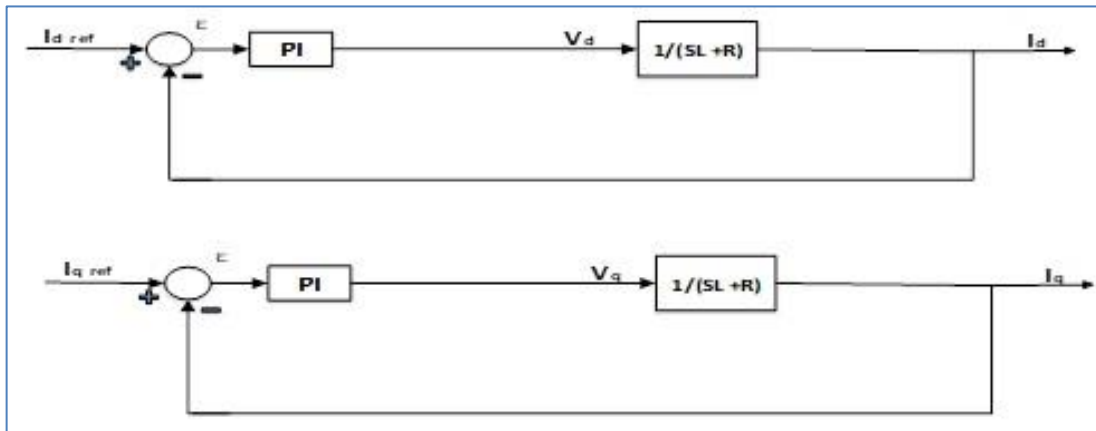


Figure 4.17

Shunt active power filter controller by using MATLAB/SIMULINK

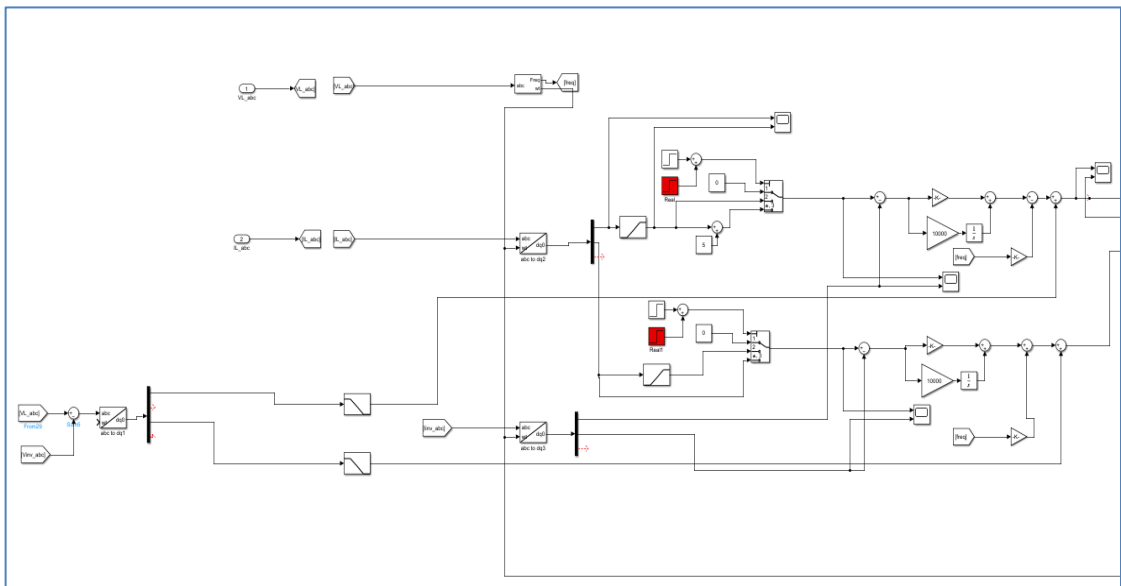
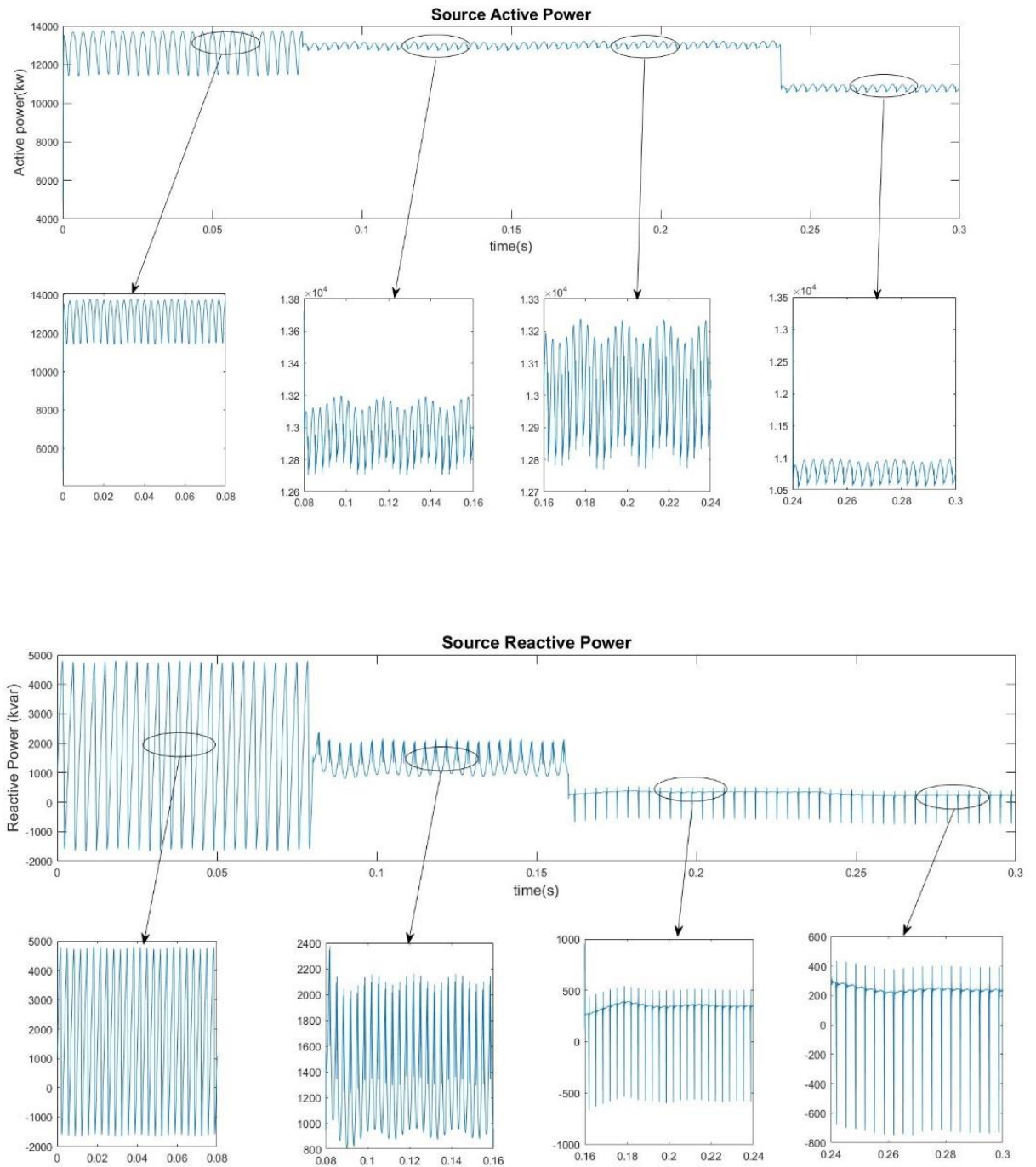


Figure 5.2.1

Schematic of System active power and reactive power behavior under different operation scenarios a- source power b- Inverter power

a- Source Power



b- Inverter Power

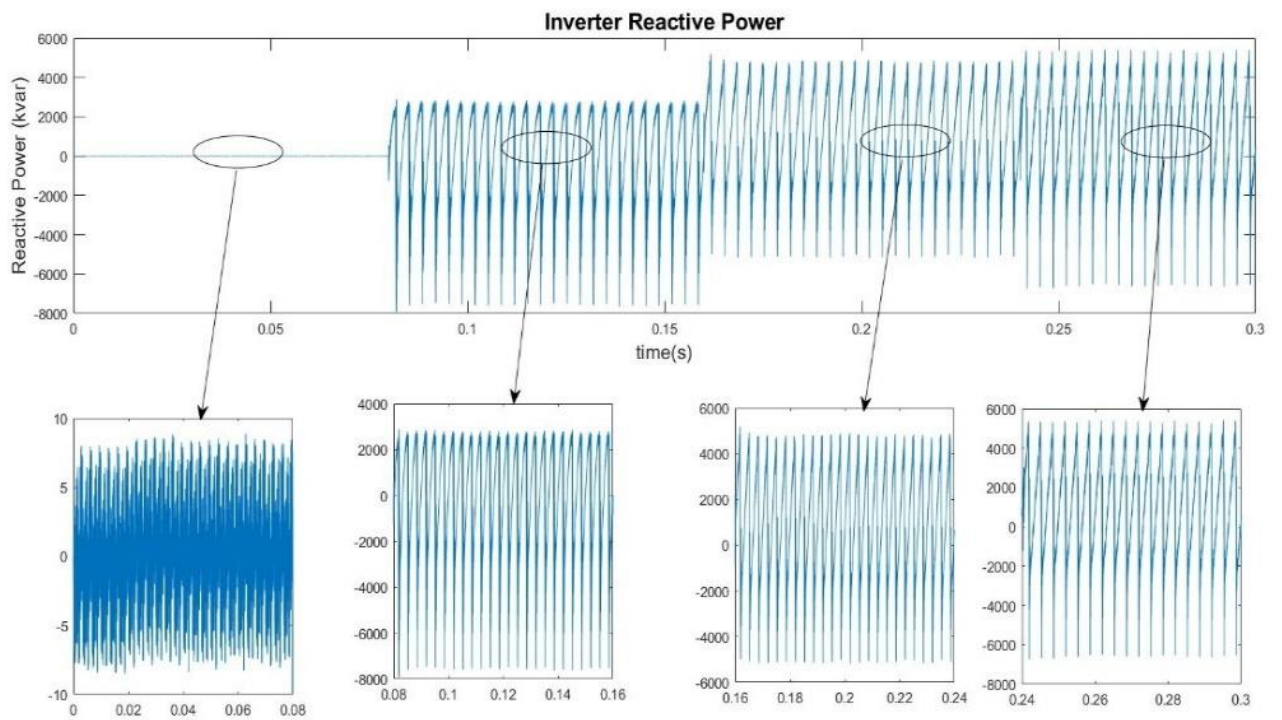
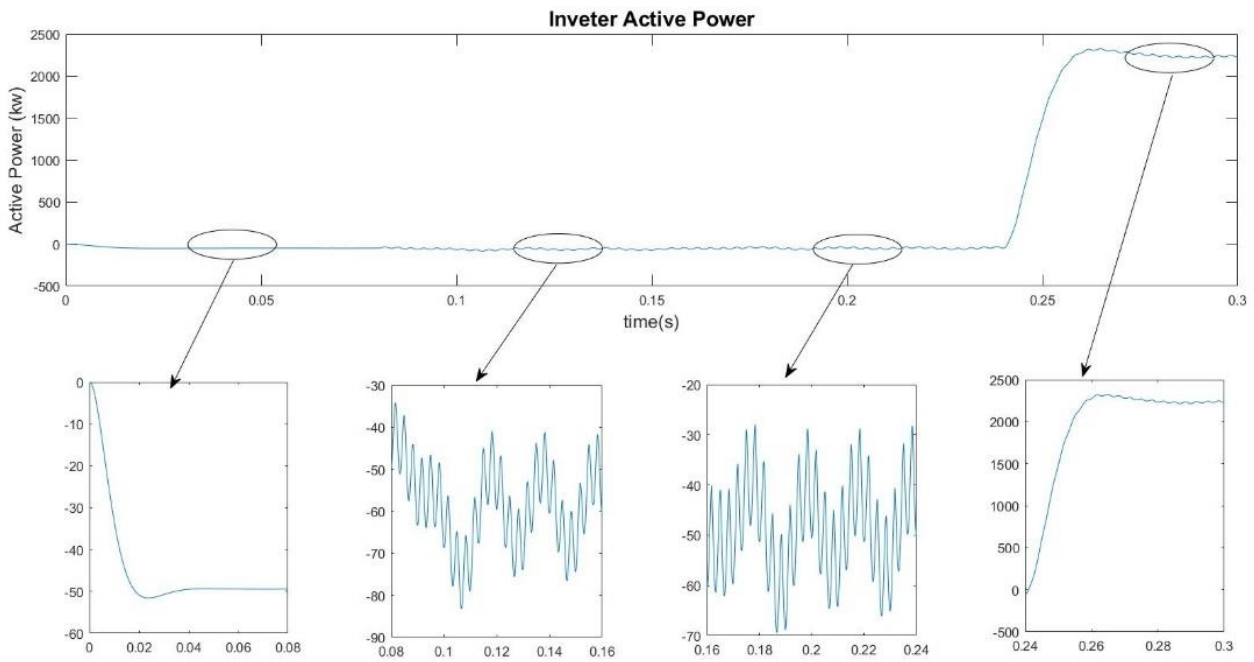
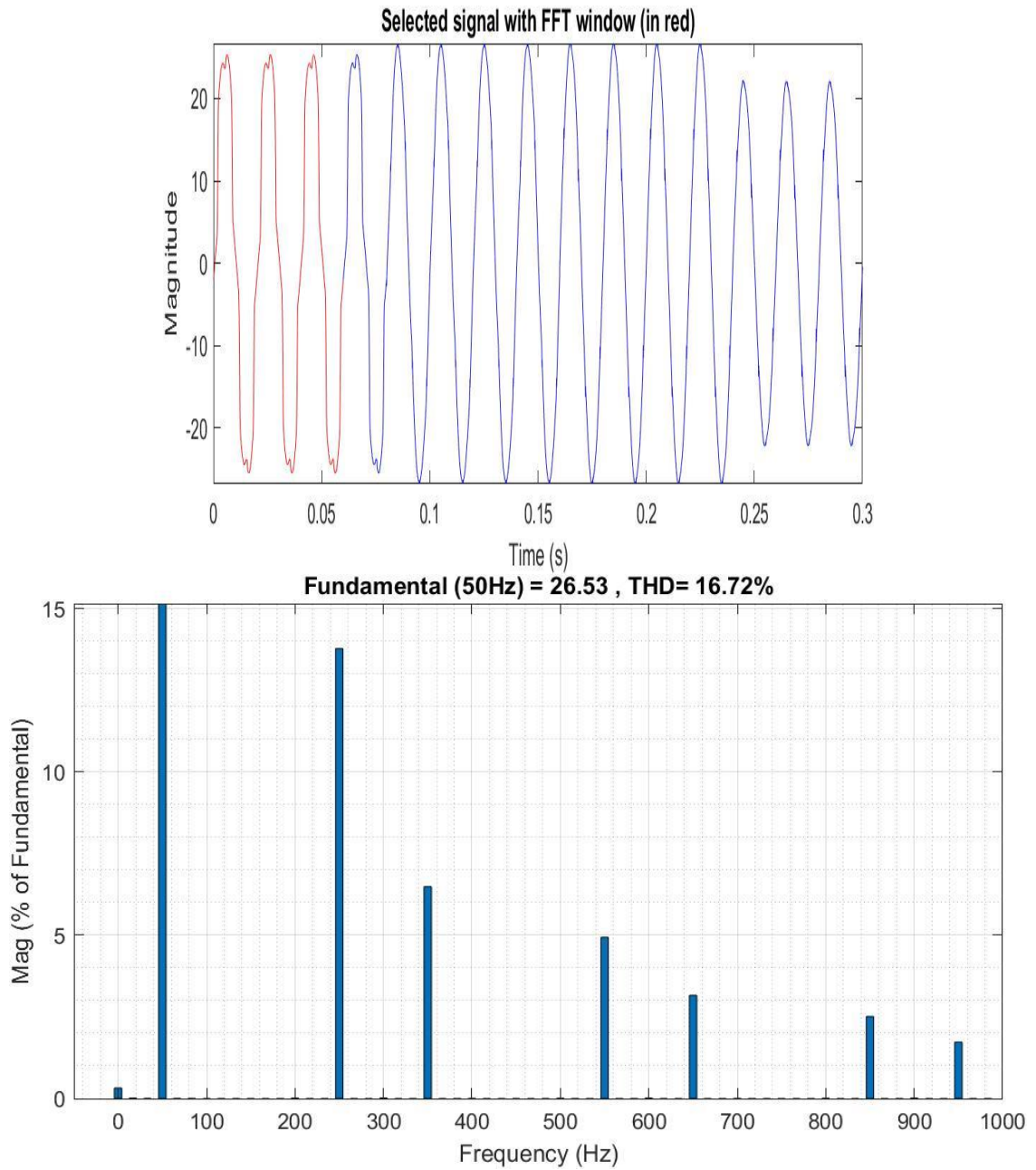
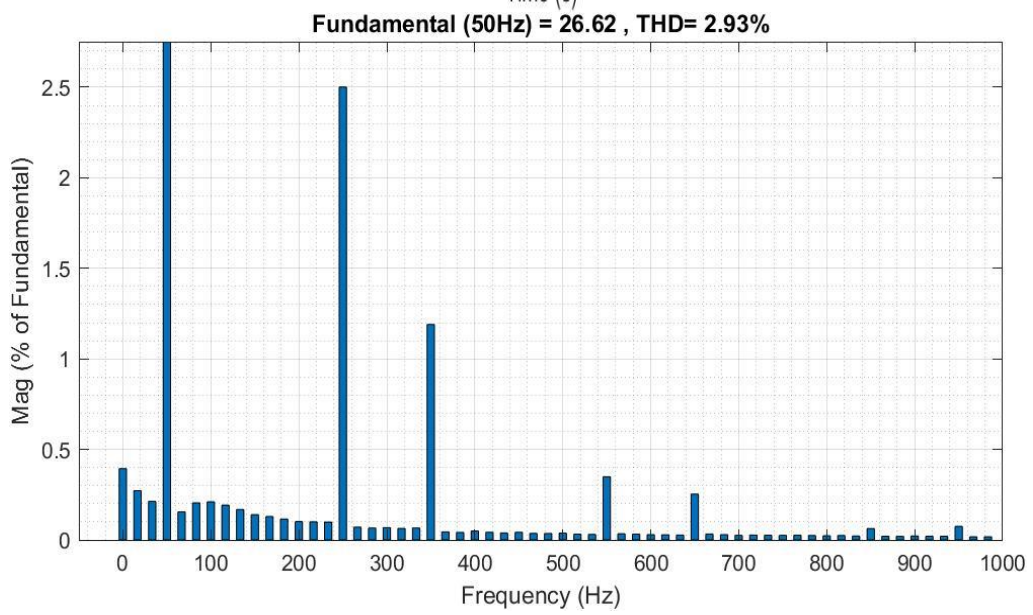
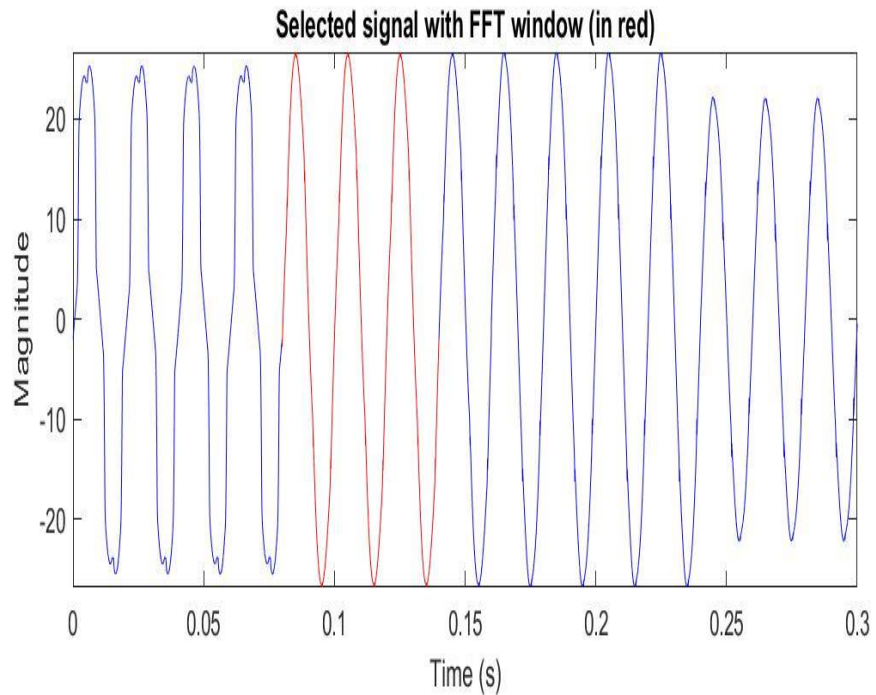
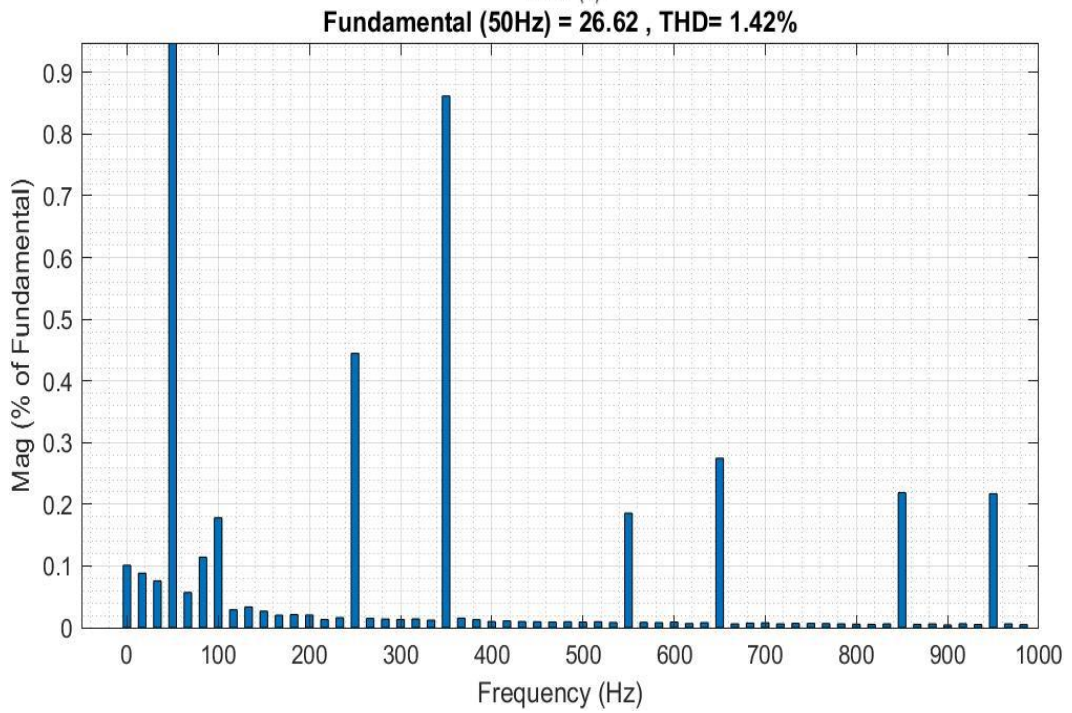
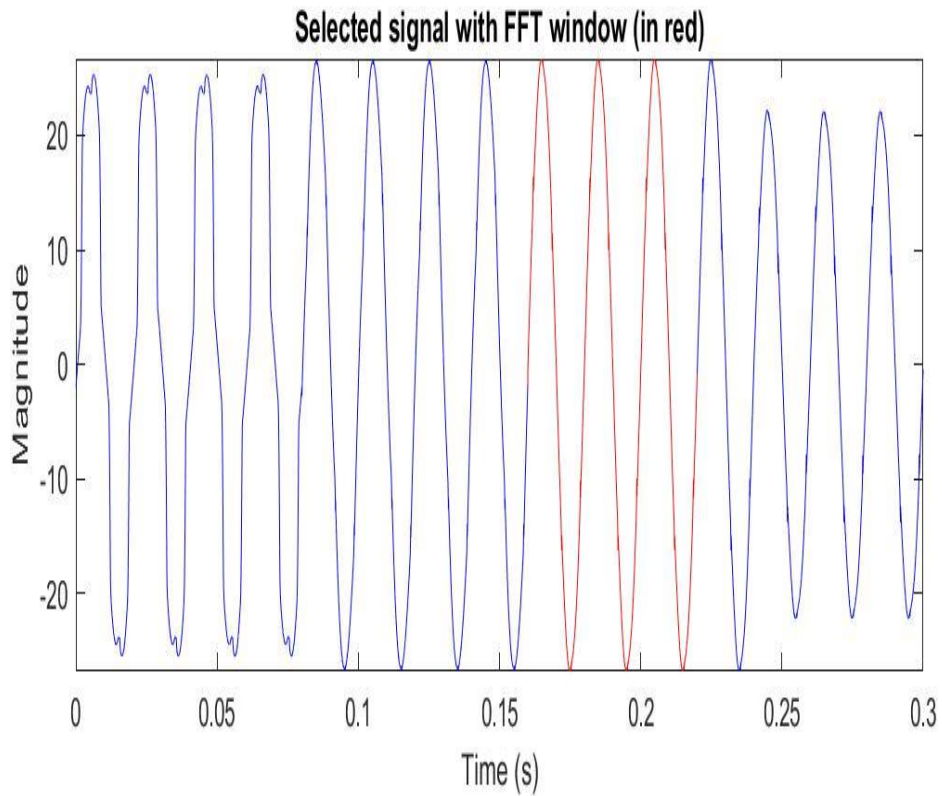


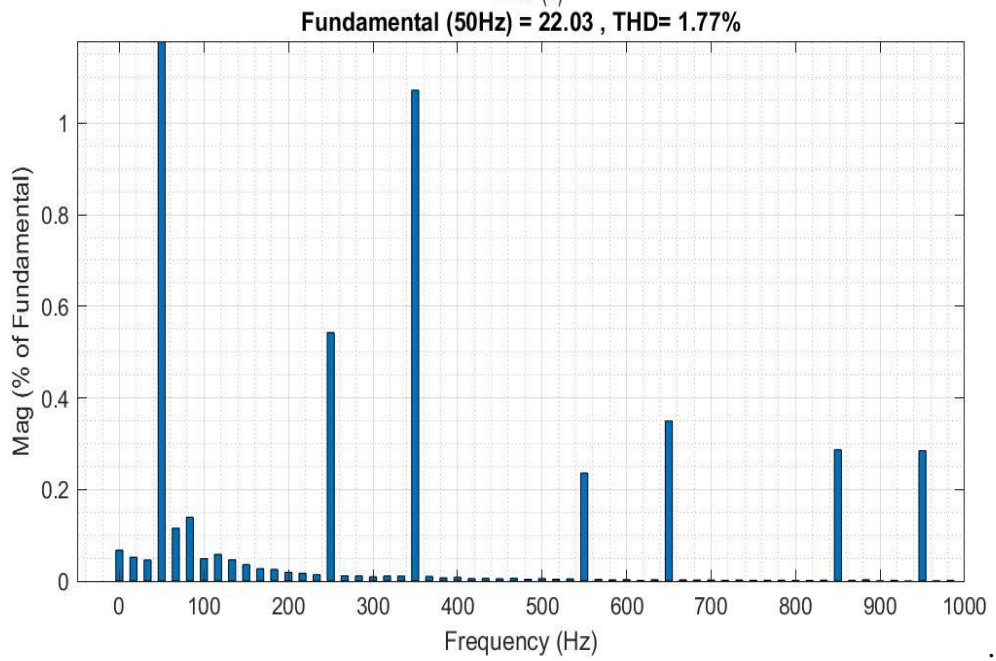
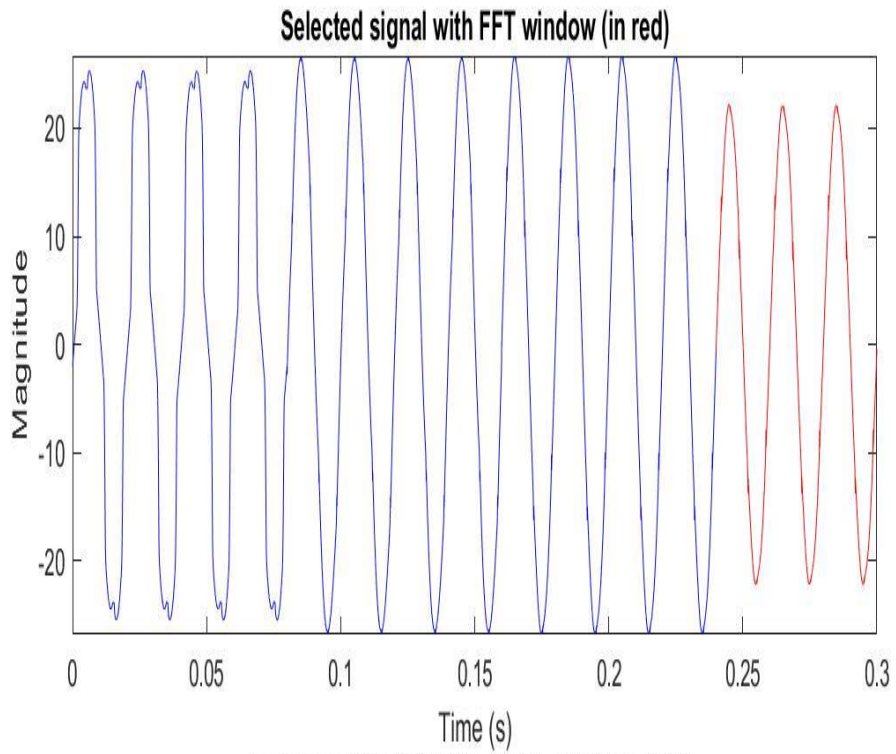
Figure 5.2.1

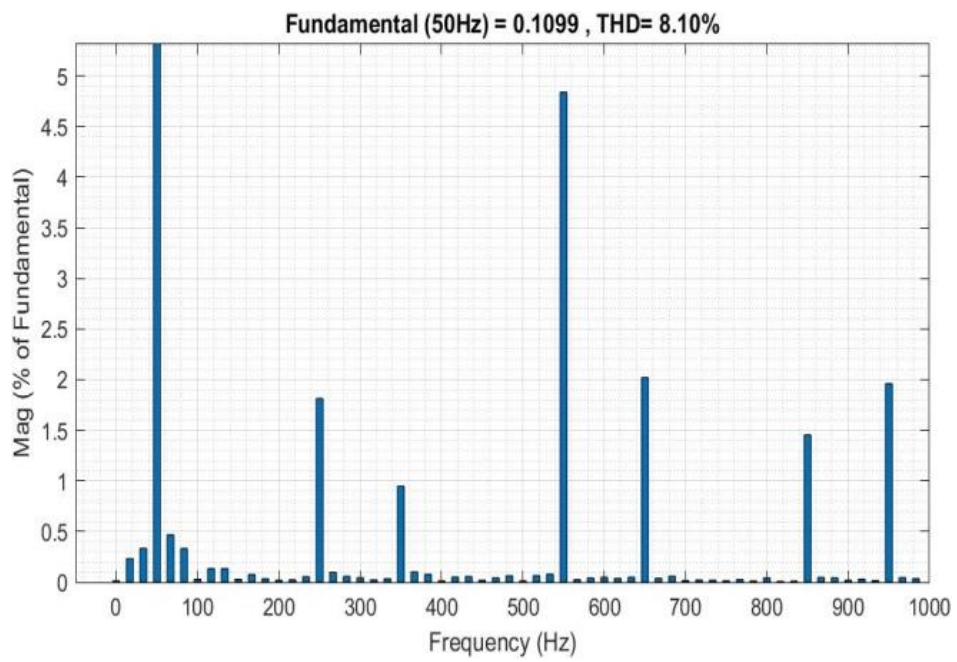
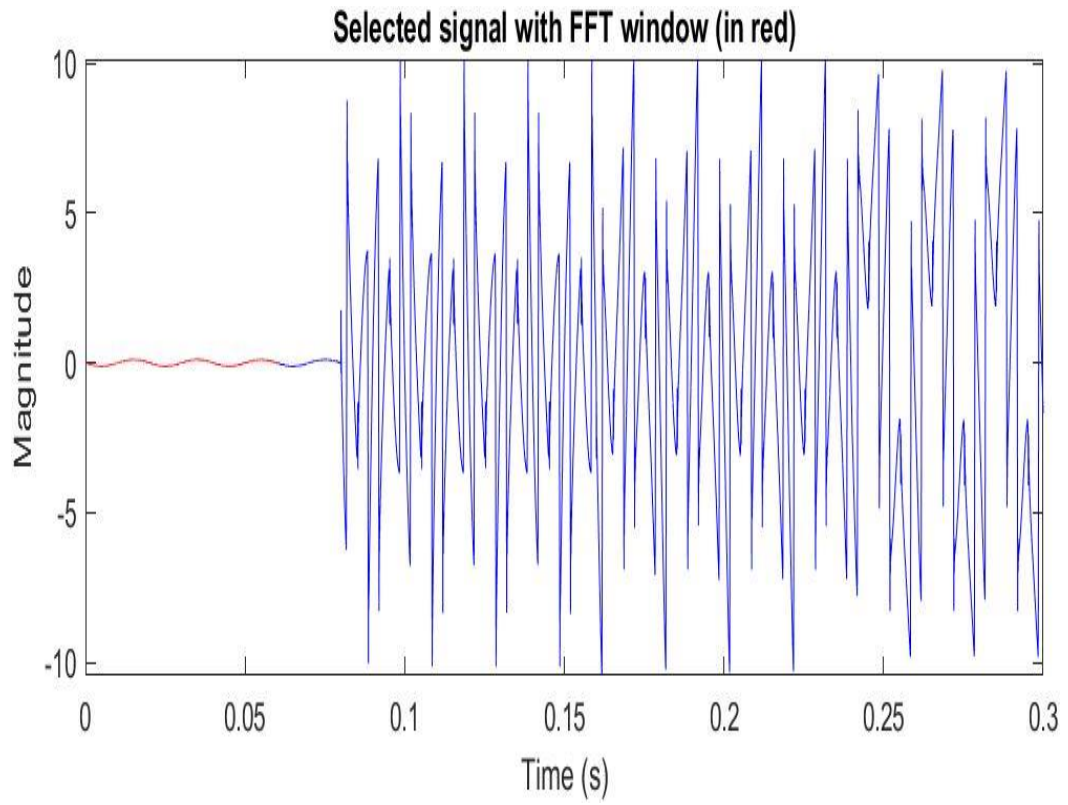
Schematic of System result of FFT analysis for source and inverter behavior under different operation scenarios

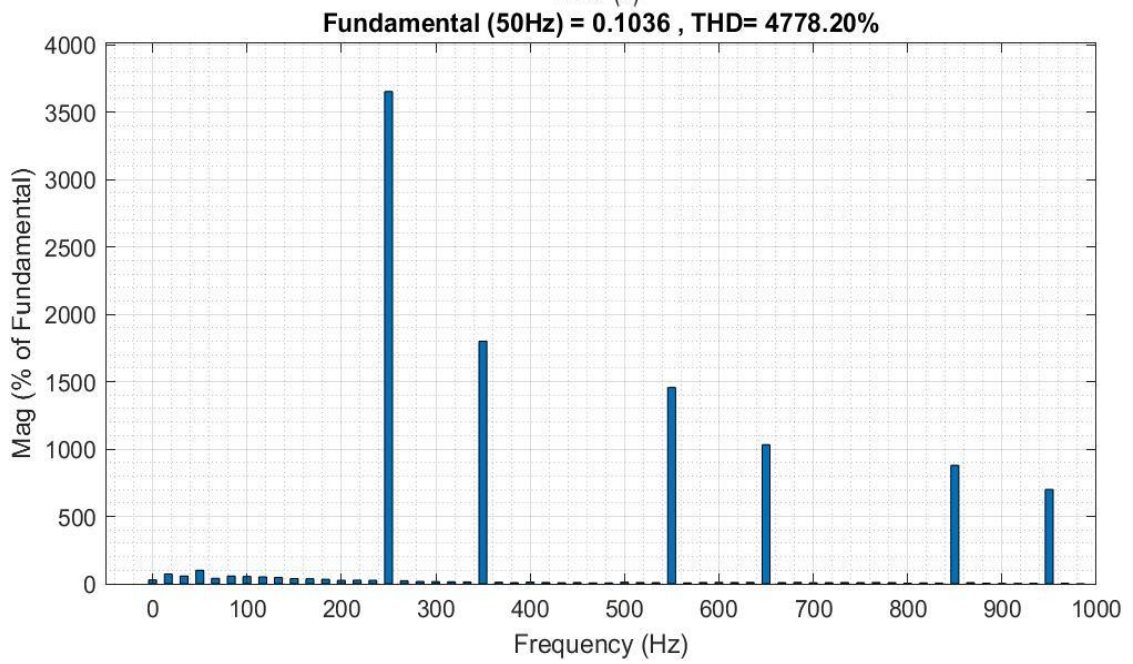
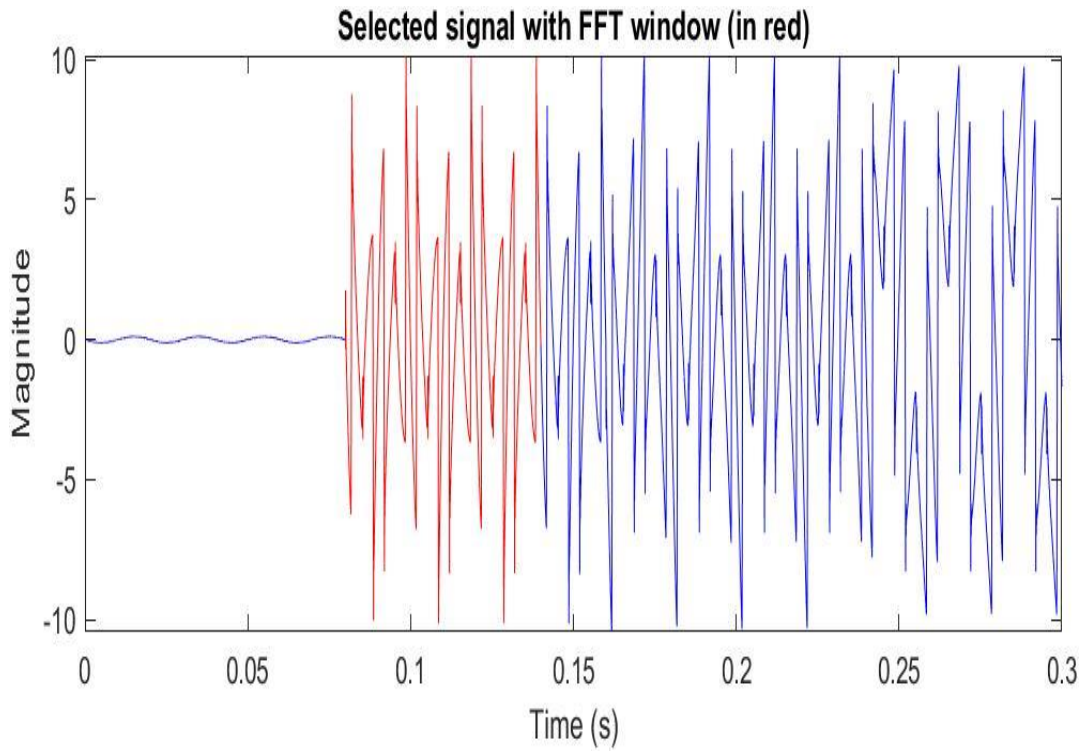


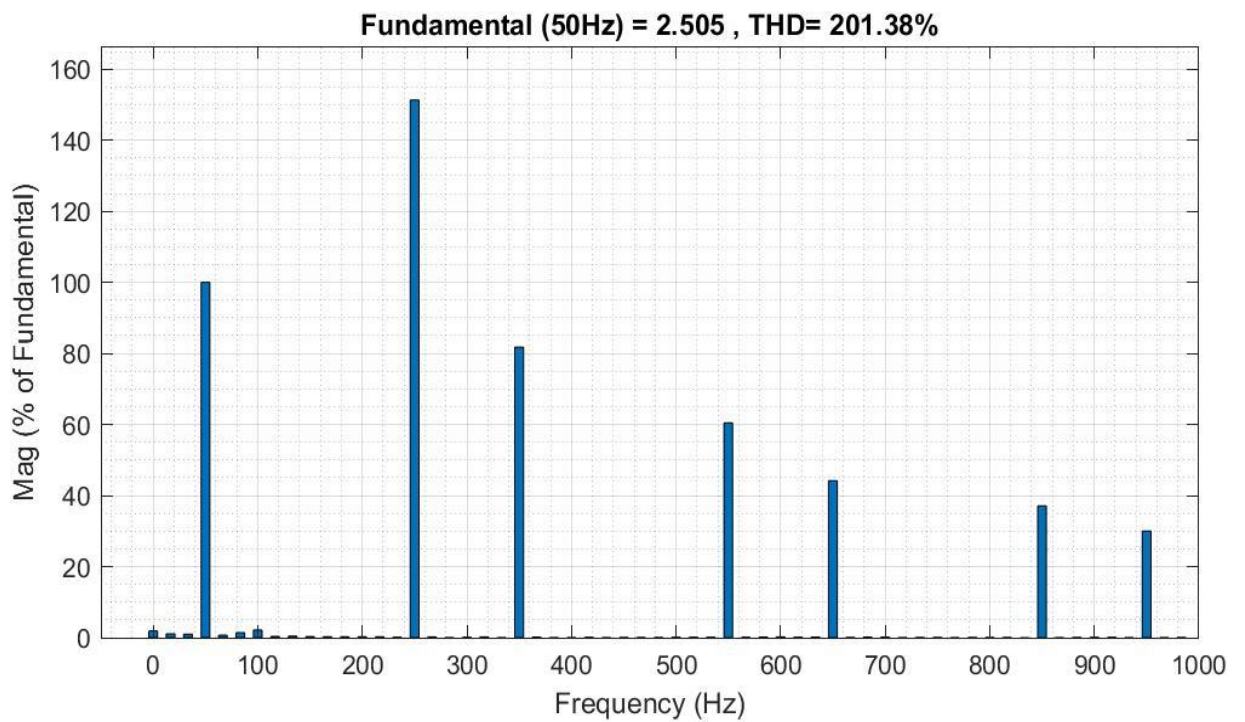
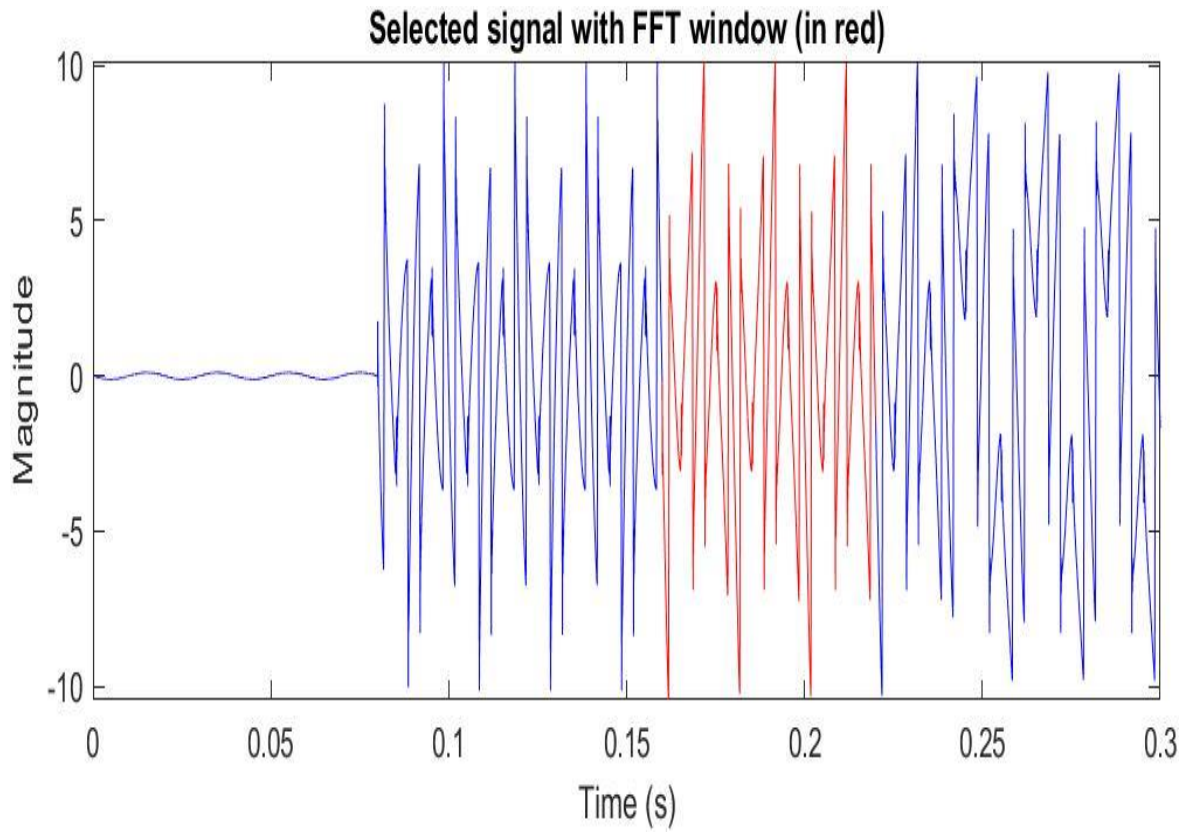












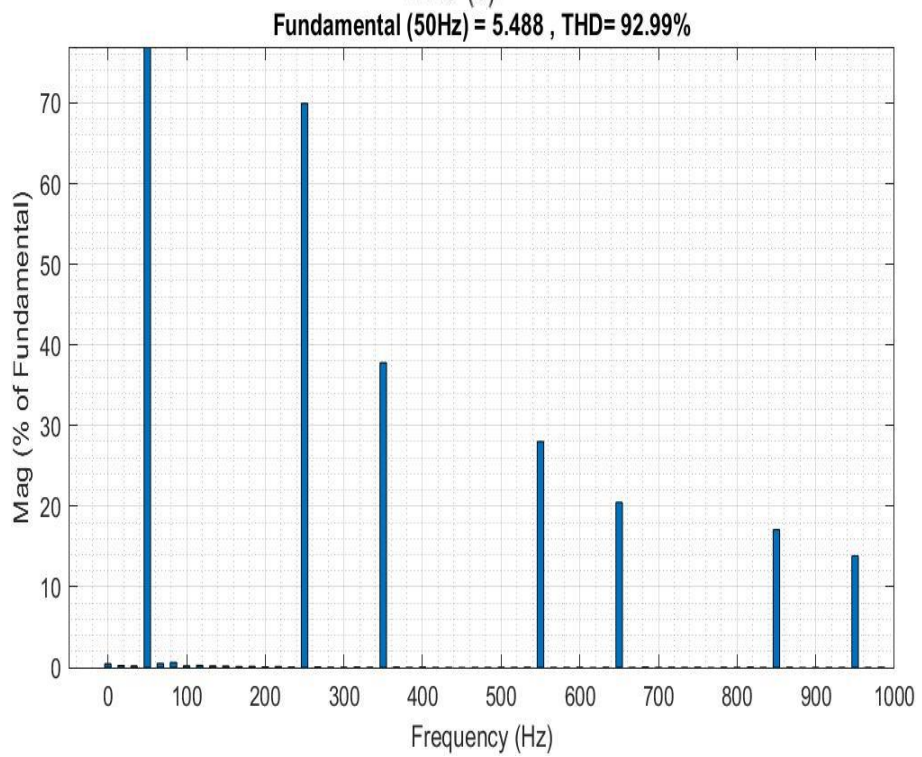
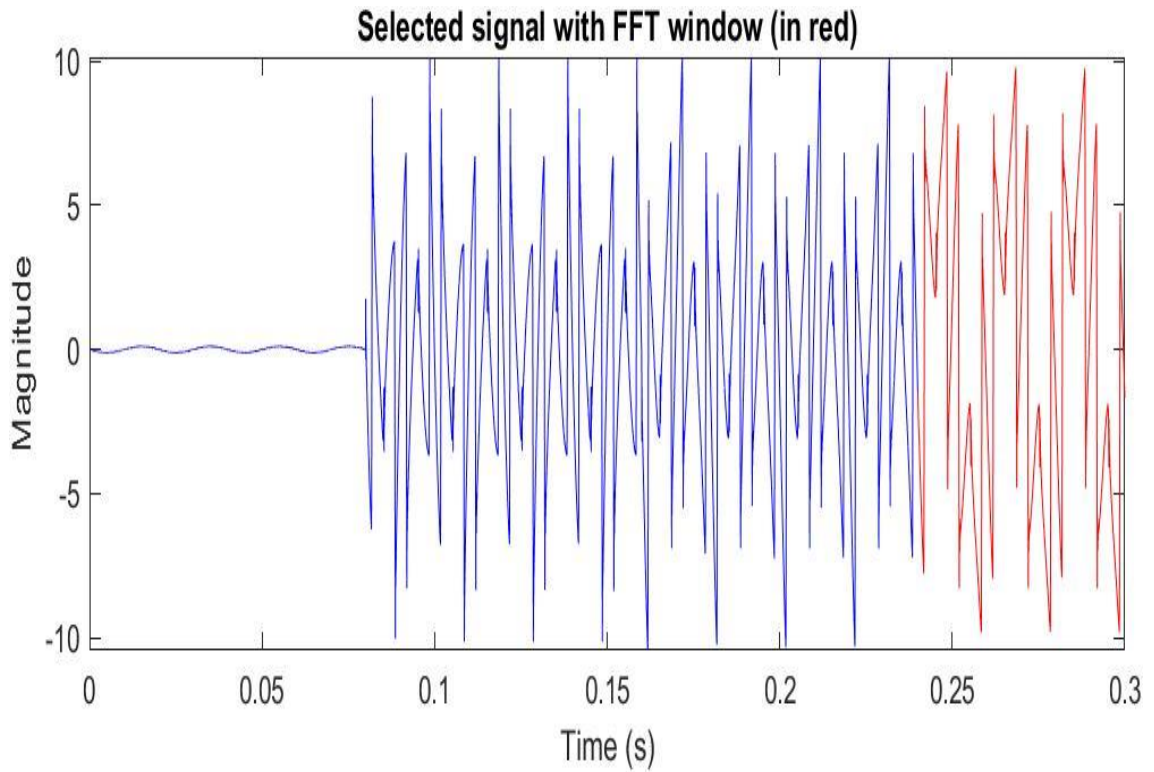
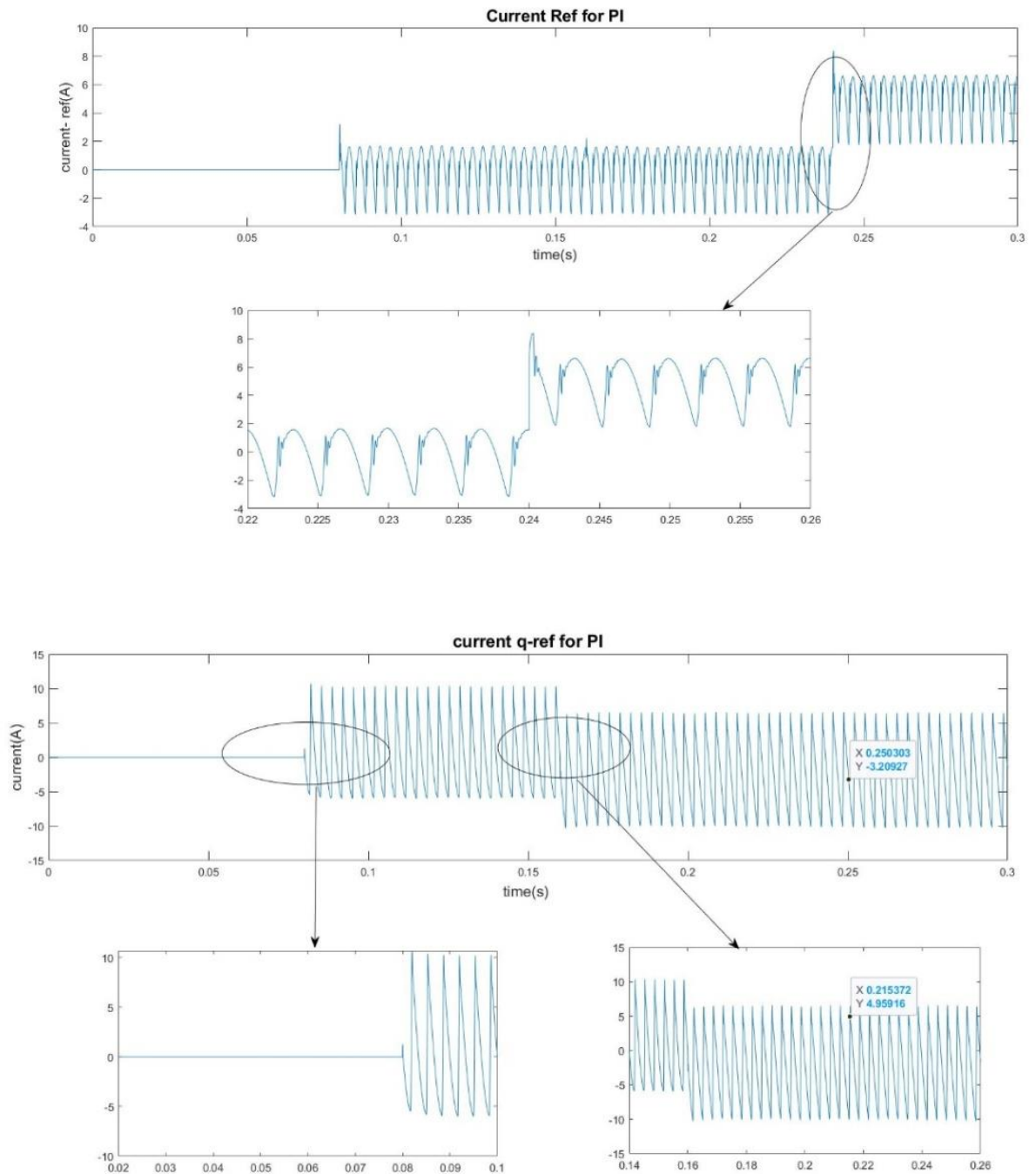


Figure 5.5

Schematic a- I_d / I_q ref and measured for PI system / b- I_d / I_q ref and measured for Fuzzy system simulation with non-linear load in combination

a- PI system



b- Fuzzy logic System

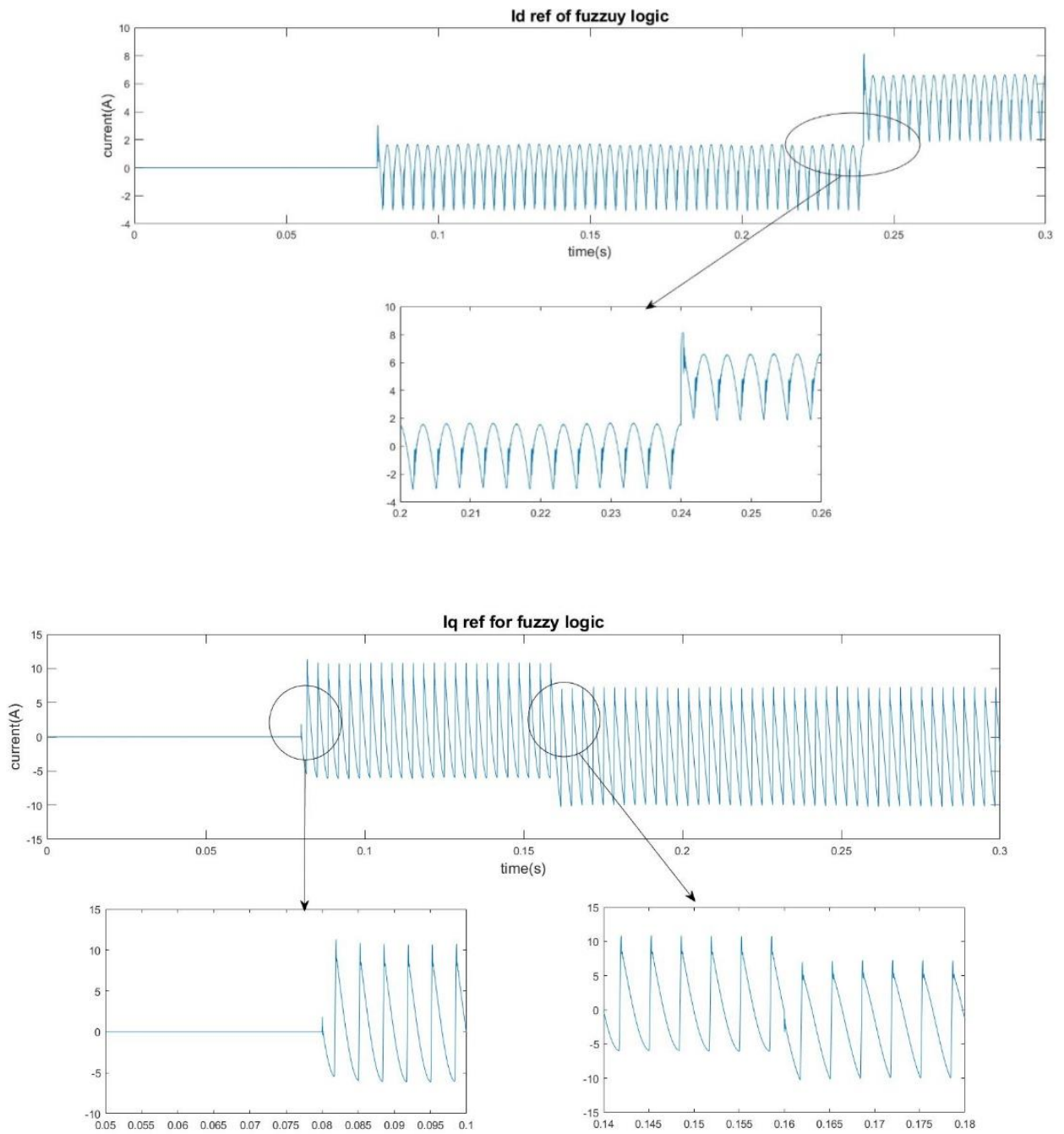
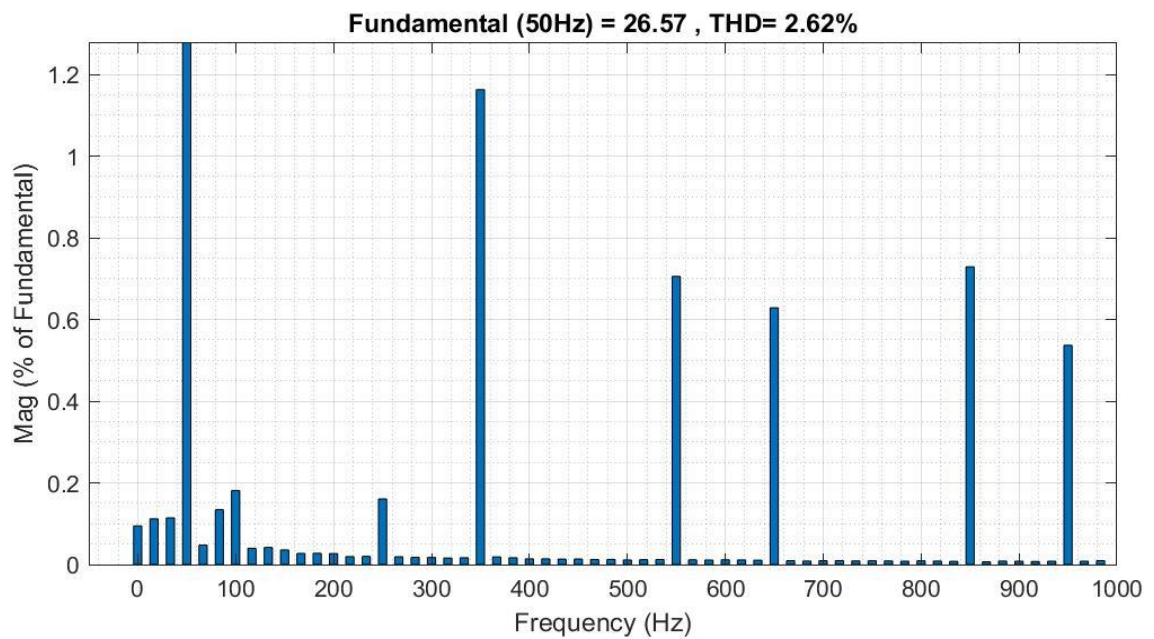
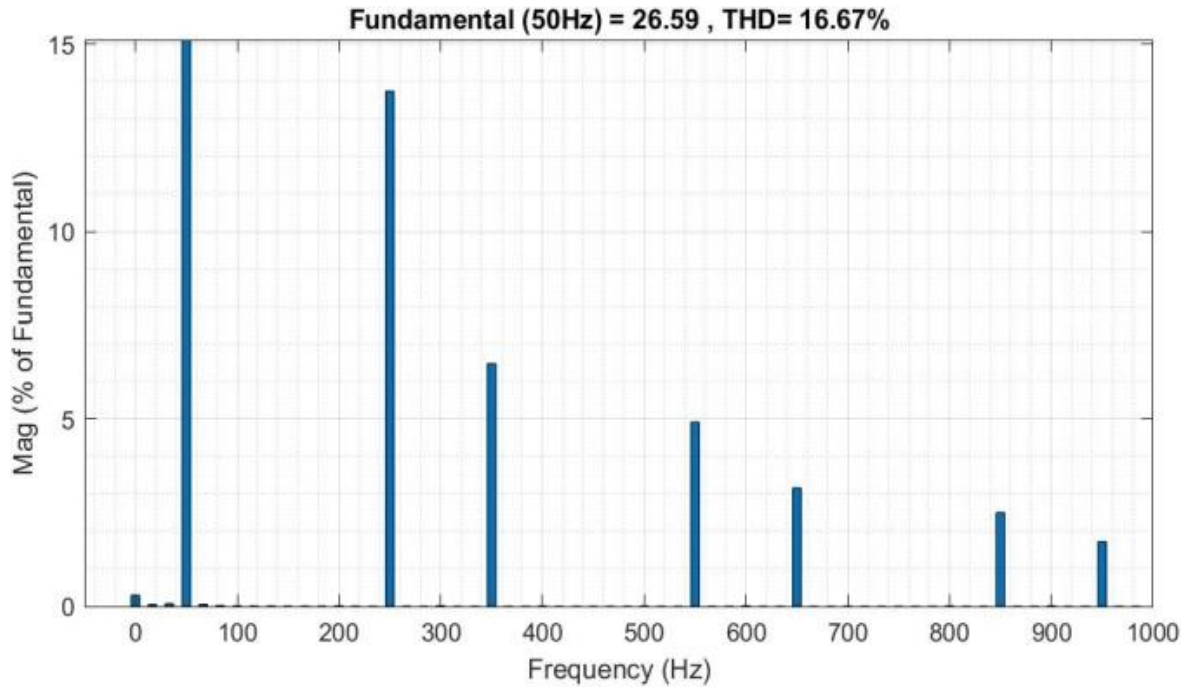


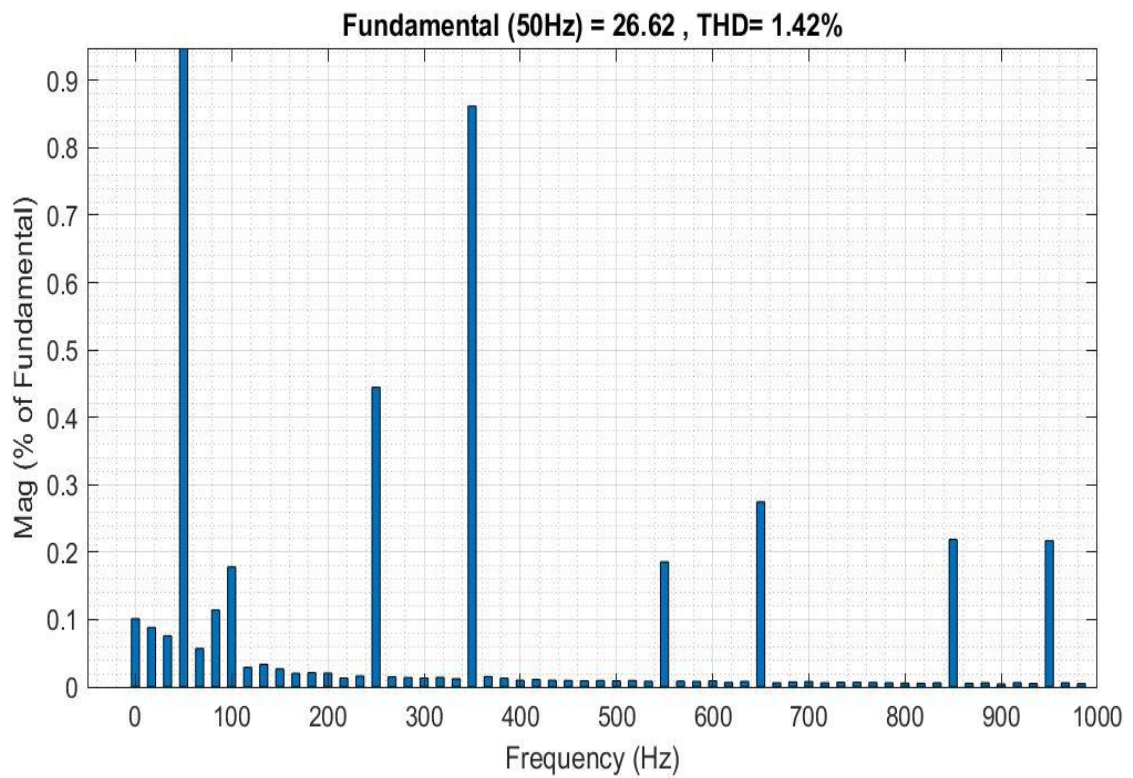
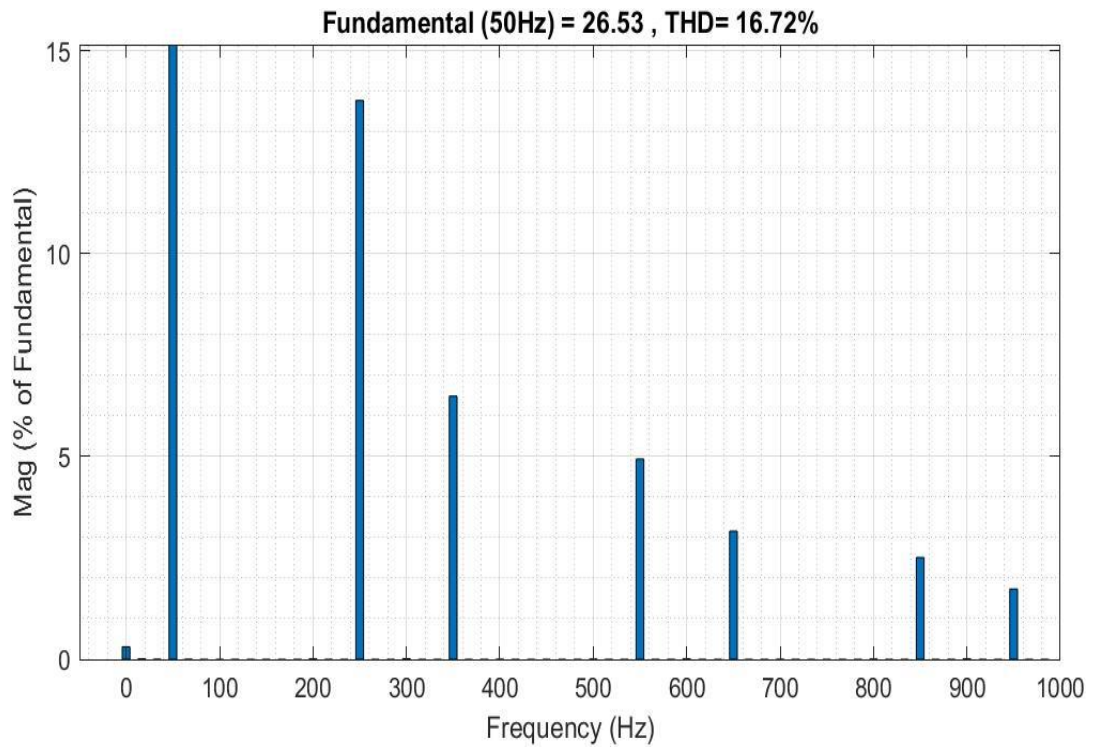
Figure 5.6.1

THD without and with APF of : a-PI controller without and with APF / b- Fuzzy Logic controller.

a- PI controller



a- Fuzzy Logic controller



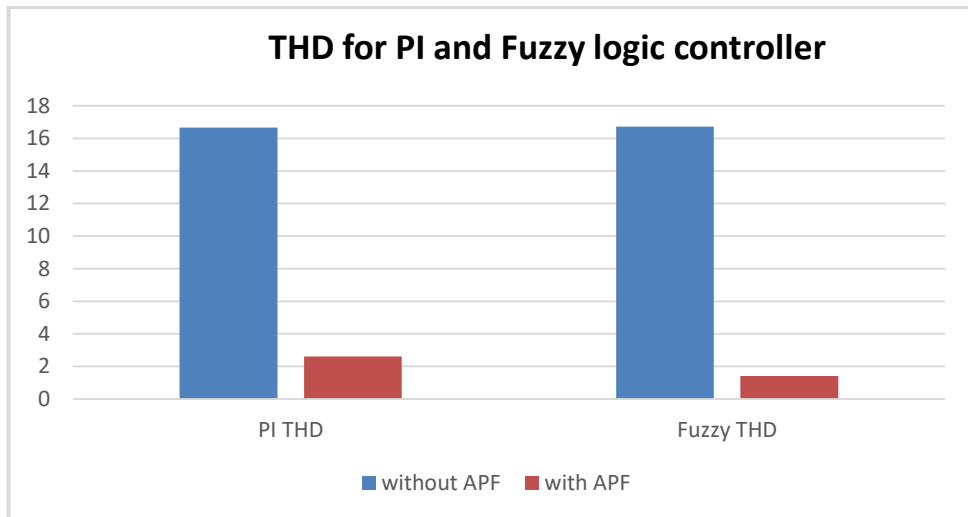


Figure 5.9

Operation of the SAPF during under load disturbance

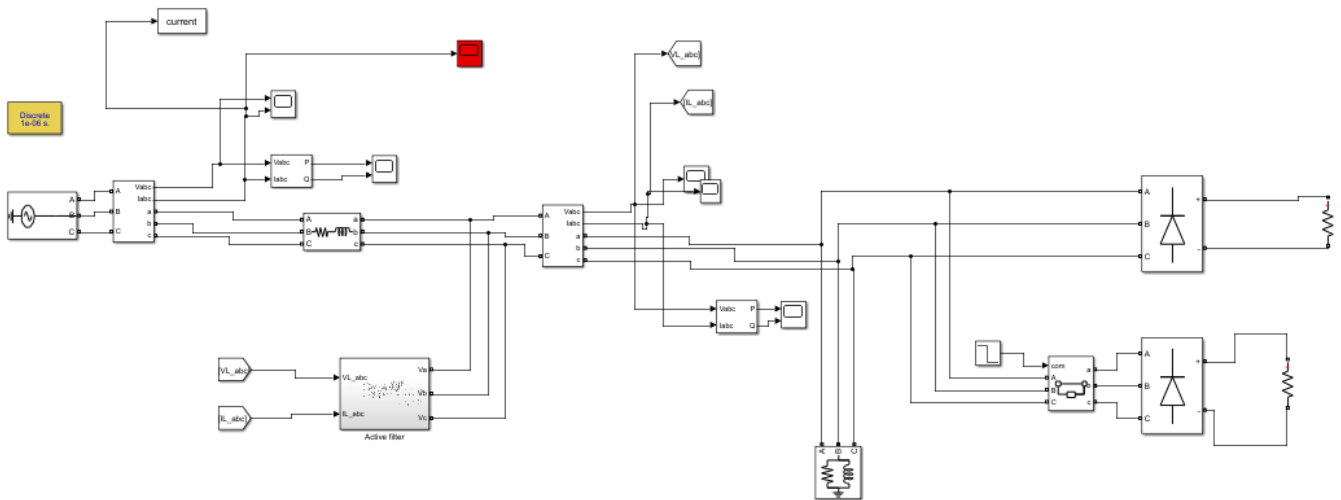


Figure 5. 10

The source current of operation of the SAPF during under load disturbance

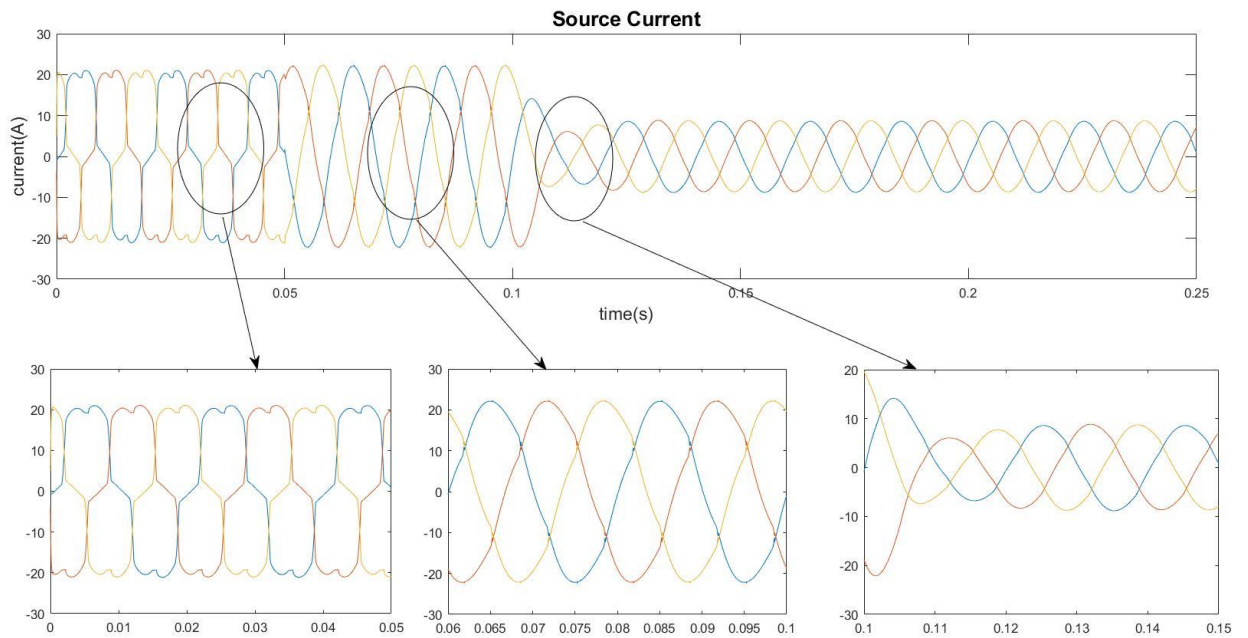
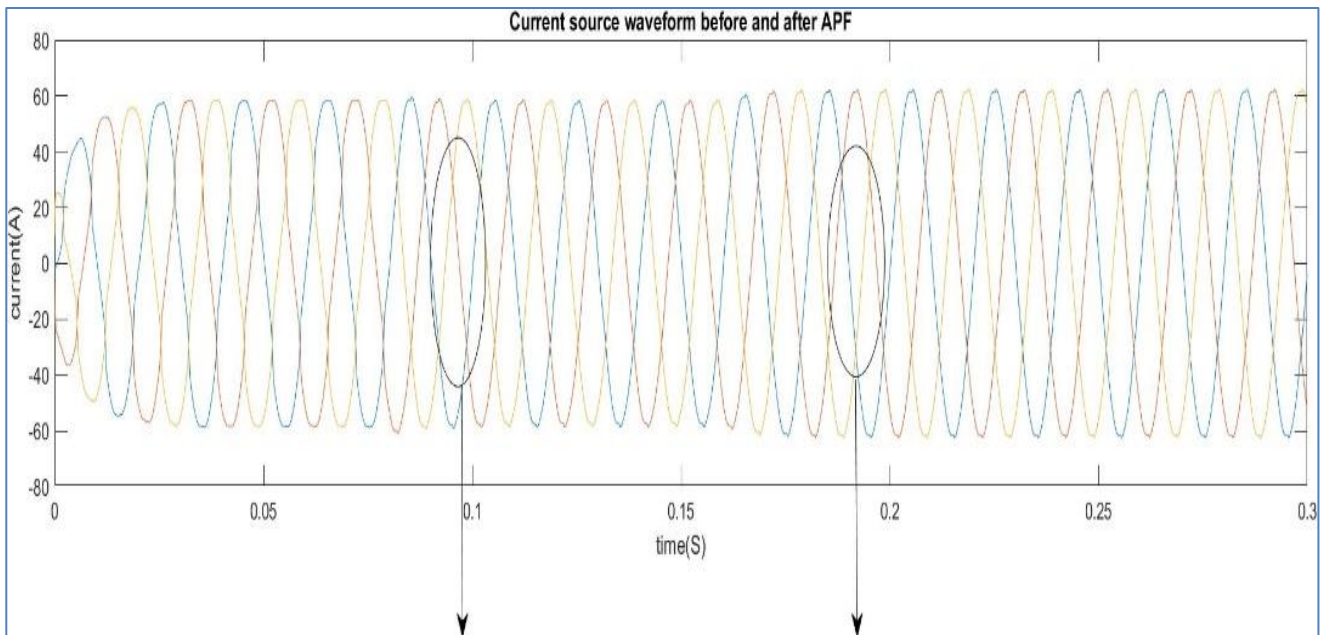


Figure 5. 11

source current when APF connected to bus no 1 of the IEEE 15 bus networks



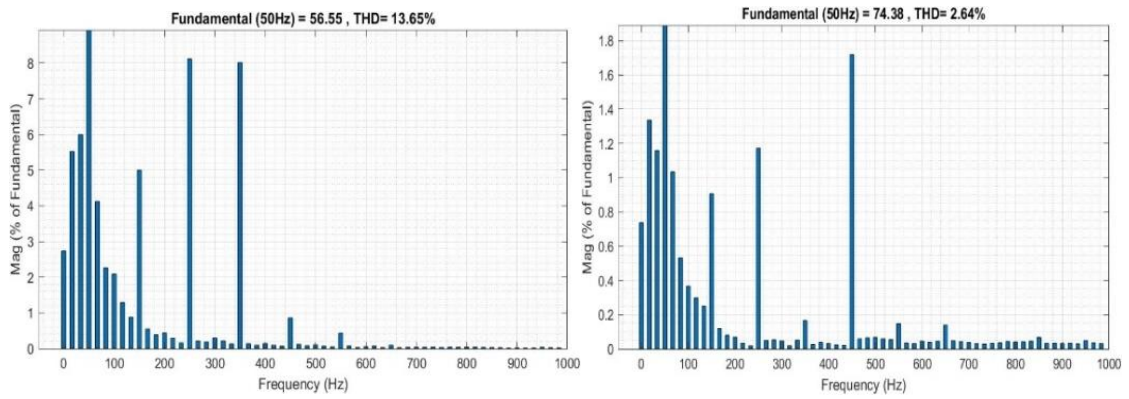


Figure 5.10
currents waveforms at buses 9,11,15 when APF connected to bus 1 of the IEEE 15 bus network

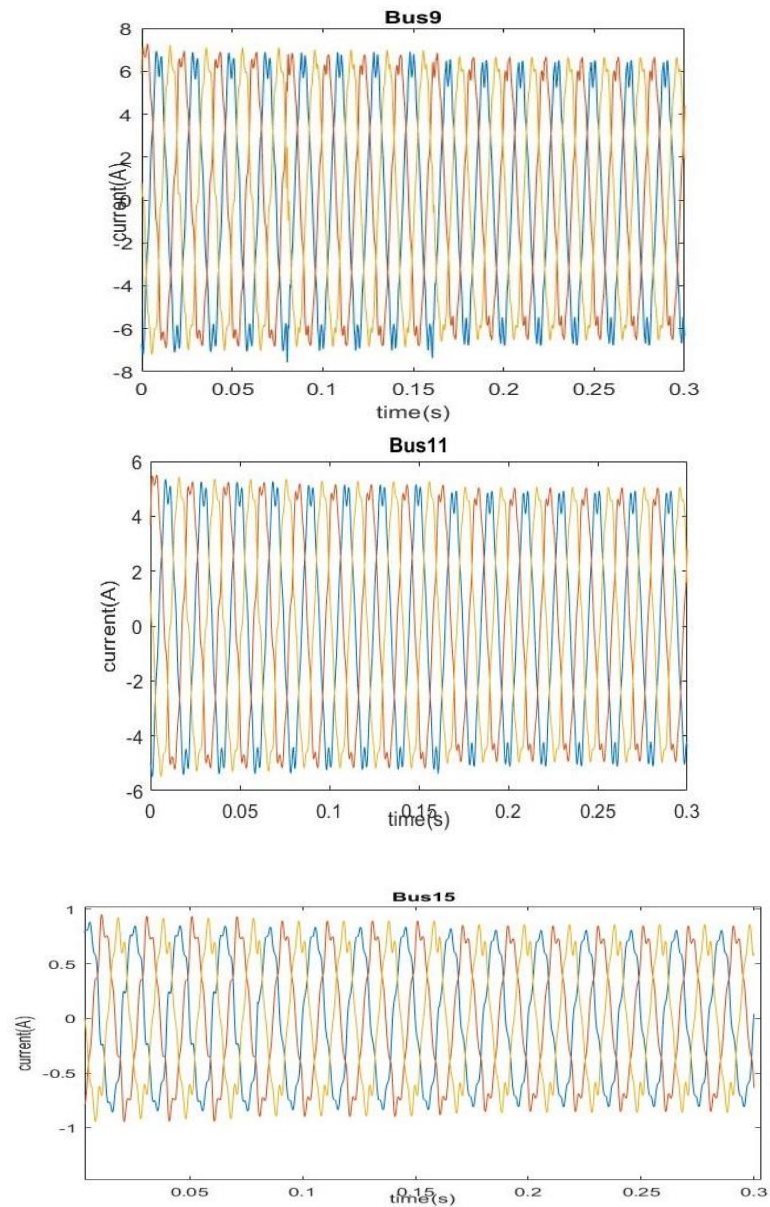


Figure 5.11

THD at buses 9,11,15 when APF connected to bus no 1 of the IEEE 15 bus network

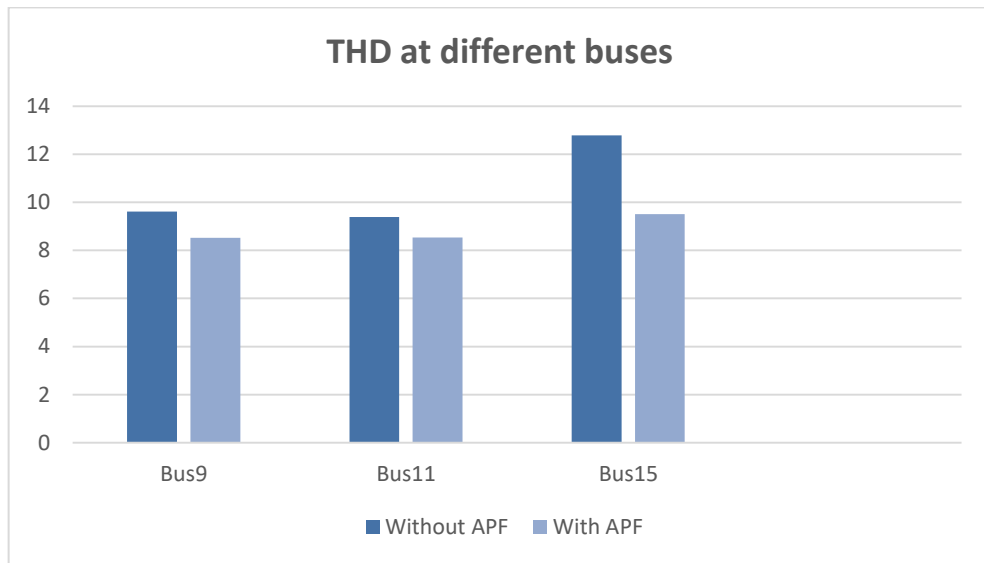


Figure 5.12

Source current when APF connected to bus no5 of the IEEE 15 bus network

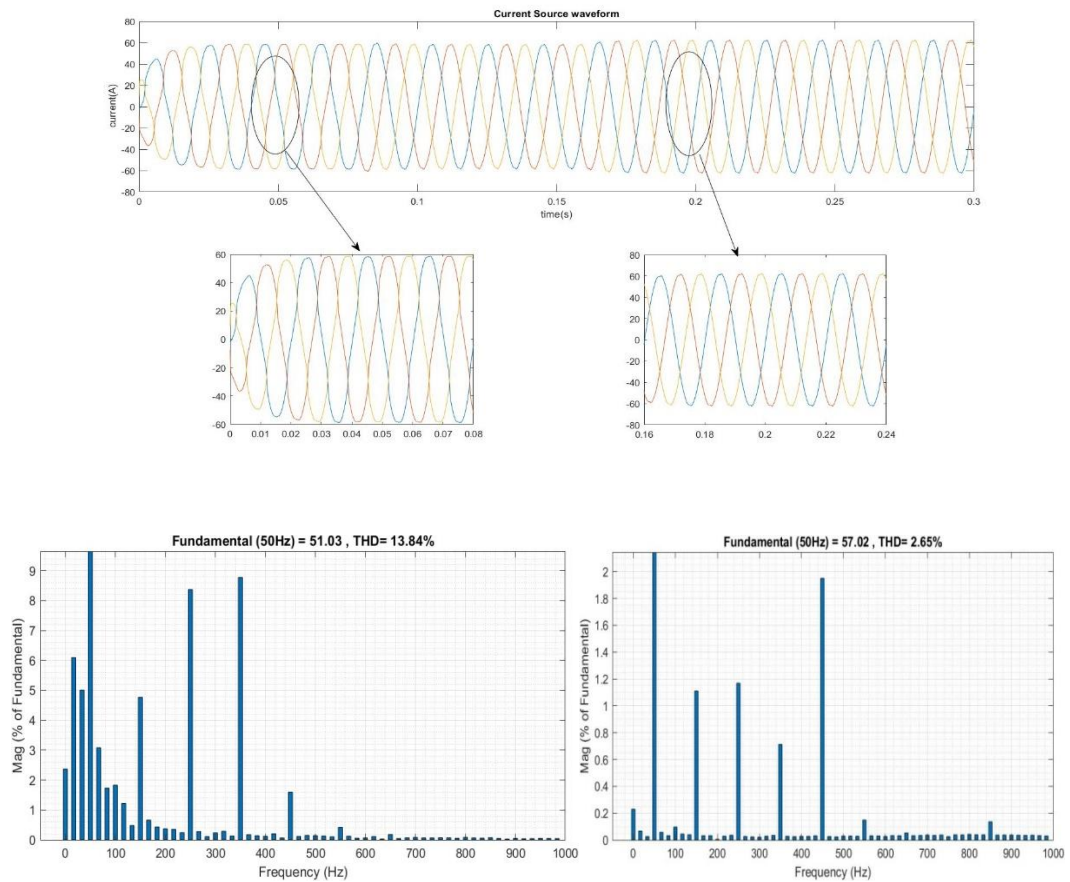


Figure 5.13

currents waveforms at buses 9,11,15 when APF connected to bus 5 of the IEEE 15 bus network

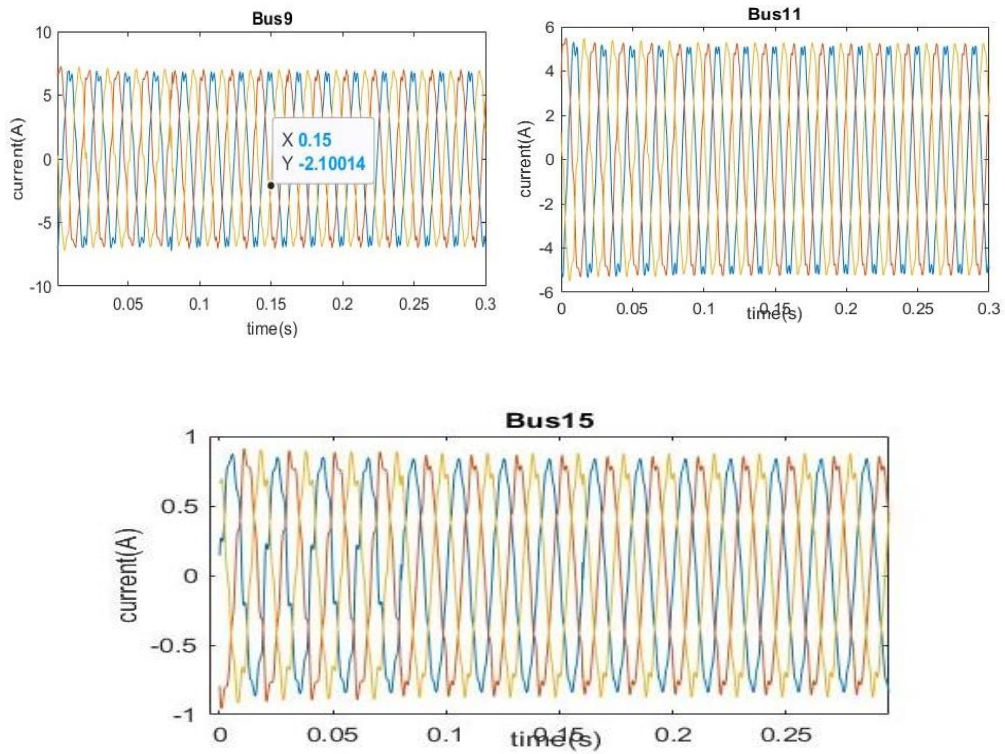


Figure 5.14

THD when APF connected to bus no5 of the IEEE 15 bus network

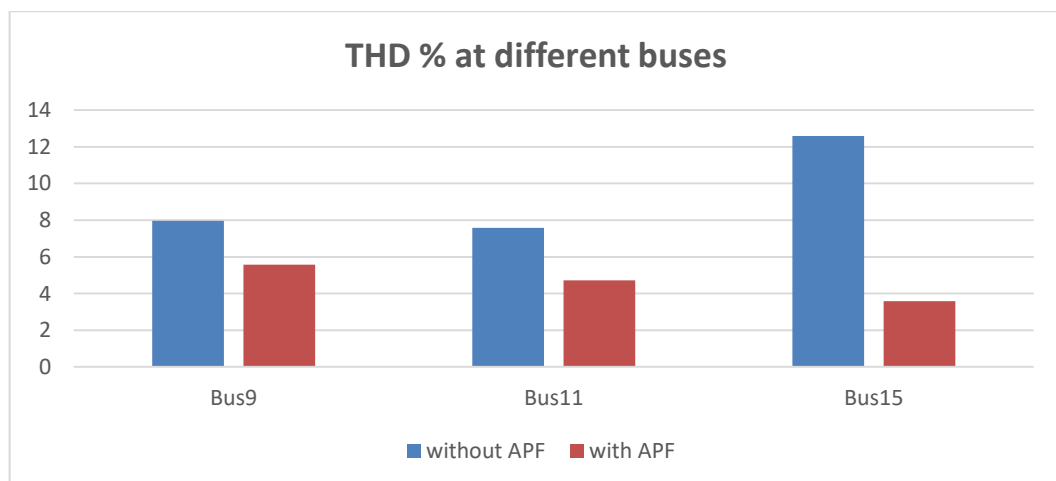


Table 2.2*Error and Change of Error for FLC with 27*27 membership*

	-13	-12	-11	-10	-9	-8	-7	-6	-5	-4	-3	-2	-1	0	1	2	3	4	5	6	7	8	9	10	11	12	13
-13	13	13	12	12	11	11	10	10	9	9	8	8	7	7	6	6	5	5	4	4	3	3	2	2	1	1	0
-12	13	12	12	11	11	10	10	9	9	8	8	7	7	6	6	5	5	4	4	3	3	2	2	1	1	0	0
-11	12	12	11	11	10	10	9	9	8	8	7	7	6	6	5	5	4	4	3	3	2	2	1	1	0	0	-1
-10	12	11	11	10	10	9	9	8	8	7	7	6	6	5	5	4	4	3	3	2	2	1	1	0	0	-1	-1
-9	11	11	10	10	9	9	8	8	7	7	6	6	5	5	4	4	3	3	2	2	1	1	0	0	-1	-1	-2
-8	11	10	10	9	9	8	8	7	7	6	6	5	5	4	4	3	3	2	2	1	1	0	0	-1	-1	-2	-2
-7	10	10	9	9	8	8	7	7	6	6	5	5	4	4	3	3	2	2	1	1	0	0	-1	-1	-2	-2	-3
-6	10	9	9	8	8	7	7	6	6	5	5	4	4	3	3	2	2	1	1	0	0	-1	-1	-2	-2	-3	-3
-5	9	9	8	8	7	7	6	6	5	5	4	4	3	3	2	2	1	1	0	0	-1	-1	-2	-2	-3	-3	-4
-4	9	8	8	7	7	6	6	5	5	4	4	3	3	2	2	1	1	0	0	-1	-1	-2	-2	-3	-3	-4	-4
-3	8	8	7	7	6	6	5	5	4	4	3	3	2	2	1	1	0	0	-1	-1	-2	-2	-3	-3	-4	-4	-5
-2	8	7	7	6	6	5	5	4	4	3	3	2	2	1	1	0	0	-1	-1	-2	-2	-3	-3	-4	-4	-5	-5
-1	7	7	6	6	5	5	4	4	3	3	2	2	1	1	0	0	-1	-1	-2	-2	-3	-3	-4	-4	-5	-5	-6
0	7	6	6	5	5	4	4	3	3	2	2	1	1	0	0	-1	-1	-2	-2	-3	-3	-4	-4	-5	-5	-6	-6
1	6	6	5	5	4	4	3	3	2	2	1	1	0	0	-1	-1	-2	-2	-3	-3	-4	-4	-5	-5	-6	-6	-7
2	6	5	5	4	4	3	3	2	2	1	1	0	0	-1	-1	-2	-2	-3	-3	-4	-4	-5	-5	-6	-6	-7	-7
3	5	5	4	4	3	3	2	2	1	1	0	0	-1	-1	-2	-2	-3	-3	-4	-4	-5	-5	-6	-6	-7	-7	-8
4	5	4	4	3	3	2	2	1	1	0	0	-1	-1	-2	-2	-3	-3	-4	-4	-5	-5	-6	-6	-7	-7	-8	-8
5	4	4	3	3	2	2	1	1	0	0	-1	-1	-2	-2	-3	-3	-4	-4	-5	-5	-6	-6	-7	-7	-8	-8	-9
6	4	3	3	2	2	1	1	0	0	-1	-1	-2	-2	-3	-3	-4	-4	-5	-5	-6	-6	-7	-7	-8	-8	-9	-9
7	3	3	2	2	1	1	0	0	-1	-1	-2	-2	-3	-3	-4	-4	-5	-5	-6	-6	-7	-7	-8	-8	-9	-9	-10
8	3	2	2	1	1	0	0	-1	-1	-2	-2	-3	-3	-4	-4	-5	-5	-6	-6	-7	-7	-8	-8	-9	-9	-10	-10
9	2	2	1	1	0	0	-1	-1	-2	-2	-3	-3	-4	-4	-5	-5	-6	-6	-7	-7	-8	-8	-9	-9	-10	-10	-11
10	2	1	1	0	0	-1	-1	-2	-2	-3	-3	-4	-4	-5	-5	-6	-6	-7	-7	-8	-8	-9	-9	-10	-10	-11	-12
11	1	1	0	0	-1	-1	-2	-2	-3	-3	-4	-4	-5	-5	-6	-6	-7	-7	-8	-8	-9	-9	-10	-10	-11	-12	-12
12	1	0	0	-1	-1	-2	-2	-3	-3	-4	-4	-5	-5	-6	-6	-7	-7	-8	-8	-9	-9	-10	-10	-11	-12	-12	-13
13	0	0	-1	-1	-2	-2	-3	-3	-4	-4	-5	-5	-6	-6	-7	-7	-8	-8	-9	-9	-10	-10	-11	-12	-12	-13	-13

-1,-1,-1	-1,-1,0	-1,-1,1	-1,0,-1	-1,0,0	-1,0,1	-1,1,-1	-1,1,0	-1,1,1
NNN	NN0	NNP	NON	N00	N0P	NPN	NP0	NPP
0,-1,-1	0,-1,0	0,-1,1	0,0,-1	0,0,0	0,0,1	0,1,-1	0,1,0	0,1,1
0NN	0N0	0NP	00N	000	00P	0PN	0P0	0PP
1,-1,-1	1,-1,0	1,-1,1	1,0,-1	1,0,0	1,0,1	1,1,-1	1,1,0	1,1,1
PNN	PN0	PNP	P0N	P00	P0P	PPN	PP0	PPP

The figure 2.12 in appendix a below shows the design Fuzzy Logic Controller (FLC) by using MATLAB/SIMULINK.



جامعة النجاح الوطنية

كلية الدراسات العليا

التصميم والتحكم بالمرشحات الفعالة باستخدام وحدة التحكم
الضبابي وتغذية المرشح بعكس متعدد المستويات وخلايا ضوئية.

إعداد

غدير أحمد عبده

إشراف

د. كامل صالح

قدمت هذه الرسالة استكمالاً لمتطلبات الحصول على درجة الماجستير في هندسة القوى الكهربائية، من كلية الدراسات العليا، في جامعة النجاح الوطنية، نابلس - فلسطين.

2023

التصميم والتحكم بالمرشحات الفعالة باستخدام وحدة التحكم الضبابي وتغذية المرشح بعكس متعدد المستويات وخلايا ضوئية.

إعداد

غدير أحمد عبده

إشراف

د. كامل صالح

المخلص

تستخدم الأحمال غير الخطية على نطاق واسع في الأنظمة الكهربائية الحديثة مما يؤدي الى زيادة التوافقيات والتي تؤثر سلبا على الشبكة الكهربائية.

تؤثر التيارات التوافقية الناتجة عن استخدام الأجهزة الالكترونية المزودة للطاقة مثل أجهزة شحن الهواتف المحمولة أو المحولات أو أي جهاز كهربائي يحتوي على شبه موصل على جودة الطاقة الكهربائية وتخلق تيارات غير جيبية من مصدر التيار المتردد.

عملية التحويل التي تقوم بها محولات الطاقة تسبب انقطاع في التيار والذي ينتج عنه زياده التوافقيات في النظام. تعمل هذه الأجهزة على احداث تلوث في نظام الطاقة وتسبب مشاكل في جودة الطاقة وتؤثر على الأحمال الحساسة. التوافقيات في نظام الطاقة تسبب العديد من المشاكل مثل تشوه الجهد وتغيير القيمة القصوى الفعالة لتيار الخط والذي ينتج عنه خسائر إضافية.

بالإضافة إلى التحديات التي تسببها التيارات المتناسقة، فإن القدرة الحقيقية هي مشكلة أخرى تؤثر على جودة التيار الكهربائي في النظام الكهربائي. فالتيار النشط لا يعمل فعليًا على النظام الكهربائي، مما يجعله مصدر طاقة بحيث يصبح غير فعال. وتتسبب ارتفاع قيمة التيار يؤدي إلى تحميل المكونات التي يمر

بها في خسائر إضافية. ولتحسين جودة الطاقة المستلمة من الشبكة، يجب استخدام مرشحات كهربية لإلغاء التيارات المتناسقة والقدرة الحقيقية.

تم تطوير جودة الطاقة باستخدام مجموعة متنوعة من المرشحات، بما في ذلك المرشحات السلبية والنشطة والهجينة. ويتم استخدام مرشح نشط للتيار لزيادة جودة الطاقة الكهربائية. يمكن لهذا المرشح النشط تنفيذ مجموعة متنوعة من المهام، بما في ذلك تقليل التشوهات المتناسقة وضبط الطاقة النشطة وتطوير معامل القدرة وإدخال مصدر طاقة حقيقي..

تم استخدام برنامج MATLAB / SIMULINK في هذه الدراسة لدمج مصادر الطاقة المتجددة المختلفة مع محول متعدد المستويات مع H-Bridge بـ 27 مستوى مع مرشح نشط للطاقة الكهربائية. وتم بناء النظام مجموعة متنوعة من السيناريوهات التشغيلية. بحيث تم تقييم آثار توصيل النظام بالشبكة أو حمل منفصل لكل سيناريو. ويتم عرض المخطط العام للنظام الذي تم إنشاؤه لهذه الدراسة في الشكل

الكلمات المفتاحية: المرشحات الفعالة ، وحدة التحكم الضبابي، مرشح متعدد المستويات، خلايا ضوئية، التشوه التوافقي الكلي